Title
The DNA binding properties of intercalating drugs

Author
Mirau, Peter Allen

Publication Date
1981

Peer reviewed|Thesis/dissertation

THE DNA BINDING PROPERTIES OF INTERCALATING DRUGS

by

PETER ALLEN MIRAU

DISSERTATION

Submitted in partial satisfaction of the requirements for the degree of

DOCTOR OF PHILOSOPHY

in

PHARMACEUTICAL CHEMISTRY

in the

GRADUATE DIVISION

of the

UNIVERSITY OF CALIFORNIA

San Francisco

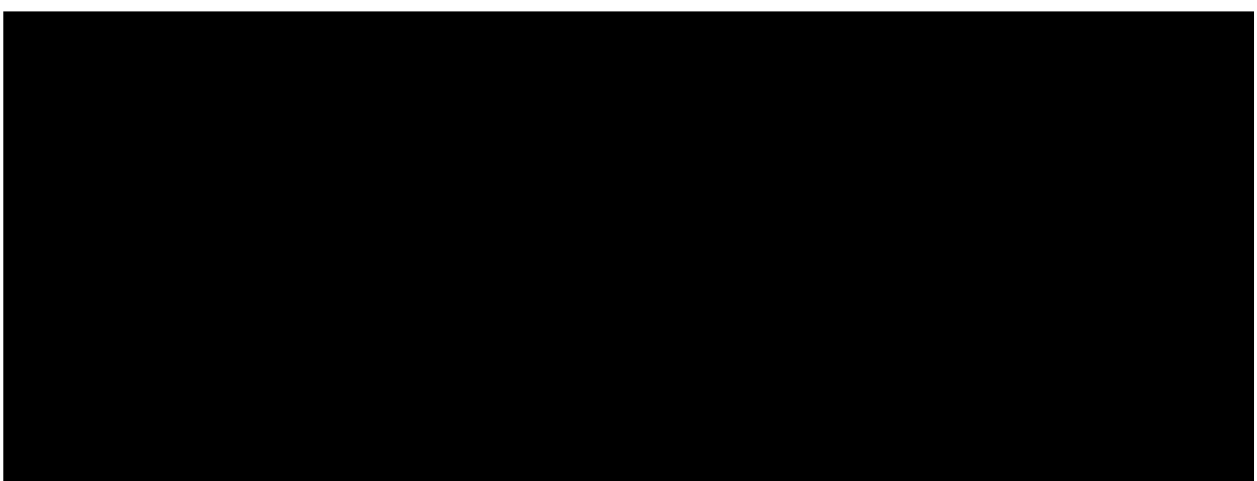

Date University Librarian

Degree Conferred: JUN 2 8 1981

In spite of the XL-100

TABLE OF CONTENTS

ABSTRACT

A variety of physical chemical techniques have been used to study the binding of intercalating drugs to nucleic acids. Of particular interest are the conformation and dynamics of the drugs, the nucleic acid equilibrium binding and kinetic properties, and the physical properties of the drug receptor complex. It is hoped that these studies may provide some insight into the molecular basis for the observed biological effects.

In one series of experiments we examined the effect of amino acid substitution on the conformational and DNA binding properties of the antitumor antibiotic actinomycin. High resolution ^{1}H NMR studies showed that the amino acid substitutions were made a unique site on either the α or the β pentapeptide lactone ring. Substitution had only a minor effect on the conformational and hydrogen bonding properties of the drug and it was concluded that the analogs may adopt a conformation similar to that of the parent compound. Also, it was observed that the dynamics of the amino acids on the the α and β pentapeptide differed.

The equilibrium and kinetic DNA binding properties of the actinomycin analogs were also studied. Both the binding and kinetic properties are sensitive to the nature of the substituted amino acid. The kinetic properties, which are believed related to the biological activity, were most affected. A thermodynamic analysis of the dissociation

rates

ing s

tion s

A

of th

molec

cally

ments,

observe

the bi

al der

Fl

were u

labeled

al sh

essentia

inaccess

used to

relative

bending

rates suggest that dissociation is a complex process involving substantial ordering of water molecules in the transition state.

Absorption and ^{31}P NMR were used to monitor the binding of the intercalating antibiotic daunomycin to DNA and nucleotides. The results revealed that the drug preferentially binds to GC sequences. In the DNA binding experiments, an average change in the ^{31}P chemical shift was observed when the drug bound one every five base pairs and the binding seemed to inhibit only the final stage of thermal denaturation.

Fluorine NMR, absorption, and fluorescence spectroscopy were used to investigate the interaction between fluorine labeled intercalators and nucleic acids. The induced chemical shifts indicate that the environment of the drug is essentially hydrophobic when intercalated and the drug is inaccessible to the solvent pool. ^{19}F NMR relaxation was used to show that the drug exhibits considerable motion relative to the base pairs when intercalated but slows the bending motions of the helix.

ACKNOWLEDGEMENTS

Several people have helped make my four years at UCSF a pleasent and learning experience. Dick Shafer has been a warm and personable mentor who has encouraged me at every step along the way. From him I have learned both science and patience. Martin Shetlar has been a great source of biochemical information and a source of entertainment. The encouragement and guidence of Tom James has also been appreciated. Phil Bolton appeared at just the right time to help me get started in NMR. The backing of my family has also helped me at every step along the way. Kent Kunze, Marv Cohen, and Kathy (the rocket) Prickett have be a constant and pleasent source of distraction. Chuck Pidgeon taught me humility (on the squash court).

INTRODUCTION

One of the goals of pharmaceutical chemistry is the study of the interaction of drugs at their receptor, or site of biological activity. Often this is an involved task which requires complex biochemistry and chromatography to isolate small quantities of the receptor. However, some receptors, such as certain proteins and nucleic acids, are easily isolated in large quantities for study of their physical properties and their interactions with drugs.

This thesis is concerned with the interaction of several antitumor drugs whose proposed mode of action involves nucleic acid binding. Since cancer cells are often delineated by their rapid growth rates, which require increased nucleic acid tanscription and protein synthesis, drugs which interfere with these processes may have some basis for selectivity (Pratt and Ruddon, 1978). In fact, most antitumor drugs in use today are directed at the inhibition of nucleic acid synthesis (Remers, 1978).

There are several classes of drugs which are important in cancer chemotherapy. Among the most used are the antimetabolites, which interrupt the de novo synthesis of nucleic acid constituents, the alkylators, which physically perturb nucleic acids and proteins by covalently linking to the macromolecule, and the intercalators, which bind noncovelently and interfere with nucleic acid replication in a variety of ways (Remers, 1978, Kersten and Kersten, 1974). Often the intercalators are mutagenic and potent inhibitors

of DNA and/or RNA synthesis at the template level. Examples of the various classes of intercalators are shown in Figure I-1. The feature common to all of these drugs is the presence of a planar chromophore which may slip (intercalate) between the bases of the double helix as schematically illustrated in Figure I-2. Several of these drugs, such as the actinomycins and anthracyclines, are further stabilized by the interaction of peptides or sugars with the nucleotides adjacent to the intercalation site. Drugs with two planar chromophores may bisintercalate into polynucleotides and offer potential as antitumor drugs. The most heavily studied of the drugs shown in Figure I-1 is ethidium.

Binding by intercalation induces changes in the physical properties of both the drug and the nucleic acid. These changes are often used to quantitate the drug-nucleic acid interactions and provide evidence for intercalation as the mode of binding. Upon binding by intercalation, the electrons of the drug are perturbed by interaction with the electrons of the bases; this interaction gives rise to changes in the optical properties of the drug (Hopfinger, 1977). In general, the absorbance maximum of the drug is shifted to longer wavelengths and the fluorescence is altered. The fluorescence may increase or decrease, depending on the photochemical details of the complex. Ethidium binding, for example, leads to a 20-fold increase in the fluorescence intensity upon binding (Le Pecq and Paoletti,

Figure I-1. The structure of intercalators.

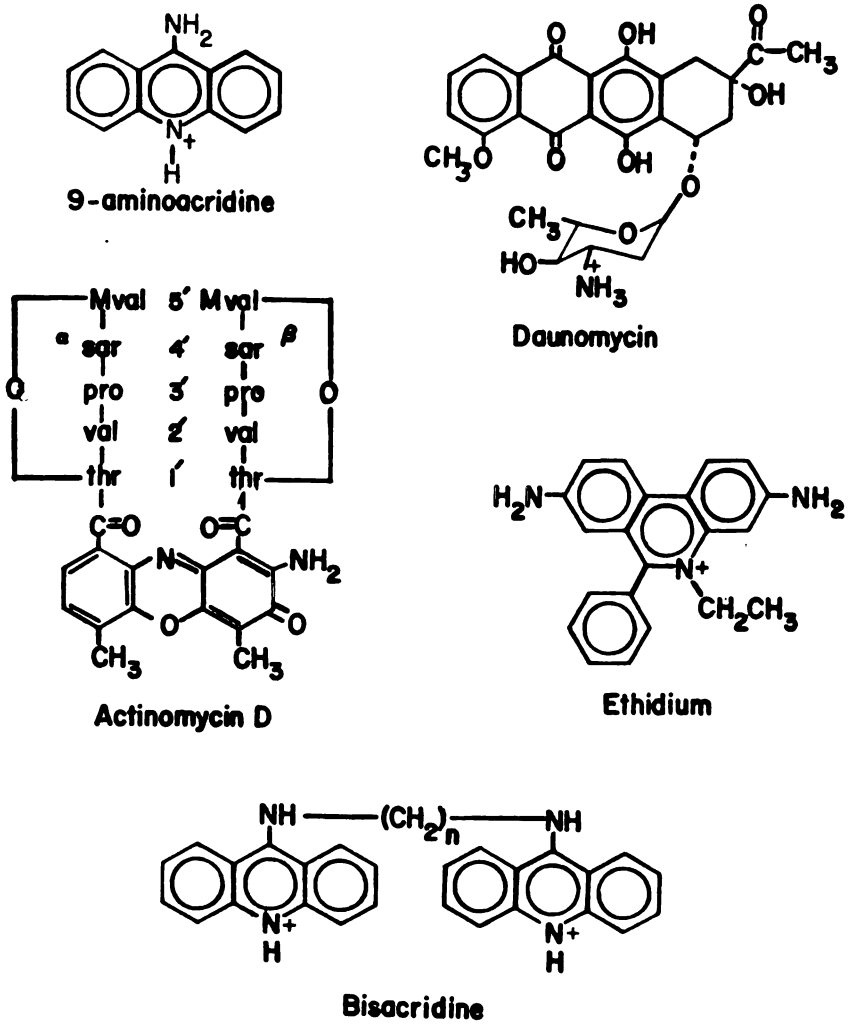

Figure I-2. Diagramatic model for the intercalation of adriamycin into DNA. The open wafers represent the base pairs while the coils are schematic for the sugar-phosphate backbone. The solid wafer represents the plane of the anthracycline ring intercalated between the base pairs. Take from Ruddon and Pratt (1980) as adapted from Waring (1972).

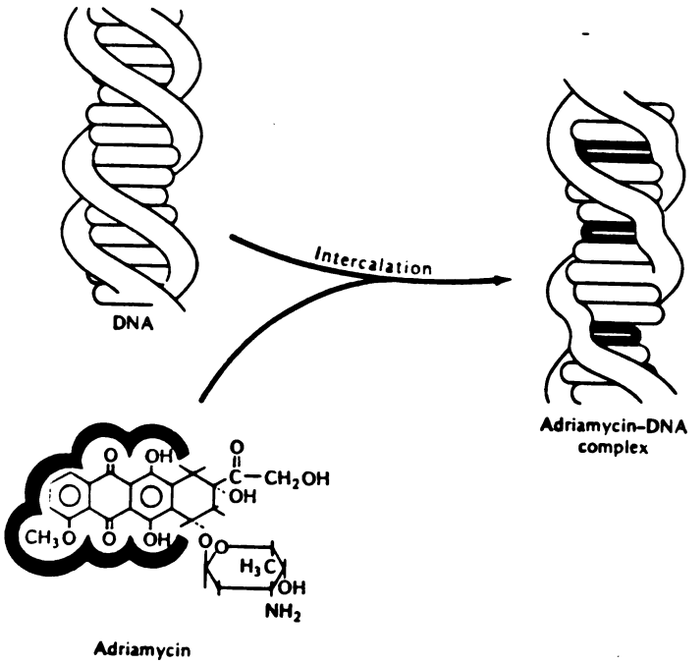

1967) while the fluorescence of 9-aminoacridine may increase or decrease depending on the base sequence at the intercalation site. AT sites enhance the fluorescence while GC sequences quench the fluorescence (Tubbs et al, 1964). Intercalation increases both the fluorescent lifetime of the drug and the anisotropy of the drug's fluorescence (Olmsted and Kearns, 1977, Plumbridge and Brown, 1975). Dynamic information may be obtained from analysis of the decay of fluorescence anisotropy of the bound drug (Genest and Wahl, 1978, Barkley and Zimm, 1979).

In addition to the optical changes of the drug, the optical and hydrodynamic properties of the polynucleotide are altered upon complex formation. Intercalation increases the temperature at which double-stranded nucleic acids cooperatively melt. The increase of the thermal denaturation temperature, Tm, results from a stronger binding (stabilization) of the double vs the single-stranded form of the nucleic acid (McGhee, 1976). Intercalation also unwinds the nucleic acid and thus affects the hydrodynamic properties (Bloomfield et al, 1974, Cantor and Schimmel, 1980). Small pieces of DNA (mw<250,000) behave hydrodynamically like rigid rods so the properties depend on the length of the macromolecule. As the drug intercalates, the helix unwinds and lengthens so changes in the viscosity and sedimentation are observed, as might be expected from Figure I-2. This is more dramatically illustrated in the study of the interac-

tion of drugs with negatively supercoiled DNA as shown in Figure I-3. Drug binding induces positive supercoils (unwinding) and the hydrodynamic volume is increased up to the point where the amount of drug unwinding is equal to the original amount of negative supercoiling (Cantor and Schimmel, 1980). The binding of more drugs induces a net positive supercoiling and the hydrodynamic volume is reduced. Useful information on the geometry of drug binding may be obtained from comparison of the unwinding angle for a given drug to that observed for ethidium (26^{o}) (Wang, 1974). The values range between 8^{o} for chlorquine to 43^{o} for some bisintercalators (Jones et al, 1980, Huang et al, 1981).

Nuclear magnetic resonance, NMR, may also provide information on the formation of drug-nucleic acid complexes. Most of the NMR studies to date have focused on the interaction of intercalators with small nucleotide fragments (Patel, 1974a, 1974b, Krugh and Neely, 1973, Krugh et al, 1977, Chaio and Krugh, 1977, Kastorp et al, 1978, Krugh and Nuss, 1980). By study of the ^{1}H chemical shifts induced upon drug binding it is possible to propose a geometry for the complex. Changes in the internucleotide ^{31}P chemical shift are also observed upon formation of the intercalation complex (Patel, 1974a, Rienhardt and Krugh, 1977, Krugh and Nuss, 1980). The ^{31}P chemical shifts are known to be sensitive to the O-P-O bond angles and torsional angles (Gorrenstien and Kar, 1975 Gorrenstien et al, 1976). It is only

Figure I-3. The effect of daunomycin on the sedimentation coefficient of ΦX174 replicative form DNA. As the amount of intercalated drug increases, the right-handed circles (A) uncoil to form the open circles (B). At higher drug concentrations, left-handed circles are formed (C). Taken from Ruddon and Pratt (1980) as adapted from Waring (1972).

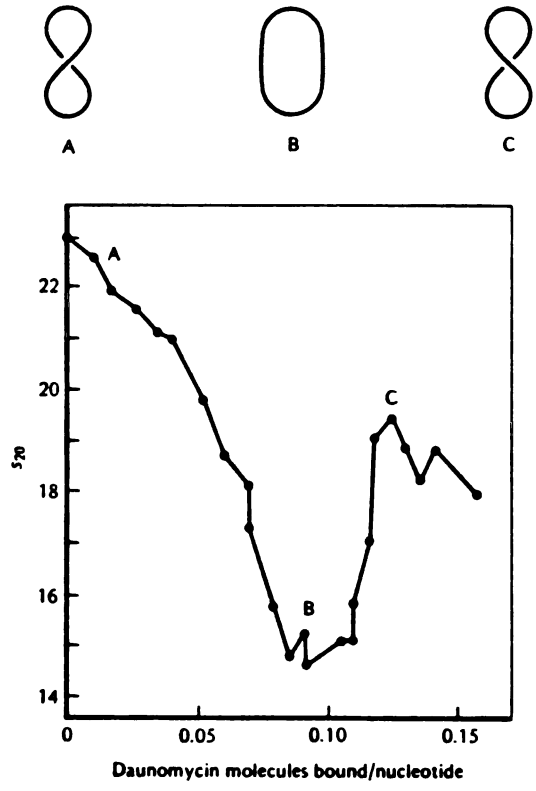

recently that NMR has been used to study the interaction of drugs with high molecular weight DNA. These experiments are complicated by the high concentrations required for the NMR experiments; addition of the cationic drugs causes precipitation of the polyanionic nucleic acids. The experiments which have been published so far are in contrast to one another. The first report demonstrated that ethidium binding effectively immobilizes the base pairs (and phosphates) at the intercalation site such that they are unobservable in the NMR experiment (Hogan and Jardetski, 1980a). A second report saw no hint of this immobilization and presented evidence that the ^{31}P chemical shift change upon intercalation is proportional to the unwinding angle of the drug (Jones and Wilson, 1980).

Although a large body of evidence suggests that DNA is the site of action for the intercalators, the physical effect by which these drug exert their biological action has yet to be demonstrated. One of the purposes of this thesis to explore the relationship between drug binding, the physical perturbations which result from drug binding, and their possible relationship to the inhibition of nucleic acid synthesis.

There are several ways in which the drugs may exert their influence. The acridines, for example, are highly mutagenic and cause transcription errors which result in improperly sequenced proteins (Kersten and Kersten, 1974).

Such mutations are often lethal. As mentioned above, the intercalators are also powerful inhibitors of DNA and RNA polymerase. Sometimes this effect is quite specific; the actinomycins, for example, inhibit RNA synthesis orders of magnitude more efficiently than they inhibit DNA synthesis (Goldberg et al, 1962). It has been proposed that the actinomycins block the progress of RNA polymerase as it translocates down the DNA template. Since actinomycins dissociate slowly from DNA (hundreds of seconds), one actinomycin molecule per thousand base pairs may have a dramatic effect on RNA synthesis. It has also been proposed that the slow actinomycin dissociation kinetics may be due to the nature of the pentapeptide lactone rings (Muller and Crothers, 1968). We have explored this possibility by studying the DNA binding and kinetic properties of actinomycin analogs which have been mono or disubstituted at the 2' and 3' amino acid position. Substitution at the 3' position has a dramatic effect on the DNA binding and kinetic properties. We have also examined the effect that amino acid substitution has on the conformational properties of the analogs. The conformational and hydrogen bonding properties are known to be intimately involved with the DNA binding ability of the actinomycins (Jain and Sobell, 1972, Sobell and Jain, 1972).

Alternatively, it may be proposed that the drugs exhibit their effects from the binding to a very specific gene

(or sequence) or which is crucial for cell growth. Thus, the proposal is that the drugs recognize a very specific sequence or conformational feature of the DNA and tend to bind in this area. Some proteins, such as the lactose operon (Caruthers, 1980) and endonucleases (Abner, 1974) have shown this property. Thus, it is desirable to study the forces involved in drug binding and how they might influence a sequence preference. We have studied this feature of drug-nucleic acid interactions by examining the binding of daunomycin to small DNA fragments as well as native and denatured DNA by ^{31}P NMR and optical spectroscopy. A sequence preference may be due either to an interaction between some base and the π electrons of the drug or some favorable interaction between the drug and some feature of the base, such as the hydrogen bond proposed between the 9 hydroxyl of daunomycin and the exocyclic amino group of guanosine (Quigley et al, 1981). Also, interactions between the drugs or conformational changes of the DNA induced upon drug binding may cause drugs to "cluster" (bind cooperatively) to one area of the lattice (Hogan et al, 1980, Winkle and Krugh, 1981).

It has also been proposed that conformational fluctuations may play a role in protein-nucleic acid interactions. Drugs which affect these fluctuations may thus inhibit the ability of the nucleic acid to bind to the protein. An example of this sort of interaction may be imagined as a

protein whose binding is sensitive to the arrangement of phosphates in the DNA backbone. The protein may bind only when there is a very well defined arrangement of phosphates along the backbone or a certain distance between them. This may not be the equilibrium conformation of DNA but may differ in energy only by a small amount, so that at ambient temperature, a fluctuation in DNA conformation may provide the geometry necessary for the protein binding. If drug binding inhibits the ability of the DNA to obtain this conformation, then drug binding may effectively inhibit the protein-nucleic acid interaction.

NMR is particularly suited for the study of conformational fluctuations; the NMR relaxation is related to molecular motion through the spectral density functions (James, 1975). However, this interaction is normally difficult to study due to the huge NMR signals from the large excess of nucleic acid required to bind up all of the drug. We have avoided this problem by using synthesized intercalators which are labeled with fluorine atoms. In addition to the motional information obtainable from the relaxation parameters, we may also monitor the environment of the drug by the ^{19}F chemical shift. In chapter 4 we show how fluorine NMR may be used to monitor the drug binding sites in the helix-to-coil transitions and the solvent accessibility of the drug. In certain cases, the NMR experiments provide information on the geometry of the complex. Since there is no

NMR signal from the macromolecule or any cellular components, these experiments may be extended to the study of the fate of intercalators in whole cell systems.

CHAPTER 1

HIGH RESOLUTION ^{1}H NMR STUDIES ON THE CONFORMATION AND DYNAMICS OF BIOSYNTHETIC ANALOGS OF ACTINOMYCIN D

INTRODUCTION

The conformation of drug molecules has been a topic of intense interest to pharmaceutical chemistry. It has been proposed that the effects of drugs may be related to their ability to adopt a specific conformation at their site of action. Drugs able to adopt several conformations may exert several effects (Hopfinger, 1977). Conformationally constrained analogs have been used to evaluate the effect of conformation on drug action.

Actinomycin D, Figure 1-1, is one of the intercalating antibiotics mentioned in the introduction which is used for the treatment of cancer in man (Remers, 1978). It is much more useful in the treatment of leukemia than solid tumors. The actinomycin molecule consists of a planar phenoxazone chromophore attached to two pentapeptide lactone rings which are believed to interact with the base pairs adjacent to the intercalation site in the DNA complex. In this chapter we examine the solution conformation and dynamics of actinomycin analogs which have been mono and disubstituted in the amino acid at the 3' position and speculate on the relationship between these properties and the DNA kinetic and equilibrium binding properties.

The conformation of actinomycin has been extensively studied by a variety of physical techniques. NMR and x-ray spectroscopy have been particularly useful tools in probing the conformational features of actinomycins (Jain and

Figure 1-1. The structure of actinomycin D and the amino acid analogs which have been mono and disubstituted into the 3' position of the pentapeptide lactone rings. Numbering of the phenoxazone ring and nomenclature for the benzoid (α) and quinoid (β) peptides is also provided. The abbreviations for the substituted amino acid analogs are azet for azetidine-2-carboxylic acid, pip for pipecolic acid, and oxypro for 4-ketoproline.

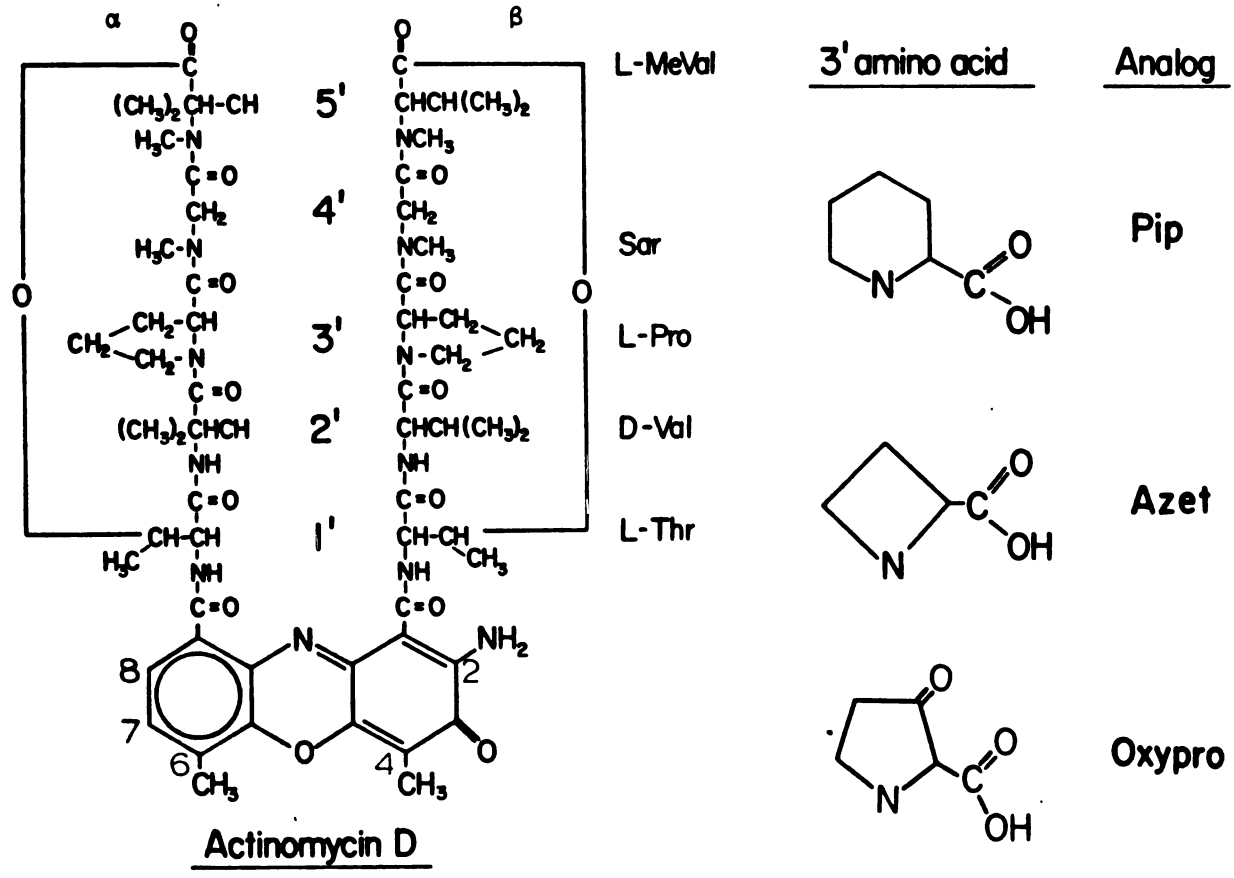

Sobell, 1972, Sobell and Jain, 1972, Lackner, 1977, Arison and Hoogsteen, 1970, Mauger , 1972). The use of high field spectrometers has helped simplify interpretation of the complex NMR spectrum of actinomycin. Conclusions from early experiments are somewhat confused by the large number of overlapping resonances.

Jain and Sobell (1972) published the x-ray structure of the 2:1 complex of deoxyguanosine with actinomycin D. From these data they constructed a model for the binding of actinomycin to a hexanucleotide (Sobell and Jain, 1972). One of the more interesting aspects of this model was the proposed interaction of the pentapeptides with the nucleotides adjacent to the intercalation site. Examination of the "tightness" with which actinomycin fits into the minor groove of the DNA helix suggests that minor structural or conformational perturbations may greatly reduce the favorable interaction between the pentapeptide and the helix. One of the goals of this chapter is to study the relationship between conformations and DNA binding ability.

Besides the steric factors which play an obvious role in DNA-actinomycin interactions, hydrogen bonding is important in the stabilization of the complex and the sequence binding (GC) preference (Wells and Larson, 1970, Muller and Crothers, 1968). Hydrogen bonds have been proposed to exist between the guanine exocyclic amino group and the threonine carbonyl to account for the GC specificity (Jain and Sobell,

1972).

One of the major successes of NMR in the past few years has been elucidation of the solution conformation of a large number of biologically interesting peptides (Bovey et al, 1972). The relationship between conformation and biological activity has been proposed for valinomycin, an ionophore antibiotic, on the basis of NMR studies (Mienhoffer and Atherton, 1977). The NMR parameters which have been most useful in the evaluation of solution conformation are the $J_{\alpha NH}$ coupling constants and the temperature coefficients of the amide protons. The magnitude of the $J_{\alpha NH}$ coupling constant is related to the dihedral angle H $-N-C^{\alpha}-H^{\alpha}$ which is of course related to the conformation about the peptide bond (Karplus, 1959). Although the relationship is empirical, a large number of studies on model compounds have suggested that this approach may be applied with confidence to amino acids (Brystrov et al, 1973). Because of the form of the relationship,

$$J_{\alpha NH} = 8.9\sin^2\vartheta + 0.9\sin^2\vartheta \qquad (1\text{-}1)$$

where θ is the dihedral angle, two possible dihedral angles may give rise to the same coupling constant. Model building studies are often required to differentiate between the two possibilities.

For the amide protons, the electron density (and chemical shift) is determined partly by the extent of hydrogen

bonding that the proton is involved in (Deslauriers and Smith, 1980). Strong hydrogen bonding leads to deshielding of the nucleus. The extent of hydrogen bonding may be probed by monitoring the chemical shift of the amide protons as a function of temperature. In hydrogen bonding solvents, such as DMSO, the possibility exist for the formation of either intermolecular or intramolecular hydrogen bonds. Increasing the temperature tends to preferentially break the intramolecular hydrogen bonds so these resonances are strongly temperature dependent (>0.003 ppm/^{o}C) while the intramolecular bonds are relatively insensitive to temperature. Benzene may also be used as a solvent in the study of hydrogen bonding and solvent exposure (Arison and Hoogsteen, 1972, Venkatachalapathi and Belaram, 1981). Interaction of the amide protons with the cloud of benzene gives rise to the temperature dependent chemical shift. Thus, the temperature coefficients are a measure of both solvent exposure and hydrogen bonding ability. The data in benzene tend to parallel those obtained in DMSO except that the temperature coefficients are about 2.5 times larger. Yet another approach to measure the hydrogen bonding strength and solvent accessibility is to measure the rate of exchange of the amide protons for deuterons from $CDCl_3$ solution.

Since actinomycins contain two N-substituted amino acids in addition to the amino acid in the 3' position, this analysis may only be applied to the study of the conforma-

tion of the 1' (threonine) and 2' (valine) amino acids. In addition, the unusually lowfield position of the H^{α} proton of the 3' amino acid allows us to study the conformation and dynamics of the amino acid which appears to play an important role in the DNA binding kinetics of the analogs.

Figure 1-1 shows the structure of the actinomycin D and the amino acid analogs substituted at the 3' position whose solution conformations are studied in this chapter. Nomenclature for the analogs is presented in Table 1-1. Chapter 2 explores the relationship between amino acid substitution and the DNA binding kinetics and thermodynamics. It is the goal of this chapter to add some insight into the molecular basis for these observations.

METHODS AND MATERIALS

Actinomycin D and deuterated solvents were obtained from Sigma. The actinomycin analogs were isolated and characterized by Dr. J. V. Formica as has been previously described (Formica et al, 1968, Formica and Apple, 1976).

^{1}H NMR experiments were performed on a Bruker HX-360 magnet equipped with a Nicolet Fourier transform accessory at the Stanford Magnetic Resonance Laboratory. The temperature was maintained by blowing cooled nitrogen over the sample. Chemical shifts are reported with respect to tetramethylsilane at zero parts per million (ppm) but were

Table 1-1. Nomenclature for actinomycin analogs.

Actinomycin	2' amino acids	3' amino acids
D	val	pro, pro
AZET II	val	azet, azet
PIP 2	val	pip, pip
C_3	alloisoleu	pro, pro
AZET I	val	azet, pro
PIP 1β	val	pip, pro
V	val	oxypro, pro

val=valine, pro=proline, azet=azetidine, pip=pipecolic acid, alloisoleu=alloisoleucine

referenced to the residual solvent resonances in organic solvents and to an external reference of 2,2-dimethyl-2-silapentane-5-sulfonate (DSS) in $^{2}H_2O$. In most spectra the concentration of actinomycin was about 2 mM. Assignments were made by comparison to published spectra of actinomycin D (Lackner, 1977, Arison and Hoogsteen, 1970, Conti and De Santis, 1972) and its analogs (Mauger, 1972), spin decoupling experiments, and known chemical shifts of the amino acids (James, 1975).

RESULTS

^{1}H Chemical Shifts

The NMR spectra of actinomycins are complex due to the relatively high molecular weight (1254) of the antibiotic and the large number of nearly equivalent methylene and methyn resonances on the two pentapeptide lactone rings. However, several conformational and dynamic features of the actinomycins become apparent with observation of the high field spectra of the drugs.

Figure 1-2 illustrates the complexity of the ^{1}H spectrum of actinomycin D. In this analog, which contains identically substituted pentapeptide lactone rings, it is important to notice that separate resonances are observed for the amino acids on the α and β pentapeptide lactones. Figures 1-3 and 1-4 show the low field portion of the spectra for the analogs and demonstrate that in all the drugs

Figure 1-2. The 360 MHz ^{1}H NMR spectrum of actinomycin D in d_6-benzene at 25°. The spectrum was gathered in 16K data points over a sweepwidth of 5 KHz using a 45° non-selective rf pulse and a 2 second recycle time. An exponential multiplication of 0.5 Hz was applied to the free induction decay prior to Fourier transformation. The concentration of actinomycin was 2 mM.

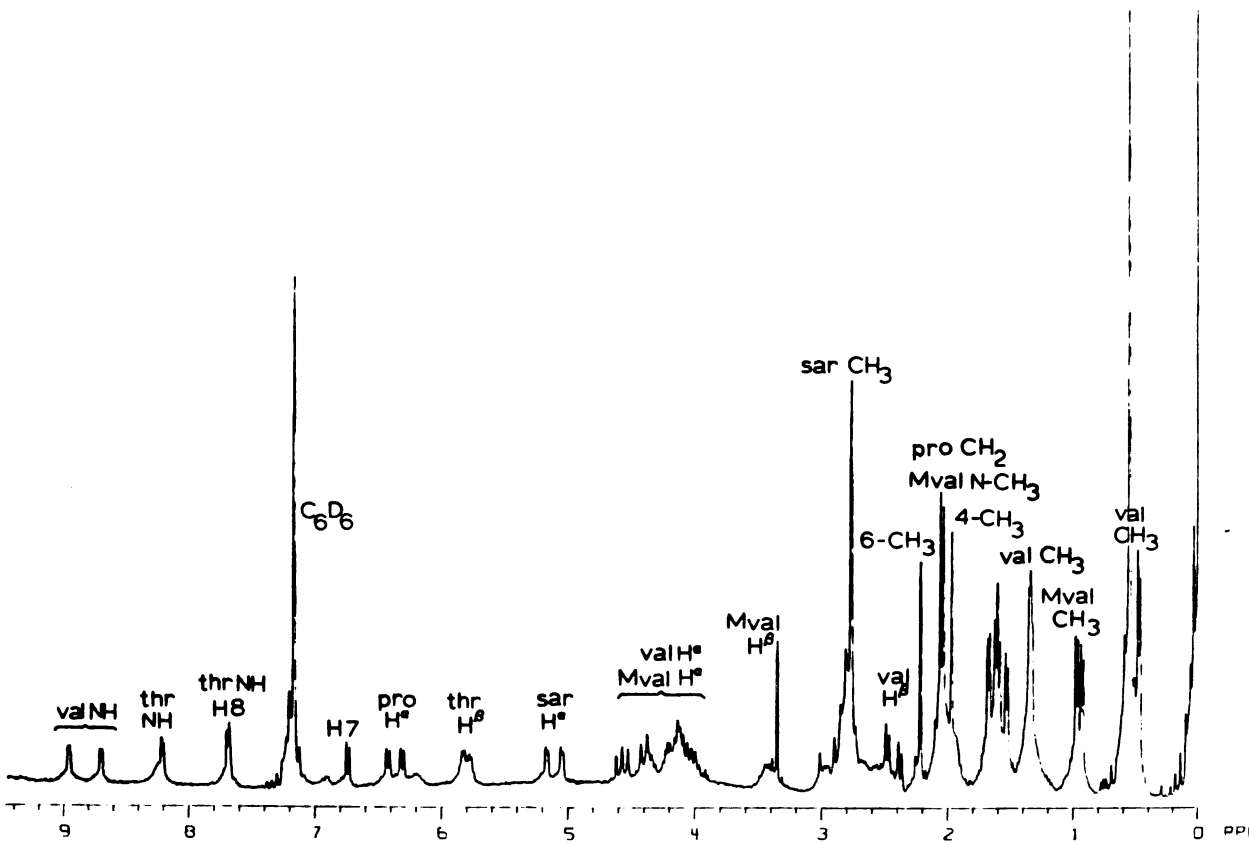

Figure 1-3. The lowfield portion of the 360 MHz NMR spectra of actinomycin analogs with identically substituted pentapeptide lactone rings. The analogs contained two azetidines (AZET II), two prolines (D), or two pipecolic acids (PIP 2) at the 3' position.

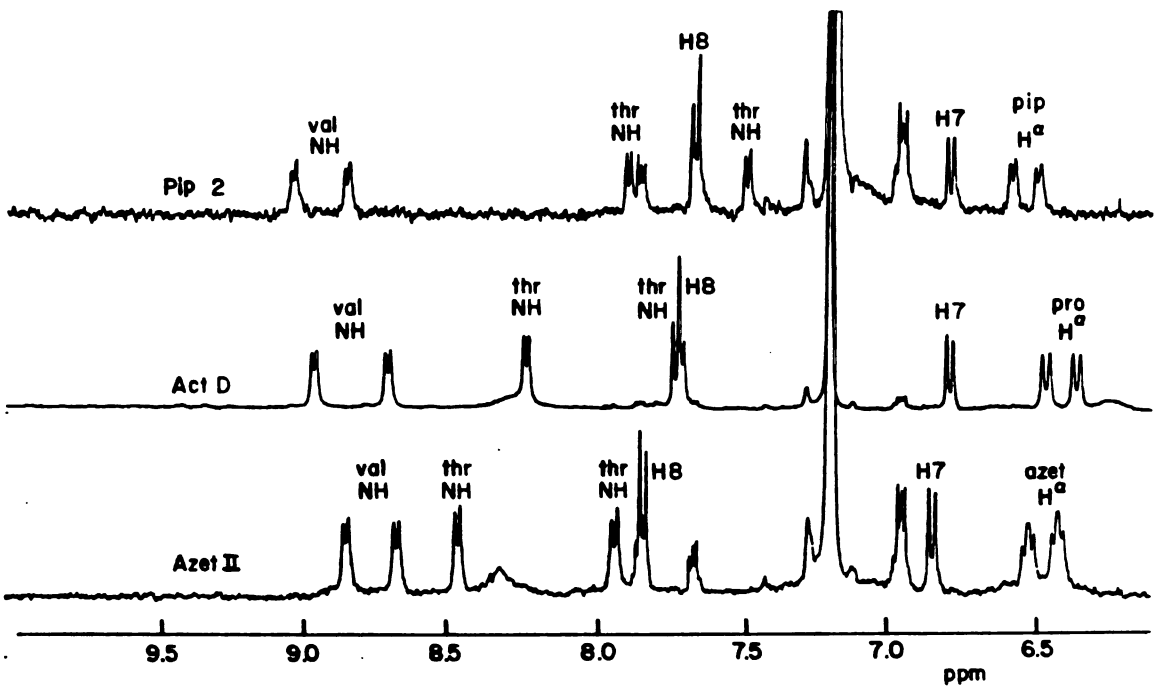

Figure 1-4. The lowfield portion of the 360 MHz ^{1}H NMR spectra of actinomycin analogs in d_6-benzene at 25°. The analogs contained one proline and one azetidine (AZET I), one pipecolic acid (PIP 1β), or one 4-ketoproline (V) at the 3' amino acid position.

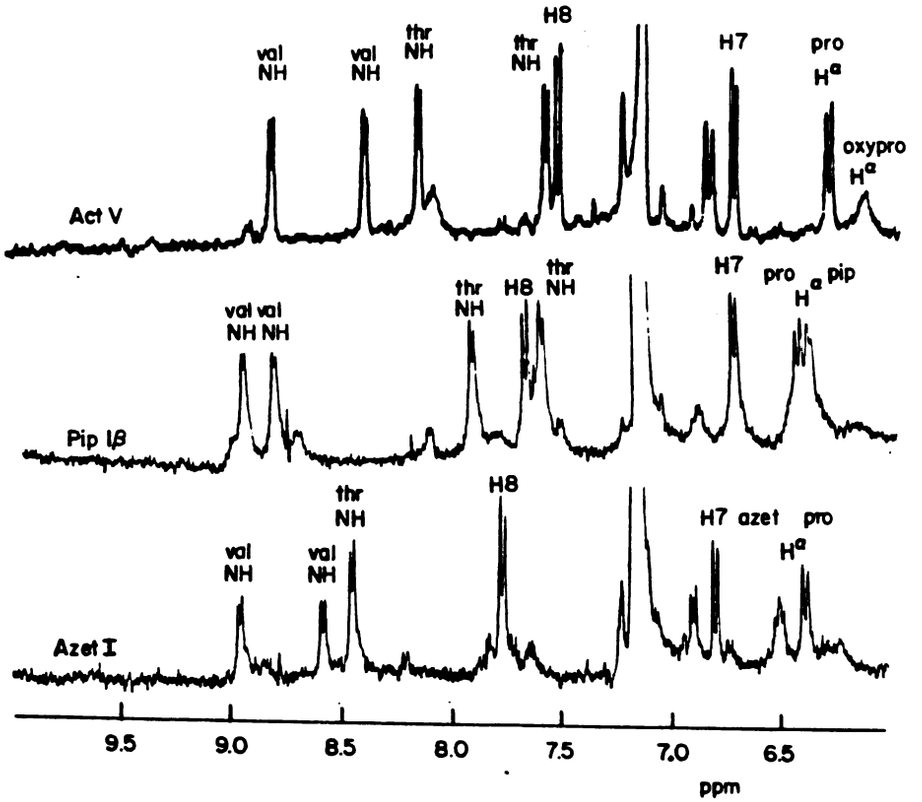

the amino acids experience different magnetic environments. The data indicate that actinomycins are asymmetric molecules; the asymmetry is also present in the amino acid substituted analogs. The source of this asymmetry is most likely attributable to the interaction of the pentapeptide lactone ring with the amino group at the 2 position of the phenoxazone chromophore. Replacement of this amino group affects the NMR spectrum of protons far from the substitution site (Mosher et al, 1977). It is easily imagined how asymmetry in the drug may be related to recognition of the highly asymmetric DNA environment.

Figures 1-3 and 1-4 depict another feature which is common to all actinomycin analogs, the low field position of the H^{α} proton of the 3' amino acid. In all analogs this proton appears between 6.0 and 6.5 ppm; the normal position of these resonances is 4.0 to 4.5 ppm (James, 1975). Lackner (1977) has proposed that the lowfield position of these resonances is due to their proximity to the threonine carbonyl on the same pentapeptide lactone ring. Evidently substitution at the 3' position does not significantly alter the distance between these two portions of the actinomycin molecule. A similar lowfield position for the H^{α}protons was observed in d_6-benzene, d_6-DMSO, $CDCl_3$ and D_2O; this feature is not an artifact of organic solutions but, more probably, a conformational feature resulting from cyclization of the pentapeptide lactones.

Most sensitive to amino acid substitution are the chemical shifts of the valine and threonine amide protons and the H8 proton on the phenoxazone ring. These differences noted in Figures 1-3 and 1-4 are clear indicators that the conformation of actinomycin is sensitive to the nature of the amino acid at the 3' position.

$J_{\alpha NH}$ Coupling Constants and Temperature Dependence of Amide Protons

A great deal of information on the conformation of peptides has been obtained by taking advantage of the relationship between the peptide bond conformation and the magnitude of the $J_{\alpha NH}$ coupling constant. With these data and the temperature dependence of the chemical shifts of the amide protons, it is sometimes possible to determine the solution conformation of molecules.

Table 1-2 lists the $J_{\alpha NH}$ coupling constants for the valine residues of the analogs. The values range between 6.3 and 4.3 Hz in no systematic way and uncertainty in the Karplus relationship is such that these small changes may not be meaningfully interpreted in terms of perturbed backbone angles upon substitution (Brystrov et al, 1973). The threonine amide protons in some of the analogs are obscured by overlap with the H8 resonance and the residual solvent peak. However, in those peaks which are observable, only a small variation in the $J_{\alpha NH}$ coupling constant is observed.

Table 1-2. $J_{\alpha NH}$ coupling constants and temperature coefficients for the valine amide protons in actinomycin analogs.

Analog	$J_{\alpha NH}$ [a] valine1	$\alpha x10^3$ [b] valine1	$J_{\alpha NH}$ [a] valine2	$\alpha x10^3$ [b] valine2
D	5.30	-4.69	5.90	-3.66
AZET II	6.19	-6.55	6.30	-6.02
PIP 2	5.43	-5.06	5.63	-4.22
AZET I	5.04	-5.50	4.32	-4.40
PIP 1β	6.12	-4.90	5.40	-4.10
V	5.76	-4.24	5.73	-4.18

a. In Hz.

b. ppm/^{o}C.

Figure 1-5 shows the effect of temperature on the chemical shift of the valine and threonine amide protons of actinomycin D and azetomycin II. The temperature coefficients for these and all of the other analogs are compiled in Table 1-2. In all cases the valines showed a strong temperature dependence, with the value of the temperature coefficient ranging between -6.19 to -4.33 ppm/^{o}C while the threonine resonances had a temperature coefficient close to zero. From x-ray studies on the 2:1 complex of deoxyguanosine with actinomycin it has been proposed that strong hydrogen bonds exist between the valine carbonyl on one pentapeptide lactone ring and the valine amide proton on the other pentapeptide (Jain and Sobell, 1972). These data are consistent with the observation the the valine protons require several days to exchange with $^{2}H_2O$ from $CDCl_3$ solution (Conti and De Santis, 1970) and that gem diols may interfere with the hydrogen bonding scheme (Asconti et al, 1972). The amino group on the phenoxazone chromophore exchanged within minutes while the threonine protons required several hours to completely exchange. Thus, it was proposed that the valines were involved in strong hydrogen bonds while the threonines were involved in weaker hydrogen bonds. It is worth noting, however, that the exchange rates, like the temperature coefficients, are sensitive to both the strength of hydrogen bonding and solvent accessibility.

Figure 1-5. The effect of temperature on the chemical shift of the valine and threonine amide protons in d_6-benzene for actinomycin D (●) and AZET II (▲).

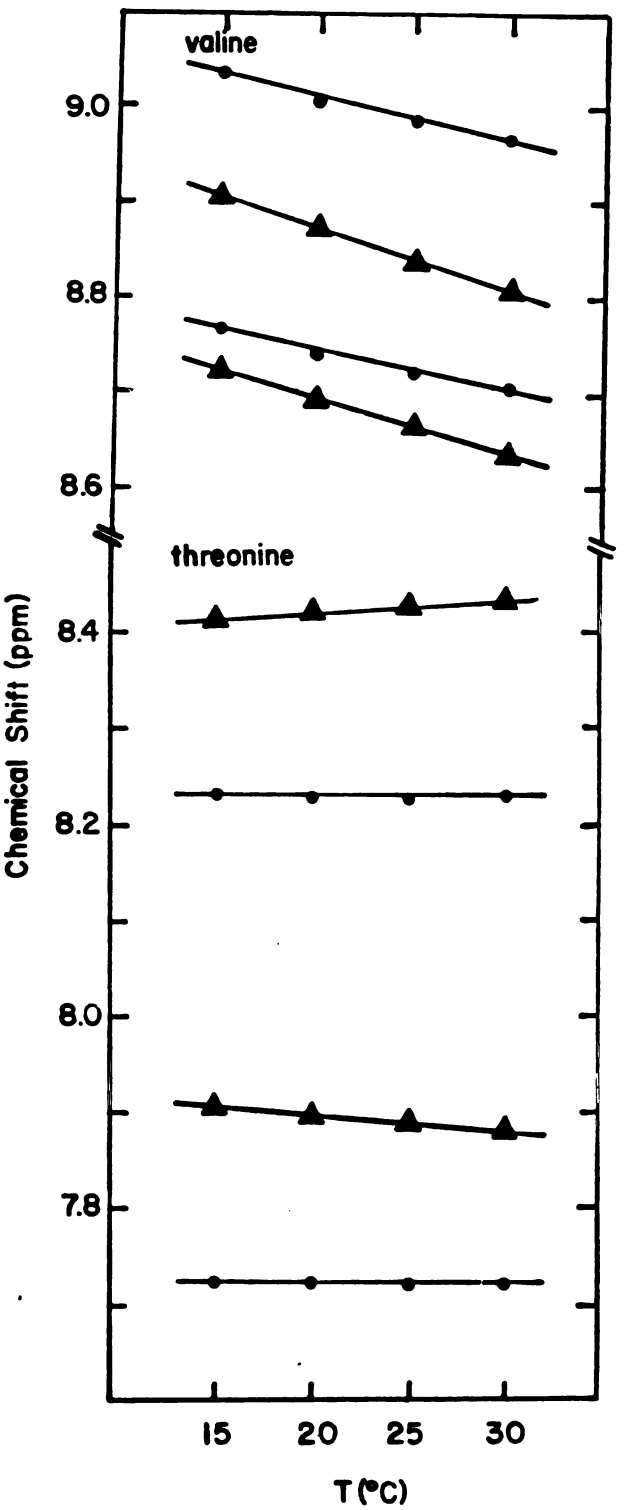

From the data presented in this section it appears that amino acid substitution at the 3' position does not greatly perturb the backbone conformation of the 1' or 2' amino acids, their hydrogen bonding, or their solvent accessibility. These data suggest that the substitutions are only a local perturbation of actinomycin conformation.

Conformation of the 3' Amino Acid

The low field position of the H^{α} proton of the 3' amino acid allows us to make a more detail study of the conformation and dynamics of this amino acid. The energetics of pyrolidine rings have been extensively studied (Ramachandran et al, 1970, Madison, 1977, De Tar and Luthra, 1977a, De Tar and Luthra, 1977b) as has the relationship between the conformation and the value and multiplicity of the $J_{\alpha\beta}$ coupling constant (Pogliani et al, 1975).

It is first worth noting, however, that separate resonances are observed for the amino acids on the and pentapeptide lactone rings. Examination of Figure 1-4 reveals that separate resonances are observed for proline, azetidine, pipecolic acid, and 4-ketoproline. These data indicate that the substitutions have been made predominantly at a unique site on either the α or β pentapeptide. In actinomycins V and PIP 1β the lowfield resonance has been substituted while the opposite is true for AZET I. Analysis of the products resulting from the chemical degradation of

have indicated that 4-ketoproline is substituted for proline on the β peptide in actinomycin V (Brockmann and Manegold, 1958, Brockmann and Manegold, 1960). Assignments for the other analogs remain to be made. It will be seen later (Chapter 2) that the actual site of of substitution plays an important role in the DNA dissociation kinetics and biological activity of the analogs.

Table 1-3 lists the chemical shift and $J_{\alpha\beta}$ coupling constants of the 3' amino acids. It is apparent from Table 1-2 and Figures 1-3 and 1-4 that the amino acids have the same conformation in all analogs. The conformation of proline is the same ($J_{\alpha\beta}$ =9.3 Hz) in actinomycin D, AZET I, PIP 1_β , and actinomycin V. A similar situation is observed for the azetidine substituted analogs ($J_{\alpha\beta}$ =5.8 Hz) and the pipecolic acid substituted analogs ($J_{\alpha\beta}$ =6.4 Hz). The H^α proton of actinomycin V appears as a singlet due to the lack of αβ coupling.

Figure 1-6 shows the Newman drawing along the C^α-C^β bond and demonstrates the the two pyrolidine ring conformers which have been observed by NMR (Pogliani, 1975) and x-ray crystalography (De Tar and Luthra, 1977a) and predicted by quantum mechanical calculations (Ramachandran et al, 1970). The two conformers differ in equilibrium energy by about 1 kcal/mole (Ramachandran et al, 1970) and may be distinguished by the value of the dihedral angle χ_1 made by the atoms N-C^α-C^β-C^γ. The "A" conformation has $\chi_1 > 0$ and

Table 1-3. Chemical shifts and $J_{\alpha\beta}$ coupling constants for 3' amino acids of actinomycin analogs.

Actinomycin	amino acid δ (ppm)	$J_{\alpha\beta}$	amino acid δ (ppm)	$J_{\alpha\beta}$
D	pro 6.42	9.3 (d)	pro 6.29	9.3 (d)
AZET I	pro 6.38	9.31 (d)	azet 6.49	5.84 (t)
AZET II	azet 6.46	5.84 (t)	azet 6.36	5.84 (t)
PIP 2	pip 6.52	6.4 (d)	pip 6.43	6.4 (d)
Pip 1β	pro 6.44	9.3 (d)	pip 6.38	6.4 (d)
V	pro 6.31	9.01 (d)	oxypro 6.12	- (s)

s=singlet, d=doublet, t=triplet

Figure 1-6. Newman projections alone the $C^{\alpha}-C^{\beta}$ bond of the pyrolidine ring. The angle is defined by the atoms N-C -C -C .

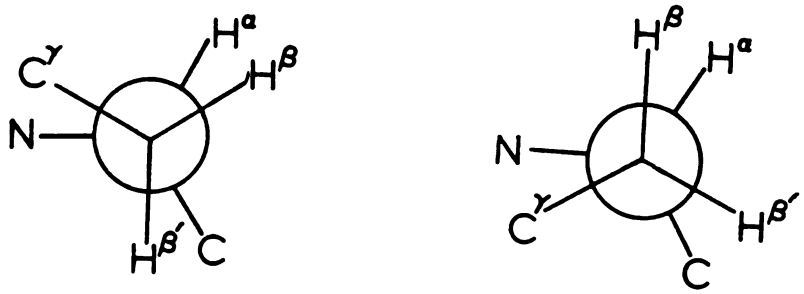

"A"
$\chi_1 = 30°$

"B"
$\chi_1 = -30°$

the "B" conformation has $\chi_1 < 0$. In x-ray crystal structures, this angle usually has a value close to plus or minus 30^{o} (De Tar and Luthra, 1977a).

The conformers may also be distinguished by the magnitude and multiplicity of the $J_{\alpha\beta}$ coupling constants as expected from Figure 1-6. The "A" conformer is expected to give rise to a triplet from $J_{\alpha\beta}$ =9 Hz ($H^{\alpha}-C^{\alpha}-C^{\beta}-H^{\beta}=30^{o}$) and $J_{\alpha\beta}$ =9 Hz ($H^{\alpha}-C^{\alpha}-C^{\beta}-H^{\beta}$=150) while the "B" conformer is expected to give rise to a psuedo-doublet from $J_{\alpha\beta}$=9Hz ($H^{\alpha}-C^{\alpha}-C^{\beta}-H^{\beta}$ =30^{o}) and $J_{\alpha\beta}$=0 Hz ($H^{\alpha}-C^{\alpha}-C^{\beta}-H^{\beta}=90^{o}$). A similar analysis may be applied to azetidine conformation (Meraldi et al, 1978).

Figures 1-3, 1-4, and Table 1-2 indicate that proline prefers the the "B" conformation while the "A" conformation is preferred by the azetidine analogs. These data are in contrast to quantum mechanical calculations which predict a 2-4 kcal/mole barrier between the two conformations (Madison, 1977). Rapid ring puckering has been demonstrated by analysis of the ^{13}C NMR relaxation of proline and proline containing peptides (London, 1978, Deslauriers et al, 1974, Deslauriers and Smith, 1977). The time scale for pyrolidine ring puckering was similar to that predicted by the theory. However, it has been noted that proline incorporated into peptides, particularly cyclic peptides, show reduced rates of ring puckering (Deslauriers et al, 1974). In actinomycin, we are observing a very strong preference for one of

the two pyrolidine conformers.

We have also studied the effect of solvent on the conformation and dynamics of the 3' amino acid (proline) in actinomycin D. Figure 1-7 shows the lowfield portion the the spectra of actinomycin D in ^2H_2O as a function of temperature. The phenoxazone rings of actinomycin in aqueous solution tend to stack; hence the H7 and H8 protons appear as a broad singlet at 7.4 ppm (Arison and Hoogsteen, 1970). The proline protons show considerable variation over the temperature range of 5-25°. At 5° the high field proton appears as a sharp doublet with a coupling constant similar to that observed in organic solution ($J_{\alpha\beta}$=9.3 Hz) while the lowfield proline appears as an unresolved multiplet. Increasing of the temperature leads to a broadening of the lowfield resonance followed by a sharpening and a superpositioning with the high field resonance at 20°. Our interpretation of these results is that there is a motion in the low field proline which is slow (k30 sec^{-1}) on the NMR time scale while the other proline remains in its preferred conformation. These data suggest the possibility that the dynamics of the amino acids on the α and the β pentapeptide lactones may differ and thus exert different effects on the dynamics of the DNA interaction.

Figure 1-7. The effect on temperature on the lowfield portion of the 360 MHz NMR spectra of actinomycin in $^{2}H_{2}O$.

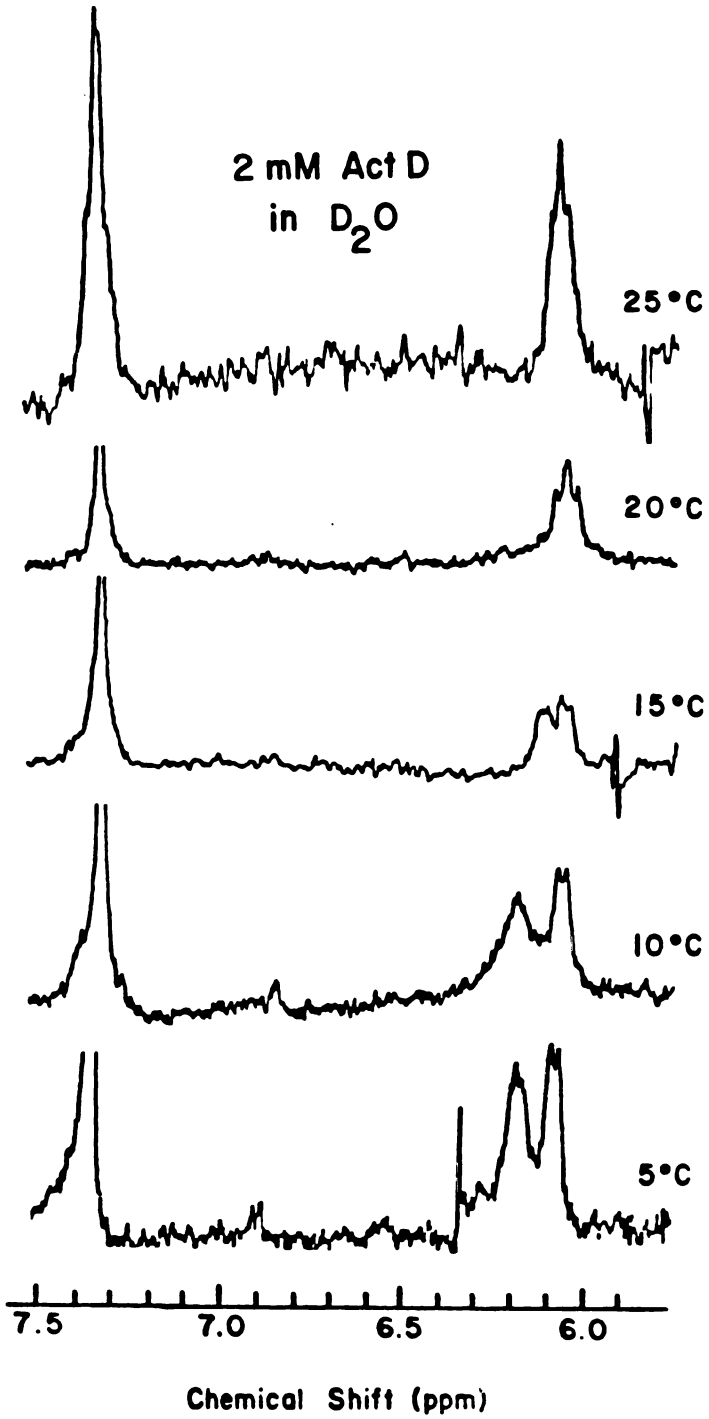

DISCUSSION

The high field NMR spectrometer allows us to make a detailed study of actinomycin conformation and the effects of amino acid substitution on the conformational features. From the spectra in this chapter it is obvious that the substitutions have an effect on the conformation of actinomycins. This is reflected in the chemical shift differences among the analogs. However, examination of the $J_{\alpha NH}$ coupling and the temperature coefficients for the valine and threonine amide protons suggests that substitution at the 3' position has little effect on the backbone conformation of the amino acids at the 1' or 2' position. This suggests that the substitutions are only a local perturbation of actinomycin conformation. The analogs also maintain the hydrogen bonding network and solvent exposure of the parent compound. The other features which appear unaltered by substitution are the general asymmetry of the molecule and the proximity of the threonine carbonyl to the H^{α} proton of the 3' amino acid. Since formation of the intercalation complex requires intimate contact between the base pairs adjacent to the intercalation site and the pentapeptide through the formation of hydrogen bonds and Van der Waal's contacts, the conformation of actinomycin must play an important role in the DNA binding. Minor perturbations in actinomycin structure, such as the substitution of hydroyproline for proline, inhibit the DNA binding ability of the drug, presumably due

to a steric interaction between the hydroxyl group on the proline and the base pair adjacent to the intercalation site (Reich et al, 1962). The GC sequence specificity observed for actinomycins is thought to be due both to the favorable electronic interaction between the phenoxazone chromophore and guanine (Muller and Crothers, 1968) and the formation of hydrogen bonds between the 2-amino of guanine and the threonine carbonyl (Sobell and Jain, 1972). The NMR data presented here suggest that the analogs may adopt similar conformations and have similar hydrogen bonding schemes. Thus, it might be expected that all of the analogs may bind DNA. Chapter 2 confirms this speculation.

Somewhat fortuitously, we may study the conformation and dynamics of the 3' amino acid. Analysis of the rather simple $J_{\alpha\beta}$ coupling pattern reveals that only one of the two possible conformers of the 3' amino acid is observed in the analogs. Normally the barrier for interconversion of the two conformers is low, and rapid flipping between the "A" and "B" conformer is expected (Ramachandran et al, 1970). Similar, though less severe, motional constraints have been observed for other proline containing peptides (Deslauriers et al, 1974). ^{13}C spin-lattice relaxation time measurements for the proline carbons in cyclic peptides show a reduced rate of puckering compared to proline free in solution (Deslauriers and Smith, 1977). The constraint is much stronger for the prolines in actinomycins, suggesting that

actinomycin is a relatively inflexible molecule. It is interesting to note that in the crystal structure of the 2:1 complex of deoxyguanosine with actinomycin D the prolines on the α and the β pentapeptides have different puckers; the proline is in the "A" conformation and the proline is in the "B" conformation (Jain and Sobell, 1972).

The spectra of actinomycin D in ^2H_2O show a difference in the dynamics of the prolines on the α and β pentapeptides. However, from this data it is not possible to determine if the difference is just in the proline conformation or a conformational fluctuation in one of the pentapeptides. These data suggest that actinomycin retains at least part of its inflexibility in aqueous solution. Thus, it is not unreasonable to postulate that the slow DNA binding kinetics of the actinomycins may be related to a conformational fluctuation within the peptide which has a high (20 kcal/mole) energy of activation. The dynamics of the lowfield proline are much faster that the kinetics of DNA binding; most likely it is the proline that remains in the preferred conformation which is most important in the DNA binding kinetics.

The observation of a difference in the dynamics of the pentapeptides and the observation that the amino acid substitutions are made at a unique site on the pentapeptide allow us to speculate on a possibly different role for the and the peptides in the kinetics. The data presented in

chapter 2 will strongly indicate that the 3' amino acid plays an important role in the DNA dissociation rate constants and the thermodynamics of dissociation. Dissociation of the disubstituted analogs appears related to the size of the ring in the 3' amino acid. The smaller this ring, the more slowly the analog dissociates. Analysis of the monosubstituted analogs is more complex, and does not follow this simple pattern. Actinomycin V dissociates an order of magnitude more slowly than the parent compound while monosubstitution with azetidine or pipecolic acid has little effect on the dissociation rate. The data presented here suggest the possibility that the dynamics of the pentapeptides may differ from each other. Thus we may postulate that one of the pentapeptides plays a dominant role in dissociation of the drug. The dissociation data for the monosubstituted analogs may then be explained by proposing that in the azetidine and pipecolic acid substituted analogs the amino acid substitution has been made on the pentapeptide lactone ring which is least important in the dissociation process, while the opposite is true for actinomycin V. The substitution of 4-ketoproline for proline has been made on the pentapeptide which is most important in the dissociation process.

In summary, we have used ^{1}H NMR to study the conformation and dynamics of actinomycin analogs and have used these data to provide some insight into the molecular basis for

DNA binding. Both the conformational and dynamic features appear to be important in DNA-actinomycin interactions.

CHAPTER 2

KINETIC AND EQUILIBRIUM BINDING PROPERTIES OF ACTINOMYCIN ANALOGS

INTRODUCTION

The DNA binding properties of actinomycins have been extensively studied over the past two decades both as an antitumor antibiotic and as a model for protein-nucleic acid interactions (Remers, 1978, Mauger, 1980, Mienhofer and Atherton, 1977). The binding and kinetic properties of actinomycins are more complex than those observed for other intercalators and various investigators have searched for a correlation between the physical properties of drug and its mode of action.

Prior to 1968 it was widely believed that actinomycin binding did not involve intercalation, but rather the drug bound to the outside of the helix and was stabilized by hydrogen bonds (Hamilton et al, 1963). In an extensive study of the equilibrium, kinetic, and hydrodynamic properties of actinomycin binding, it was concluded that the most consistent interpretation of the spectroscopic data was that the drug bound by intercalation (Muller and Crothers, 1968). The authors observed absorbance changes similar to those which accompany the binding of other intercalators and an increase in the viscosity of DNA solutions upon addition of the drug. These and previous authors have noted a specificity in actinomycin binding (Goldberg et al, 1962, Cerami et al, 1967, Wells and Larson, 1970, Gellert et al, 1970, Krugh, 1972). Actinomycin binds only to double-stranded

DNA; not denatured DNA, RNA, or DNA-RNA hybreds. In addition, actinomycin showed a preference for guanine at the intercalation site. Removal of the guanine exocyclic amino group resulted in a loss of binding affinity (Cerami et al, 1967, Wells and Larson, 1970). The specificity is thought to be due both to a favorable electronic interaction between the phenoxazone chromophore and guanine (Muller and Crothers, 1968) and hydrogen bonds between the guanine exocyclic amino group and the threonine carbonyl on the pentapeptide lactone rings (Jain and Sobell, 1972).

The complex of actinomycin D with deoxyguanosine (1:2) has been studied by x-ray diffraction (Jain and Sobell, 1972) and a model for actinomycin binding to a hexanucleotide has been proposed (Sobell and Jain, 1972). This model details some of the conformational features, Van der Waal's contacts, and hydrogen bonds in the actinomycin-DNA complex. Some of these proposals have been confirmed by NMR studies on the complex of actinomycin with nucleotides (Patel, 1974a, 1974b, 1976, Krugh et al, 1977, Krugh and Neely, 1973a, 1973b).

Another interesting aspect of the DNA binding of actinomycins is the relatively slow kinetics. Muller and Crothers (1968) observed that the DNA dissociation was orders of magnitude slower than that observed for ethidium (Bresloff and Crothers, 1975), proflavin (Li and Crothers, 1969), and daunomycin (Gabbay et al, 1976). The authors

suggested that the slow kinetics were due to a conformational transition within the pentapeptides. They proposed a complex scheme to account for the five rate processes observed in the association and three rate processes observed in the dissociation. However, more recently it has been shown that the dissociation of actinomycin from poly(dG-dC)poly(dG-dC) is characterized by a single rate process (Krugh et al, 1979). Furthermore, it was demonstrated that the amplitude that each rate process contributed to dissociation from calf thymus DNA was dependent upon the ratio of P/D. These data are consistent with the hypothesis that dissociation from DNA is characterized by a single exponential process; the multiexponential dissociation from DNA may arise from different dissociation rates from alternate binding sites on the helix. The various sites may have different binding properties and thus the populations will be sensitive the the ratio of P/D. One possibility is that the alternate binding sites are intercalation sites of different base sequence (Krugh and Nuss, 1980). The time constant for actinomycin dissociation from poly(dG-dC)poly(dG-dC) was similar to the slowest rate observed in DNA dissociation, suggesting that the most slowly dissociating DNA binding site has the GC sequence. Somewhat anomalously, the time constant for actinomycin dissociation from poly(dG-dC)poly(dG-dC) was dependent upon the ratio of P/D; this is not observed in DNA binding (Krugh et al, 1979).

It has also been proposed that the slow kinetics may be due to a property of the double helix rather than the drug (Sobell, 1974). However, since none of the simple intercalators, such as ethidium, proflavin, etc., show the slow kinetics, it is most likely that the peptides dominate the slow binding kinetics. The hypothesis that the peptides are responsible for the slow kinetics is consistent with the observation that the association kinetics of actinomycin binding to linear DNA are the same as those observed for binding to supercoiled DNA (Bittman and Blau, 1976). Also, it has been observed that the binding kinetics of actinomine (the phenoxazone chromophore with out the peptides) are very fast (Muller and Crothers, 1968).

Actinomycins are toxic to cells in very low concentrations (Remers, 1978, Meinhoffer and Atherton, 1977). Several lines of experimental evidence have suggested that the biological activity is related to the ability of the drugs to bind DNA. However, this hypothesis is still open to question. It has been suggested, for example, the the cytotoxic effects may be related to the ability of actinomycins to interact with cell membranes (Fico et al, 1977). The DNA binding hypothesis has been reinforced by chromosomal staining experiments which show actinomycins localized in the genetic material (Zelenin et al, 1976) and studies on the effect of actinomycin on DNA and RNA synthesis (Goldberg et al, 1962, Hyman and Davidson, 1970, Waring, 1965).

Actinomycin D has been shown to be a potent inhibitor of DNA dependent RNA polymerase (Waring, 1965). As much as 20% inhibition of RNA synthesis has been observed with one actinomycin bound per thousand base pairs. Much higher concentrations are required for inhibition of DNA synthesis (Goldberg et al, 1962). In fact, inhibition of DNA synthesis is observed only at levels of actinomycin high enough to elevate the temperature of the helix-to-coil transition of the complex. It has been proposed that the potent inhibition of RNA synthesis by actinomycin is due to the slow dissociation of the drug (Muller and Crothers, 1968). This hypothesis maintains that the polymerase translocates along the template until it encounters a bound drug. Progress of the enzyme is inhibited until the drug dissociates. A mathematical description of the process predicts that plots of the inverse fraction of control activity v.s. r (the average number of drugs bound per nucleotide) should be linear and the slope of the line should be related to the dissociation time constant. Similarly, inhibition should be related to the dissociation time constant at constant value of r for analogs with different dissociation rates. This comparison has only been made for daunomycin analogs (Gabbay et al, 1976) where a qualitative agreement with this theory was observed.

In this chapter we examine the equilibrium and kinetic DNA binding properties of actinomycin analogs which have

been mono and disubstituted in the amino acid at the 2' and 3' position in the pentapeptide lactone rings. Structure and nomenclature for the analogs are provided in Figure 1-1 and Table 1-1. We evaluate the effect of substitution on the DNA binding constant, the number of binding sites, the thermal denaturation temperature of the actinomycin-DNA complexes, the dissociation rate constants, and the thermodynamics of dissociation. We may combine these results with those obtained in Chapter 1 to speculate on the relationship between the physical properties of the drug and the biological activity.

METHODS AND MATERIALS

Calf thymus DNA was purchased from Sigma, as was actinomycin D. Actinomycins C_3, V, AZET I, AZET II, PIP 2, and PIP 1β were the generous gift of Dr. M.A. Apple and Dr. J.V. Formica. The analogs were isolated and characterized by Dr. Formica as previously described (Formica et al, 1968, Formica and Apple, 1976). Sodium laurel (dodecyl) sulfate (SDS) was obtained from Calbiochem. Binding and kinetic experiments were performed in BPES buffer, which contained 0.08 M Na_2HPO_4, 0.02 M NaH_2PO_4, 0.18 M NaCl, and 0.01 M Na_2EDTA at pH 7.0. For thermal denaturation experiments the buffer was diluted 1:100. Concentrations were determined spectrophotometrically using the extinction coefficients of 6600 per nucleotide at 260 nm for DNA and 24,500 for actinomycin at 440 nm. All actinomycin analogs were assumed

to have the same extinction coefficient.

The actinomycin-DNA dissociation kinetics were measured as described by Muller and Crothers (1968). Actinomycin-DNA complexes were allowed to equilibrate until the association was complete (30-120 min.) at the desired temperature. SDS was added to a final concentration of 3%, the solutions were gently mixed by inversion, and the absorbance at 440 nm was monitored as a function of time. Typically, the mixing consumed the first 30-40 seconds of the reaction. It has been determined that SDS irreversibly dissociates drug-nucleic acid complexes (Muller and Crothers, 1968). The experiments were performed at P/D>20 in all experiments. P/D ratios of about 60 were used in the later experiments to increase the amplitude of the slowest dissociation step. The P/D ratio had no effect on the DNA dissociation time constants. The temperature of the sample was maintained by coils of circulating water wrapped around the 10 cm absorbance cells.

Thermal denaturation of the actinomycin-DNA complexes was performed at a P/D ratio of 20 and the absorbance at 260 nm was monitored as a function temperature. Experiments were performed on a Beckman Acta CIII equipped with a multisample accessory in water-jacketed 1 cm cells. The temperature was measured by insertion of a temperature probe into the reference sample. The data are normalized as the fractional increase in absorbance as a function of temperature and are not corrected for thermal expansion.

DNA binding constant were measured by titrating a concentrated DNA solution into a solution of actinomycin in the 10 cm absorbance cells. The extinction coefficient of the fully bound actinomycin was measured in a large excess of DNA and the concentration free and bound was calculated from the absorbance.

Analysis of Data

Scatchard plots were constructed by monitoring the absorbance of the drug as a function of DNA concentration at 440 nm. The concentration of free drug is given by

$$C_f = \frac{A_{440} - \varepsilon_b C_o}{\varepsilon_f - \varepsilon_b} \qquad (2\text{-}1)$$

where C_f is the concentration of free drug, C_o is the total drug concentration, and ε_f and ε_b are the extinction coefficients for the free and the bound drug, respectively. The average number of drugs bound per site, r, is

$$r = \frac{C_b}{(DNA)} \qquad (2\text{-}2)$$

where where C_b is the concentration of bound drug and (DNA) is the total DNA concentration in base pairs. The data were plotted as r/C_f v.s. r. The binding constants were obtained from a fit of the Scatchard plot described in equation 2-3,

$$\frac{r}{C_f} = K(1-nr)\left\{\frac{1-nr}{1-(n-1)r}\right\}^{n-1} \qquad (2\text{-}3)$$

where K is the binding constant, and n the number of sites

occluded by the binding of the drug (McGhee and von Hippel, 1974).

The dissociation data were analyzed by digitizing the absorbance traces into the Prophet system for multivariate regression analysis. The Prophet system is a national computer resource developed by the Chemical/Biological Information Handling Program of the Division of Research Resources, National Institutes of Health. Curves were fit to two exponentials, as shown in equation 2-4, using the Marquardt-Levenberg algorhythm.

$$\ln(A(t)-A(f))=B_1e^{-k_1t}+B_2e^{-k_2t}+const. \qquad (2\text{-}4)$$

In this equation A(t) is the absorbance at 440 nm at time t, A( ) is the absorbance at infinite time, k_1 and k_2 are the rate constants for the dissociation processes, and B_1 and B_2 are the amplitudes contributed to the total dissociation by the various processes. Results are reported in terms of the characteristic dissociation time τ_i, which is the inverse of the rate constant k_i.

Arrhenius plots of the data were constructed using the equation

$$\ln(\frac{k}{T})=\frac{\Delta H^{\ddagger}}{RT}+ln(\frac{k_B}{h})+\frac{\Delta S^{\ddagger}}{R} \qquad (2\text{-}5)$$

where $\Delta H^{\ddagger}$ in the enthalpy of activation, $\Delta S^{\ddagger}$ is the entropy of activation, k_B is Boltzman's constant, and h is Plank's constant. Values for the entropy and enthalpy of activation

were obtained from a least-squares fit of the data. The reported uncertainties are the standard errors in the slope and intercept which are defined in the usual manner.

RESULTS

DNA Binding Properties of Actinomycins

It has long been known that actinomycins bind strongly to DNA (Reich et al, 1962, Muller and Crothers, 1968, Wells and Larson, 1970). In this section we examine the effect of substitution at the 2' and 3' position on the DNA binding properties of the actinomycins and the helix-to-coil transition of the actinomycin-DNA complexes. Figure 2-1 and 2-2 shows the effects of the di and monosubstituted analogs on the melting transitions of calf thymus DNA (Shafer et al, 1980). The induced Tm for all of the analogs are compiled in Table 2-1. It may be easily demonstrated that the induced Tm is a measure of the affinity of the drug for the helix vs the coil form of DNA (McGhee, 1976). Drugs which bind more strongly to the helix increase the Tm while those which bind more strongly to the coil form are helix destabilizing. For drugs with the same number of binding sites, the induced Tm may be regarded as a measure of the binding affinity of the drug for the double helix.

Table 2-1 shows that a whole range of helix stabilizations are induced by the binding of the analogs. Most notably the substitution of pipecolic acid for proline reduced

Figure 2-1. The effect of disubstituted actinomycin analogs on the thermal denatureation temperature of calf thymus DNA. The data are plotted as F, the fraction single-stranded v.s. temperature for DNA free (○) and in the presence of PIP 2 (●), actinomycin D (△), AZET II (▲), and C_3 (□) at a P/D ratio of 10. The concentration of DNA was $7x10^{-5}$ M and the experiments were performed in BPES buffer diluted 1:100. Replotted from Shafer et al (1980).

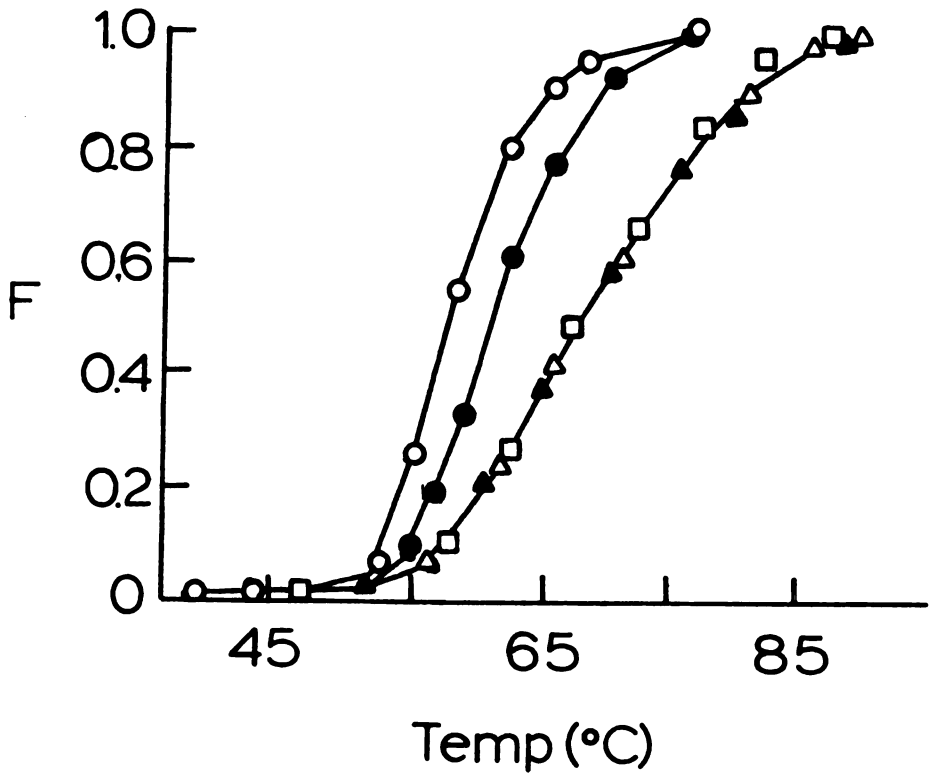

Figure 2-2. The effect of monosubstituted actinomycin analogs on the thermal denatureation of calf thymus DNA. The data are plotted as in Figure 2-2 for DNA free (○) and in the presence of AZET I (△), , PIP 1^{β} (●), and V (▲) at a P/D ratio of 10.

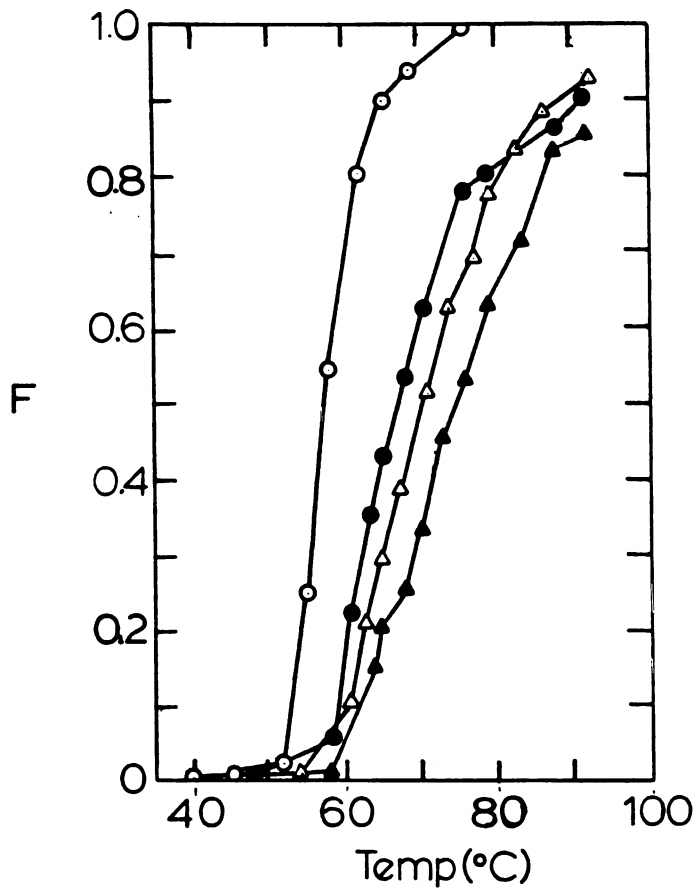

Table 2-1. Induced thermal denaturation temperature, binding constant, and number of binding sites for actinomycin analogs binding to DNA.

Actinomycin	ΔT_m (°C)	K $\times 10^{-6} M^{-1}$	n
D	10.6[a]	3.2	9.8
AZET II	10.6[a]	2.2	8.6
PIP 2	3.3[a]	0.3	10.8
AZET I	12.9	3.3	9.1
PIP 1β	9.4	0.6	9.9
V	17.4	30	9.9
C_3	10.6	3.1	9.8

a. From Shafer et al, 1980.

the induced Tm, with disubstitution being the greater perturbation. It is interesting to note that monosubstitution of azetidine has a greater effect than disubstitution. Substitution of alloisoleucine for valine at the 2' position (C_3) has no effect and the greatest perturbation is noted for 4-ketoproline substitution.

The DNA binding affinities of the analogs have also been measured by monitoring the absorbance of the drug at 440 nm as a function of DNA concentration. The binding constants reported in Table 2-1 were fit in the manner of McGhee and von Hippel (1974), which statistically accounts for "gaps" in the drug-saturated lattice which are smaller than the drug binding site. Figure 2-3 shows typical binding isotherms for the analogs. The conclusions reached from this analysis are similar to those reached from the Tm analysis. Pipecolic acid decreases the binding constant, 4-ketoproline greatly increases the binding constant, and the other substitutions have little effect. It should be noted, however, that construction of the binding isotherms requires the subtraction of two large and similar numbers at low values of r, the average number of drugs bound per base pair, which depend on an accurate determination of the bound extinction coefficient. Small errors (a few percent) can lead to large uncertainties in the magnitude of the binding constant. Even with this caution, we may come to the general conclusions reached above. Perhaps most importantly we

Figure 2-3. Scatchard plots for the binding of actinomycin analogs to calf thymus DNA at 25°. The data are plotted as r/C_f, the average number of drugs bound over the concentration of free drug v.s. the average number of drugs bound. The data were fit according to the theory of McGhee and Von Hippel (1974) and the concentration of actinomycin was 4×10^{-6} M.

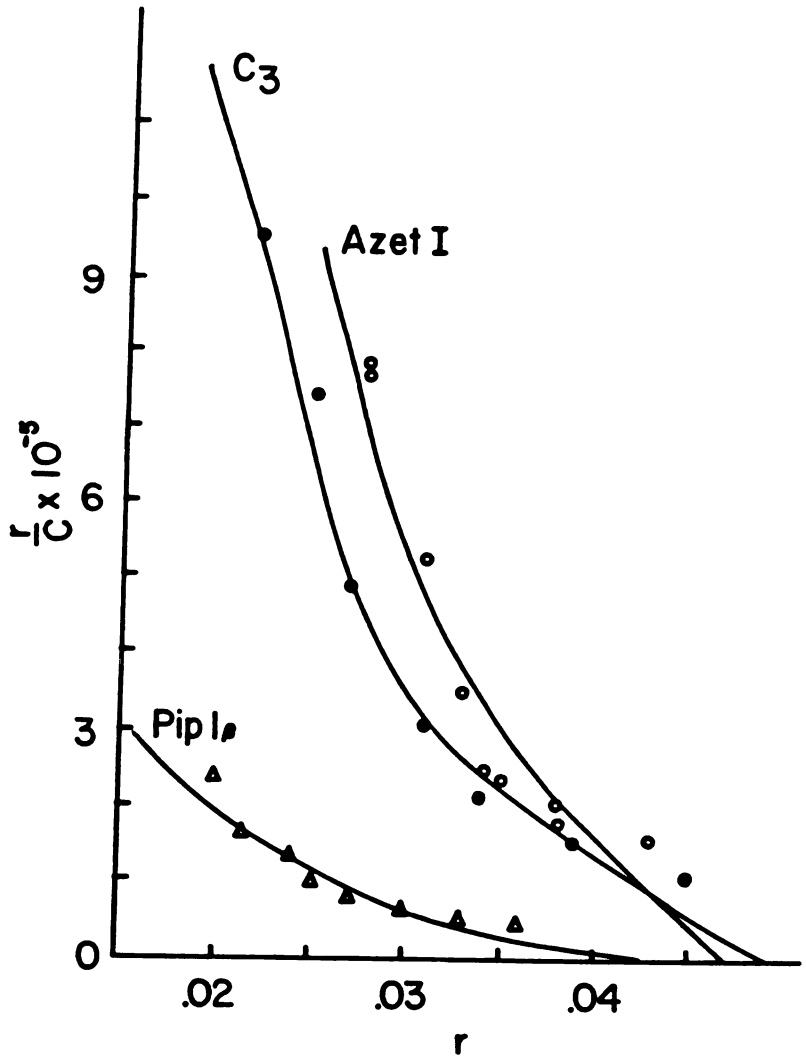

should note that all analogs bind strongly to DNA ($K.10^5$). The observed variation presumably reflects the details of the interaction between the peptides and the nucleotides adjacent to the intercalation site.

Additional information may be obtained from analysis of the number of drug binding sites along the lattice. Table 2-1 shows this value is close to 10 for all analogs. Examination of the model built from the 2:1 complex of deoxyguanosine with actinomycin D suggests that drug binding physically occludes two binding sites on either side of the site of intercalation (Sobell and Jain, 1972). Thus, we might expect maximum saturation to occur with 5 sites occluded per bound drug instead of 10. However, actinomycins are known to have a strong preference for the GC sequence, so every free site on the DNA lattice will not be a potential binding site. It has been reported that actinomycin binding to poly(dG-dC)poly(dG-dC) occludes 4 or 6 base pairs per bound drug (Winkle and Krugh, 1981, Wells and Larson, 1970). The larger values of n observed in these studies suggest that some sequence specificity is retained in the analogs.

Actinomycin Dissociation Kinetics

We have also studied the effect of 3' amino acid substitution on the DNA binding kinetics of actinomycins. In an early analysis of actinomycin-DNA kinetics, a complex

scheme was proposed, which included 5 steps in the association process and 3 steps in the dissociation (Muller and Crothers, 1968). As mentioned above, this is now thought to be due to dissociation from a number of different affinity binding sites (Krugh et al, 1980). Figures 2-4 and 2-5 show semi-log plots of the dissociation data for the analogs at 25°. In all cases the data were fit well by a double exponential. Preliminary stopped-flow experiments show the existence of a faster rate process similar to that observed by Muller and Crothers (1968) (Shafer et al, 1980). Figure 2-6 shows a semilog plot of the dissociation of actinomycin V from DNA. The double exponential dissociation only becomes apparent at longer times. The time constants for the rate processes are compiled in Table 2-2. These data demonstrate that the faster rate processes, with the exception of actinomycin V, are relatively insensitive to the amino acid substitution while the slow time constant is highly dependent upon the amino acid at the 3' position. The data may be divided into three classes based upon the magnitude of the slowest time constant; the analog faster than actinomycin D (PIP 2), those analogs which dissociated like actinomycin D (C_3, AZET I, PIP 1β), and those which dissociate more slowly (AZET II and V).

In the disubstituted analogs the dissociation rate appears to be related to the ring size of the amino acid at the 3' position. The larger the ring in this amino acid,

Figure 2-4. Plots of the SDS induced dissociation of disubstituted actionmycin analogs from calf thymus DNA at 25°. The data are plotted as the log of the difference between the final absorbance and the absorbance at time t v.s. time. The data were fit to two exponential decay as described in materials and methods. The concentrations were 4×10^{-6} M, 8×10^{-5} M, and 0.3% for actinomycin, DNA, and SDS respectively. Taken from Shafer et al, 1980.

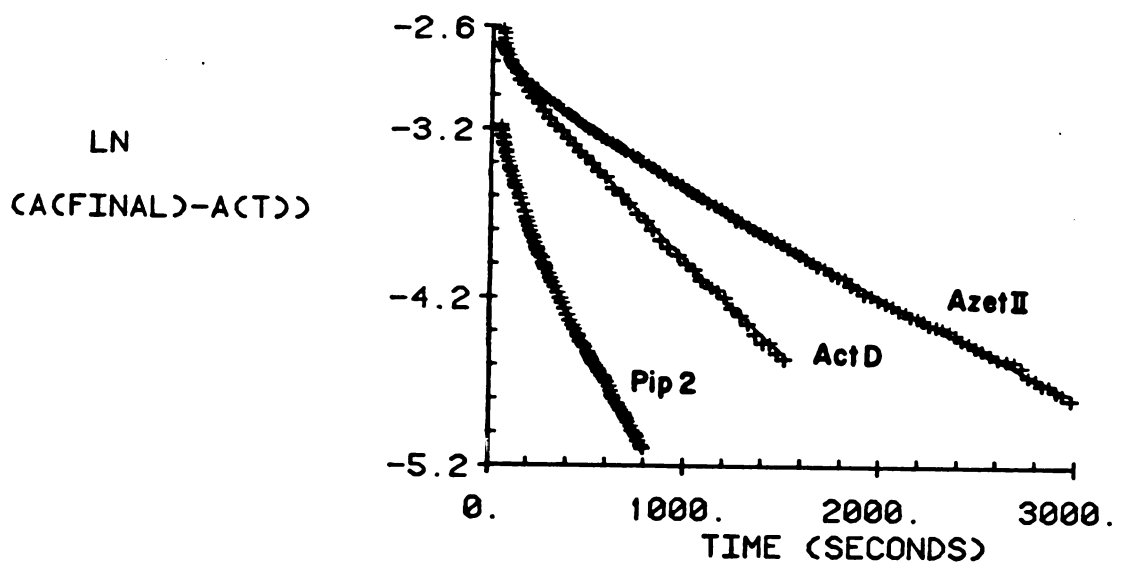

Figure 2-5. The SDS induced dissociation of monosubstituted actionomycin analogs at 25 °. See Figure 2-4 for details.

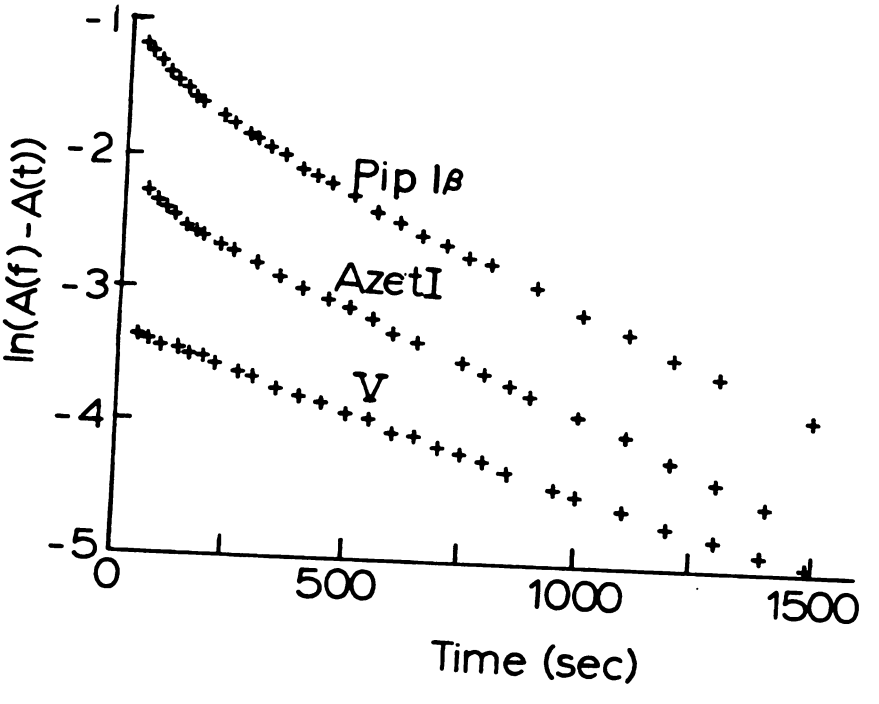

Figure 2-6. The SDS induced dissociation of actinomycin V from DNA at 25°. Note the expanded time axis for comparison to Figures 2-4 and 2-5.

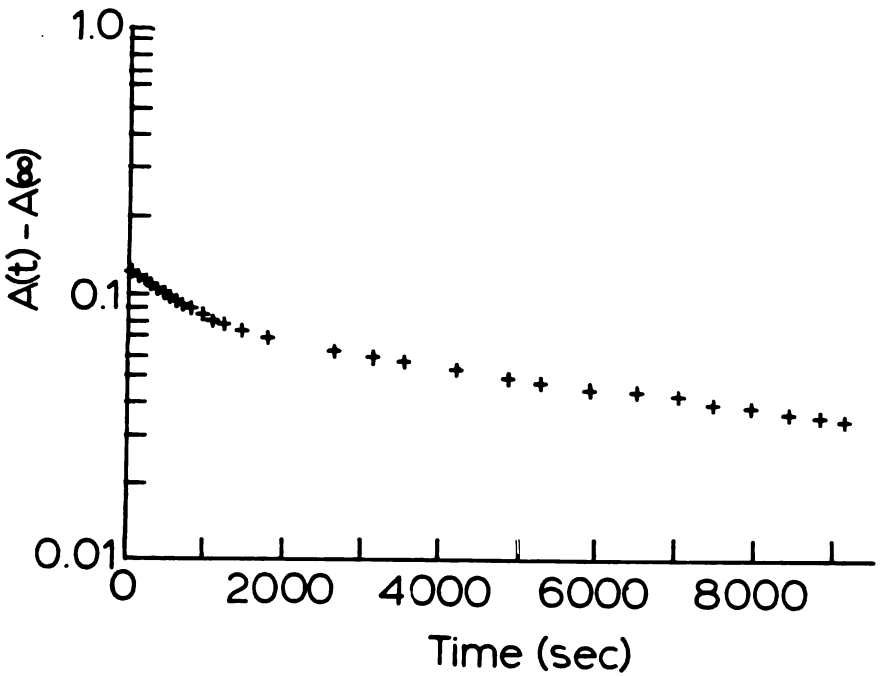

Table 2-2. Dissociation times of actinomycin analogs at 25°C

Actinomycin	τ_{fast} (sec)	τ_{slow} (sec)
PIP 2	57	278
D[a]	40	735
AZET II[a]	77	1360
C_3	45	592
AZET I	75	671
PIP 1β	70	490
V	662	10,940

a. Data from Shafer et al, 1980.

the faster it dissociates. The six membered ring analog dissociates faster than the five which is faster than the four membered ring analog. Substitution at the 2' position has no effect on the dissociation rate, hence dissociation is not thought to involve the 2' amino acid.

Analysis of the monosubstituted analogs is more complex and does not follow the predicted order. Table 2-2 shows that monosubstitution with azetidine or pipecolic acid has no appreciable effect on the dissociation rate constants while substitution with 4-ketoproline increases the dissociation time constant by an order of magnitude. Recalling two conclusions from the ^{1}H study of actinomycin conformation these data may be explained. In the last chapter we saw evidence that the amino acid substitution was made at a unique site on the pentapeptides, either on the α or β the chain. We also saw a difference in the dynamics of the prolines of actinomycin in aqueous solution. From these data we may consider the possibility that the dynamics of the and the pentapeptide are different and thus the individual pentapeptides may play a role in the dissociation process. Specifically, we would consider the possibility that the dynamics of one of the pentapeptides was slower and played a more important role in the dissociation kinetics. If this hypothesis is correct, then the site of substitution is expected to play an crucial role in the dissociation kinetics. We may explain the dissociation data by proposing that

the substitutions of azetidine and pipecolic acid for proline have been made on the pentapeptide lactone ring which is least important in the slow step in dissociation. In actinomycin V, the substitution has been made on the peptide which is important in the dissociation process. As mentioned above, chemical degradation studies have shown this substitution to be made on the pentapeptide lactone ring (Brockmann and Manegold, 1958, 1960).

Thermodynamics of DNA Dissociation

The thermodynamics of actinomycin dissociation may be investigated by analyzing the temperature dependence of the dissociation rate constants to extract the entropy and enthalpy of activation for the rate processes. Figure 2-6 and 2-7 show the effect of temperature on the slowest dissociation rate constant for the analogs. Since the slow step in dissociation is most likely related to the biological activity, we have concentrated our analysis on this step. The entropy, enthalpy, and free energy of activation for the slow step are compiled in Table 2-3. Examination of this table indicates that the observed rate constants are the result of large perturbations in both the entropy and enthalpy of activation. These two parameters change in such a way as to minimize the difference in the free energy of dissociation for the various analogs. For example, the difference in the free energy of dissociation for actinomycin D and azetomycin I is only 0.2 kcal/mole. This

Figure 2-7. Arrhenius plots for the dissociation of disubstituted actinomycin analogs from calf thymus DNA. The data are presented for the slowest rate process only (Shafer et al, 1980).

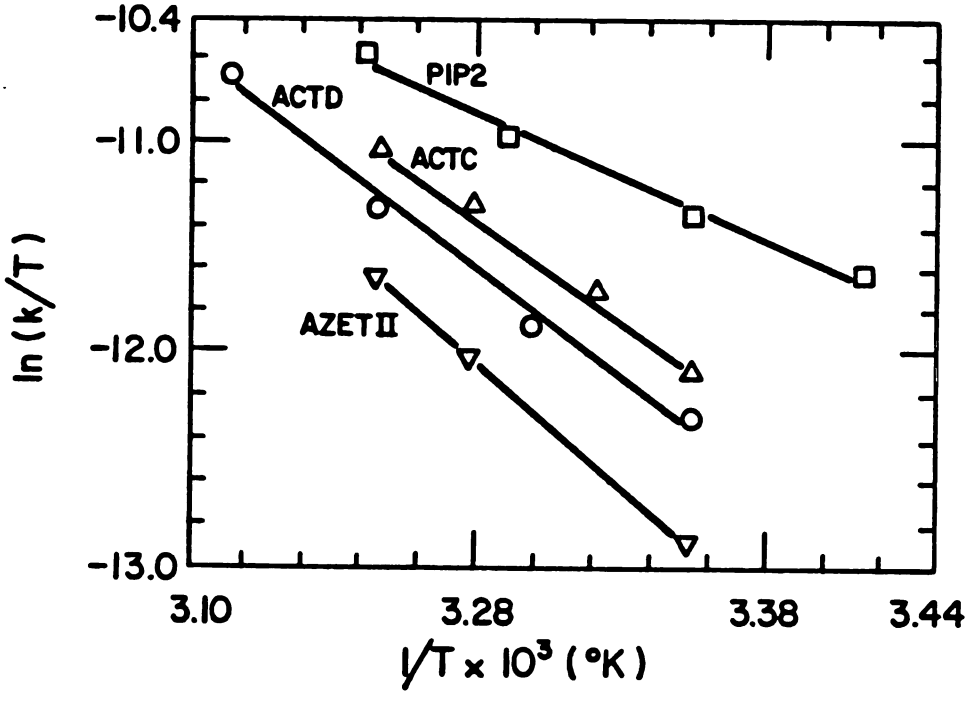

Figure 2-8. Arrhenius plots for the dissociation of monosubstituted actinomycin analogs from calf thymus DNA.

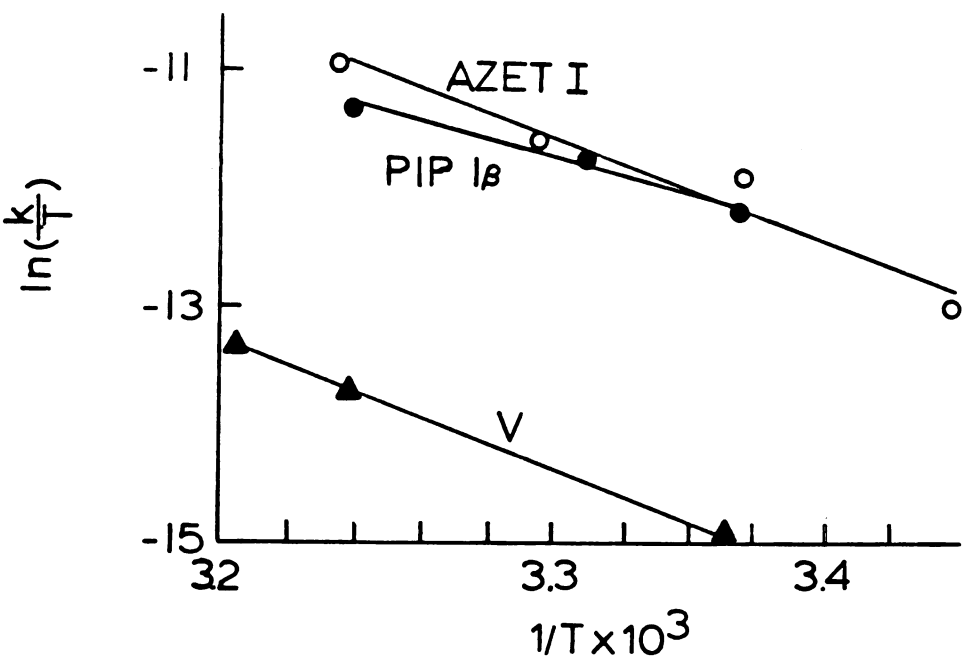

Table 2-3. Activation parameters for dissociation of actinomycin analogs at 25°C.

Actinomycin	$\Delta H^{\ddagger}$ (kcal/mole)	$\Delta S^{\ddagger}$ (e.u./mole)	$\Delta G^{\ddagger}$ (25°C) (kcal/mole)
D[a]	20.1±1.3	-4.4±4.3	21.4
C_3[a]	19.1±0.8	-7.1±2.7	21.2
AZET II[a]	23.0±0.4	4.4±1.4	21.7
PIP 2	11.4±2.6	-31.6±8.6	20.8
AZET I	15.3±2.0	-19.79±5.9	21.2
PIP 1β	21.3±3.4	0.2±11.6	21.6
V	21.9±0	-3.29±0	22.8

a. Data from Shafer et al, 1980.

translates to a difference in dissociation rate constants of only 144 seconds at 25°. This small change in the free energy of dissociation is due to a difference in the enthalpy of activation of 4.8 kcal/mole and a difference in the entropy of activation of 15.4 e.u./mole. Since the enthalpy of activation decreases the rate relative to actinomycin D and the entropy increases the rate relative to actinomycin D only the small difference in free energy of activation is observed. Although the faster rate process appears unaffected by by amino acid substitution, large perturbations in the entropy and enthalpy of activation are observed (data not shown). Again these changes oppose each other such that similar dissociation time constants are observed.

It is obvious from examination of Table 2-3 that entropy plays an important role in the dissociation process. Although a molecular interpretation of the entropic contribution to dissociation is somewhat difficult to visualize, several features are obvious from the activation energy analysis. In a general sense, we may conclude that solvation plays an important role in the stability of the dissociation transition state. It has been observed, for example, that the dissociation time constant is smaller by a factor of two for actinomycin D dissociation in $^{2}H_{2}O$ (Krugh, T. R. personal communication). The high lipophilicity of the drug may be important in its biological properties. It

may be noted that the the temperature coefficient for actinomycin solubility is opposite of most compounds; its solubility increases with decreasing temperature (Gellert et al, 1965).

The enthalpies of activation may give some insight into the dissociation process if the entropic contribution to dissociation is comparable. Actinomycins D and C_3 exhibit the same temperature dependence of the rate constants. Thus, the thermodynamic analysis is consistent with the other kinetic and equilibrium observations; the 2' amino acid does not appear important in the dissociation or binding process. Comparing actinomycin D with actinomycin V, we observe that the large difference in free energy of dissociation is due to a difference in the enthalpy of activation. It is interesting to note that while monosubstitution has little effect on the rate constants of AZET I and PIP 1β, perturbations of the activation parameters are observed. One possible explanation for this observation is that some interactions between the pentapeptides are important. Thus, while one peptide plays a dominate role in dissociation, both rings are involved.

DISCUSSION

The data presented in this chapter demonstrate that the amino acid at the 3' position plays an important role in the equilibrium and kinetic properties of actinomycin-DNA

interactions. The binding isotherms and the Tm analysis show that the binding is perturbed by substitution. Substitution of pipecolic acid for proline decreases the DNA binding affinity with disubstitution being the greatest perturbation. Monosubstitution of 4-ketoproline for proline leads to the greatest increase in binding affinity.

These studies are of use in determining that the analogs bind DNA in a similar fashion as might be expected from the NMR data presented in Chapter 1. Those data showed that the actinomycin analogs could adopt conformations similar to the parent compound. Also, the analogs showed a similar number of binding sites along the the helix (10 sites per bound drug) suggesting that the drugs maintain some sequence preference. If the drugs showed no sequence preference, the expected number of binding sites would be 4 to 6, as observed for actinomycin D binding to poly(dG-dC)poly(dG-dC) (Winkle and Krugh, 1980, Wells and Larson, 1970).

It may be argued, however, that the binding constant are not necessarily related to the biological activity. The inhibitory effects of actinomycin become obvious at very low levels of drug, about 1 drug per 1000 base pairs. Even the most weakly binding analog, PIP 2, would be completely bound under these conditions. Thus, binding constant alone cannot account for the difference in biological activity among the analogs.

It has been proposed that the in vivo effects of actinomycin binding are related to the slow dissociation kinetics (Muller and Crothers, 1968). As mentioned above, actinomycins are much more potent inhibitors of DNA dependent RNA synthesis than DNA synthesis (Goldberg et al, 1962, Waring, 1965). The kinetics of nucleotide incorporation into RNA has been described and this theory may be simply extended to include the effects of drug dissociation on the velocity of incorporation (Hyman and Davidson, 1970). In an excess of nucleotide, the initial rate of incorporation of nucleotides into RNA, v, is related to the time required for incorporation of a single nucleotide t_n by equation 2-6

$$\frac{1}{v}=\sum_n t_n \qquad (2\text{-}6)$$

where the sum is over the four nucleotide species. In the presence of the drug, polymerization proceeds until the polymerase encounters a bound drug, where it waits until the drug has dissociated before polymerization continues. It has been experimentally demonstrated that the polymerase will not dissociate while waiting for the drug to dissociate (Hyman and Davidson, 1970). The mathematical description of this process is

$$\frac{1}{v}=\sum_n (t_n(1-r)+t_d r) \qquad (2\text{-}7)$$

where r is the average number of drugs bound per site, (1-r) is the number of drug free sites, and t_d is the time required to incorporate a nucleotide at a drug bound site.

If dissociation is the rate limiting step for incorporation of the nucleotide at the drug binding site, then:

$$t_d = \sum_n t_n + \tau \qquad (2\text{-}8)$$

where τ is the time constant for dissociation. Equation 2-6 now may be simplified to:

$$\frac{1}{v} = \sum_n t_n + r\tau \qquad (2\text{-}9)$$

This predicts that the inverse of the velocity of nucleotide incorporation into the growing RNA chain should be linearly related to the the average number of drugs bound (with the same value of τ) or that a given value of r, the velocity should be related to the dissociation time constant. The first prediction has been verified (Waring, 1965, Hyman and Davidson, 1970) for actinomycin and the second has been show to be qualitatively correct for a series of daunomycin analogs (Gabbay et al. 1976).

The biological activity of the actinomycin analogs studied in this chapter have been evaluated and compiled (Remers, 1978). Table 2-4 compares the dissociation time constant of the analogs with the concentration of drug required for inhibition of bacterial growth. This comparison is chosen as it is the only assay which has been carried out on all of the analogs. While it may be argued that <u>in vivo</u> data are complicated by other factors, such as the uptake and distribution of the analogs, the data presented

Table 2-4. Relationship between actinomycin dissociation and biological activity.

Actinomycin	τ_{slow} (sec)	Antibacterial[a] Activity MIC (mg/ml)
PIP 2	278	1.25
PIP 1β	490	0.25
C_3	592	0.25
AZET I	671	0.31
D	735	0.25
AZET II	1360	0.35
V	10,940	0.13

a. Antibacterial activity is measured for B. subtilis.

MIC=Minimum Inhibitory Concentration.

Data are compiled by Remers (1978).

in Table 2-4 are in qualitative agreement with the predictions of equation 2-9. The biological data may be divided into three classes as was done for the dissociation constant of the analogs. The most potent analog is actinomycin V, which also has the longest dissociation time constant. In fact this is the most potent analog discovered to date; unfortunately the toxicity of the analog parallels its antitumor activity, limiting its usefulness (Remers, 1978). The fastest dissociating analog, PIP 2, is the least effective in the inhibition of bacterial growth. The compound which have dissociation time constant close to actinomycin D, analogs C_3, AZET I and PIP 1β, require similar concentrations for inhibition. The one compound which does not correlate is AZET II, which dissociated more slowly than actinomycin but required slightly higher concentrations for inhibition. On the whole, however, the correlation is quite dramatic.

The data presented here very strongly indicate that the 3' amino acid plays an important role in the DNA binding and kinetics. Substitution at the 2' position changes none of the binding or kinetic properties relative to actinomycin D. As mentioned above, the association kinetics of actinomycin binding to linear and supercoiled DNA were identical (Bittman and Blau, 1976). This strongly suggests, as does the data presented here, that the peptides determine the slow binding kinetics.

The time scale for the association/dissociation kinetics are is similar to those observed for the refolding of certain proteins (Tsang and Baldwin, 1976, Tsang et al, 1976). It has been proposed that the slow step in protein folding may be a cis-trans isomerization about the proline bond as shown in Figure 2-9 (Brandts et al, 1975). For model proline containing peptides, this isomerization has about the same free energy of activation (20 kcal/mole) as does actinomycin dissociation. In the model compounds, the rate of cis-trans isomerization is sensitive both to the bulk of neighboring amino acid and the proximity of charges (Brandts et al, 1975). The effect of ring size on the rate of cis-trans isomerization is unknown. We propose a similar scheme to account for the slow kinetics of actinomycin-DNA binding. The x-ray structure of the 2:1 complex of actinomycin D with deoxyguanosine suggest that there is a very intimate contact between the peptides and the double helix (Jain and Sobell, 1972). Since actinomycin binding is known to be affected by minor structural perturbations, it is easy to imagine how a cis-trans isomerization would alter the geometry of the peptides to make the DNA interaction highly unfavorable. From the data presented here, we propose that the slow step in actinomycin kinetics is due to a cis-trans isomerization about the amino acid at the 3' position. It is also possible, however, to have cis-trans isomerizations about one of the other two N-substituted amino acids, N-methylvaline and sarcosine, or some combination of

Figure 2-9. Schematic illustration of the cis-trans about the proline peptide bond. The cis and the trans isomer are defined by the relative orientation of the C^{α} atoms.

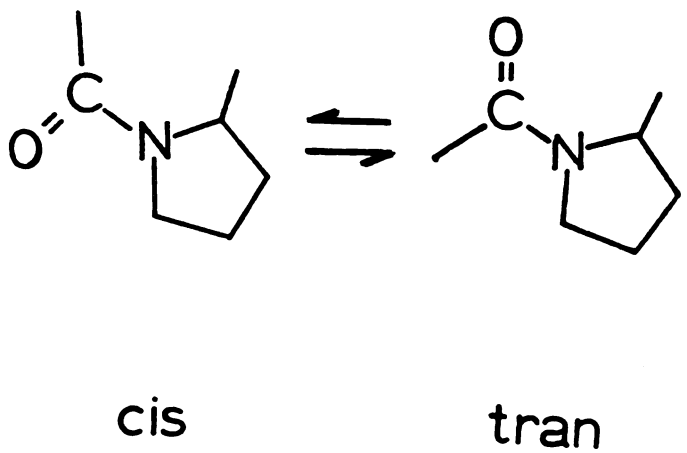

all three N-substituted amino acids. Empirical energy calculations have suggested that isomerization about the proline-sarcosine bond is much more favorable than that about the valine-proline bond of actinomycin (Kollman and Weiner, 1981). However, these calculations do not include the effect of DNA or solvent on the conformational features of actinomycin. X-ray analysis of actinomycin in its 2:1 complex with deoxyguanosine showed the conformations of the peptide linkages to be as follows: threonine-valine, trans; valine-proline, cis; proline-sarcosine, cis; sarcosine-N-methylvaline, trans (Jain and Sobell, 1972). It should be noted that the association of actinomycin with mono and dinucleotides is known to be very fast (Krugh, 1972, Davanloo and Crothers, 1976) so this model may not accurately represent the structure for actinomycin binding to DNA fragments large enough to exhibit the slow kinetics.

Analysis of the thermodynamics of dissociation indicates that dissociation is a complex process in which both entropy and enthalpy are intimately involved. Although the entropic contribution to dissociation is difficult to visualize, the transition state probably involves substantial ordering of water molecules. The complexity of the dissociation thermodynamics suggests that while one peptide may play a more important role in dissociation, both rings appear to be involved.

From these data, we have made several proposals which may be tested with additional actinomycin analogs. The hypothesis that one ring is more important in the dissociation process may be tested by examining the binding and kinetics of actinomycin analogs which are substituted with sarcosine in the 3' position. In this case, three biosynthetic isomers may be isolated, the disubstituted analog and two monosubstituted analogs, one of which is presumably substituted on the α pentapeptide lactone while the other is presumably substituted on the β chain (Mauger, 1975). We would predict that the disubstituted analog would dissociate faster from DNA that does actinomycin D, as the less bulky sarcosine should undergo cis-trans isomerization at a faster rate. We also predict that one of the monosubstituted analogs will bind much like the analog disubstituted with sarcosine. In this analog the substitution has been made on the peptide which is more important in the slow kinetics. We predict that the other analog will dissociate like actinomycin D as the substitution has been made on the peptide least important in the dissociation process. Also, we may evaluate the hypothesis that a cis-trans isomerization is related to the slow kinetics by labeling actinomycin with ^{15}N and observing the ^{15}N NMR spectrum. ^{15}N chemical shifts are very sensitive to cis-trans isomerizations (Hull and Kricheldorf, 1980) so observing the chemical shifts of the free drug and comparing that to actinomycin bound to a DNA fragment large enough to show the slow kinetics should prove

CHAPTER 3

DNA BINDING PROPERTIES OF DAUNOMYCIN.

^{31}P NMR AND OPTICAL STUDIES.

INTRODUCTION

Daunomycin, Figure 3-1, is an aminoglycoside antibiotic which is used for the treatment of cancer in man (Remers, 1978). It is a powerful inhibitor of nucleic acid synthesis and its mode of action is believed to involve intercalation into DNA (Kersten and Kersten, 1974). This hypothesis is based on a large number of *in vitro* studies on daunomycin-DNA interactions (Calendi et al, 1965, Du Vernay et al, 1980) and the ability of daunomycin to fluorescently stain chromosomes (Johnston et al, 1978). The use of daunomycin in cancer chemotherapy is limited by its cardiotoxicity. An analog which circumvents this problem, AD32, has recently reached clinical trials (Israel et al, 1980).

Since its discovery, a great deal of investigation has been directed towards an understanding of the nature of daunomycin-DNA interactions. In the presence of DNA the optical properties of the drug change in a manner similar to other known intercalators (Calendi et al, 1965). Daunomycin unwinds supercoiled DNA with an apparent unwinding angle of 12^{o}, one of the smallest observed for intercalators (Waring, 1972). The drug binds strongly to DNA, occludes three base pairs per bound drug, and increases the thermal denaturation temperature of the DNA about 15^{o} at a phosphate-to-drug ratio of 10 (Calendi et al, 1965). The binding of daunomycin appears to be sterically quite specific; analogs, such as the β anomer of the daunosamine sugar, bind DNA very

Figure 3-1. The structure of daunomycin.

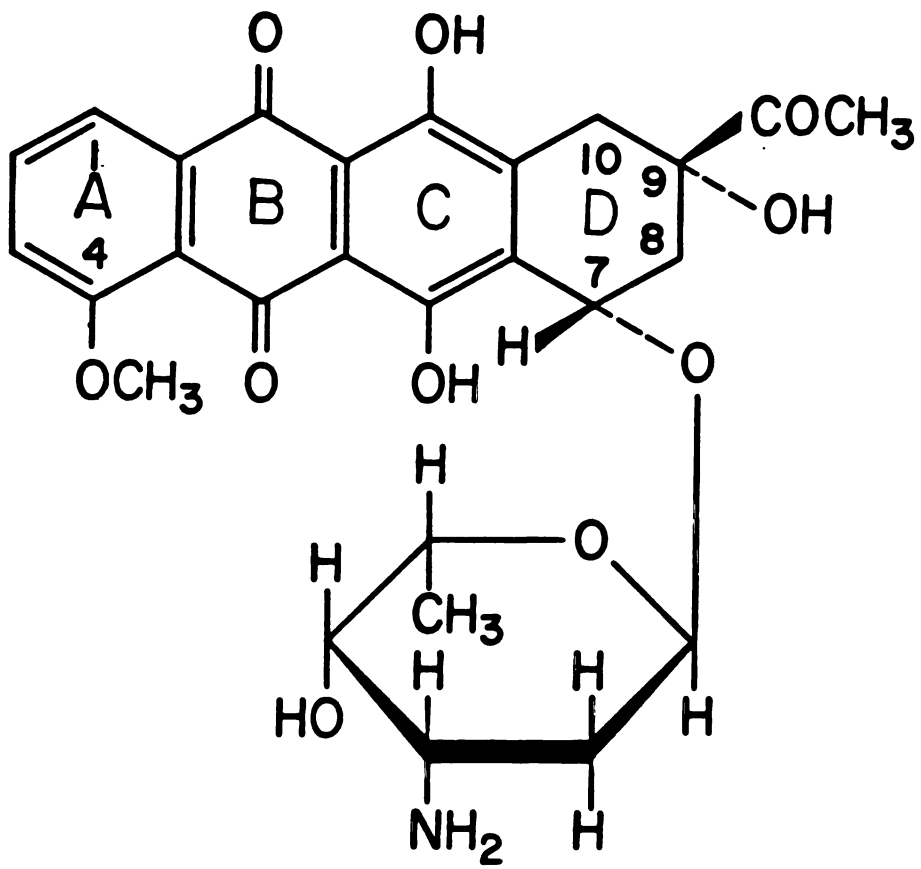

weakly (Zunino et al, 1977). Daunomycin binds to denatured DNA, but the binding constant is smaller by an order of magnitude than that observed for binding to the double helix (Calendi et al, 1965) The drug appears not to bind RNA by intercalation, with the possible exception of tRNA (Shafer, 1978). The x-ray structure of the 2:2 complex of daunomycin with d-CGATCG provides an insight into the geometry of the drug-receptor complex (Quigley et al, 1981).

Little is known, however, about the sequence preference involved in daunomycin-DNA interactions. Studies on the magnitude of the binding constant and the ability of the drug to inhibit DNA synthesis using synthetic polynucleotide templates have led to conflicting conclusions on the sequence preference of binding (Phillips et al, 1978). The binding studies showed a preference for the GC sequence while the DNA polymerase assay suggested that binding to AT sequences was most important in the biological activity. One way to approach this problem is to study the ^{31}P NMR spectra of DNA fragments in the presence and absence of intercalators (Patel, 1974a, 1974b, Reinhardt and Krugh, 1977). This approach has been successfully used to study the interaction of ethidium, actinomycin D, and 9-aminoacridine with nucleotides (Reinhardt and Krugh, 1977).

In these studies we monitor the ^{31}P chemical shift and linewidth of the internucleotide phosphate of dinucleotides and dinucleoside monophosphates in the presence and absence

of the drug. While changes in the NMR parameters may be indicative of complex formation, a quantitative analysis of the DNA unwinding which is known to accompany intercalation is not yet possible. ^{31}P chemical shifts are of course related to the electronic distribution about the phosphorus atom. Quantum mechanical calculations predict that the electronic distribution is sensitive to the O-P-O bond angle, θ, and the torsional angles ω and ω' shown in Figure 3-2 (Gorrenstien and Kar, 1975, Prado et al, 1979). There appears to be an empirical correlation between the phosphodiester bond angle and the chemical shift (Gorrenstien et al, 1975) and it has recently been demonstrated that the ^{31}P chemical shift is also sensitive to solvation (Lerner and Kearns, 1980). For DNA in the "B" conformation, the torsional angles are expected to be gauche-gauche; for the intercalated complex the angles are predicted to be gauche-trans. The theory predicts that this transition should decrease the shielding of the phosphorus atom so downfield shifts are expected. The calculations have a large degree of uncertainty and predict shifts from 6 to 22 ppm downfield (Gorrenstien et al, 1976). The largest shifts which have been observed for drugs binding to dinucleotides are those which accompany actinomycin binding to d-pGpC (-2.5 ppm) (Patel, 1974a, 1974b, Reinhardt and Krugh, 1977). While it may be demonstrated by optical absorbance, fluorescence, and ^{1}H NMR that ethidium forms the 2:1 complex with d-pCpG, the shift in the internucleotide phosphorus is only

Figure 3-2. Nomenclature for the bond and torsional angles important for ^{31}P chemical shifts of the internucleotide phosphate. The O-P-O bond angle is denoted by θ and the two torsional angles are ω and ω'.

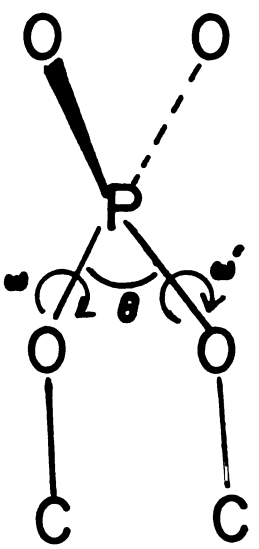

0.25 ppm downfield (Reinhardt and Krugh, 1977, Kastorp et al, 1978). In the complex with d-CpG the phosphorus is shifted 0.15 ppm upfield. Thus, while ^{31}P NMR appears to monitor complex formation, quantitative information on the nature of the complex is not obtainable from the direction and magnitude of the induced shift.

These same techniques may also be used to monitor the formation of daunomycin-DNA complexes. The experiments are more complex due to the number of binding sites excluded per bound drug. With one drug binding every three base pairs, the ^{31}P spectrum will reflect an average conformation about the phosphodiester bond of the drug-free and drug-bound phosphates. In addition, the linewidth may provide information on the effect of drug binding on the conformational fluctuations of DNA.

MATERIALS AND METHODS

Daunomycin, calf thymus DNA (Type I), d-GpC, buffer reagents, and deuterated solvents were obtained from Sigma. All other dinucleotides were obtained from Collaborative Research. Dinucleotide titrations and optical DNA binding experiments were performed in a buffer which contained 0.1 M Tris and 0.001 M EDTA at pH 7.5. For NMR experiments the buffer contained 10% $^{2}H_2O$. For Tm experiments, the buffer consisted of 0.01 M NaCl, 0.01 M cacodylate at pH 7.0. Concentrations were determined spectrophotometrically (P and L

Biochemicals catalogue #104). The concentration of dinucleotides was about 2 mM for the ^{31}P titrations. The ^{31}P DNA binding experiments were performed at both high (17 mM) and low (3 mM) concentrations of DNA with no apparent difference. Titrations were performed by additions of a concentrated solution of the drug into the nucleotide solution. Slow addition of daunomycin to DNA solutions minimized precipitation of the polynucleotide. Addition of the drug caused no decrease in intensity of the phosphorus resonance.

Optical Absorbance and ^{31}P NMR

Optical absorbance spectra were obtained on a Beckman Acta CIII equipped with water-jacketed cells and a multisample accessory. The temperature was measured by insertion of a temperature probe into the reference cell. Tm data are plotted as the absorbance relative to the absorbance at 25°. ^{31}P NMR spectra were obtained at 40.5 MHz on a Varian XL-100 spectrometer equipped with a Nicolet Fourier transform accessory. The temperature was controlled by a stream of cool air and the temperature was measured by insertion of a temperature probe into the sample. Chemical shifts in the dinucleotide experiments were referenced to an external standard of 85% phosphoric acid and the DNA binding experiments were referenced to an internal reference of trimethyl phosphate. Upfield shifts are reported with a positive

sign.

RESULTS

Daunomycin-Dinucleotide Binding

We have studied the interaction of daunomycin with a series of different sequence dinucleotides and dinucleoside monophosphates by monitoring the ^{31}P chemical shift and linewidth of the internucleotide phosphodiester linkage. This resonance appears about 1 ppm upfield from 85% phosphoric acid and is sensitive to nucleotide sequence (Reinhardt and Krugh, 1977). It is insensitive to pH changes (Patel, 1974) and control experiments showed no concentration dependence from 0.5 to 5 mM. With the temperature and ionic strength used in these experiments, the drug-free nucleotides are predominately in the single-stranded form (Young and Krugh, 1976, Krugh et al, 1976).

The internucleotide phosphate resonances of d-pGpC and d-GpC were observed to shift upfield in the presence of daunomycin. Figure 3-3 shows the effect of varying ratios of daunomycin on the 40.5 MHz ^{31}P NMR spectra of d-pGpC. A plot of the results are show in Figure 3-4 for d-pGpC, d-GpC, and d-pCpG. At a 5:1 ratio of daunomycin:d-pGpC, a 0.25 ppm upfield shift was observed, while at a ratio of 4.6:1 of daunomycin:d-GpC, a 0.14 ppm upfield shift was observed. These data show that even at these high ratios of daunomycin:nucleotide the titration is not yet complete,

Figure 3-3. The effect of daunomycin on the 40.5 MHz spectra of the internucleotide phosphate of d-pGpC at 20°. Numbers to the right of the spectra denote the ratio of daunomycin to d-pGpC. The spectra were gathered in 2 K data points with a sweep width of + 1 KHz using a 45° nonselective rf pulse, a 1 second recycle time, and broad band proton decoupling.

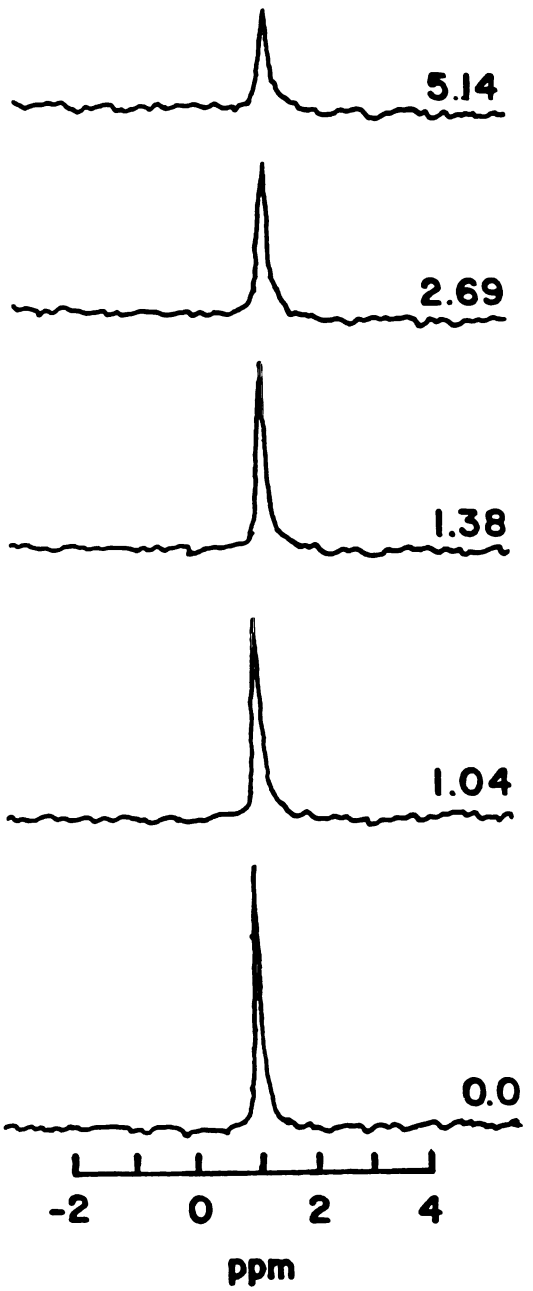

Figure 3-4. The effect of daunomycin on the chemical shift of the internucleotide phosphate of the nucleotides d-pGpC (●), d-GpC (○), and d-pCpG (△) at 20°.

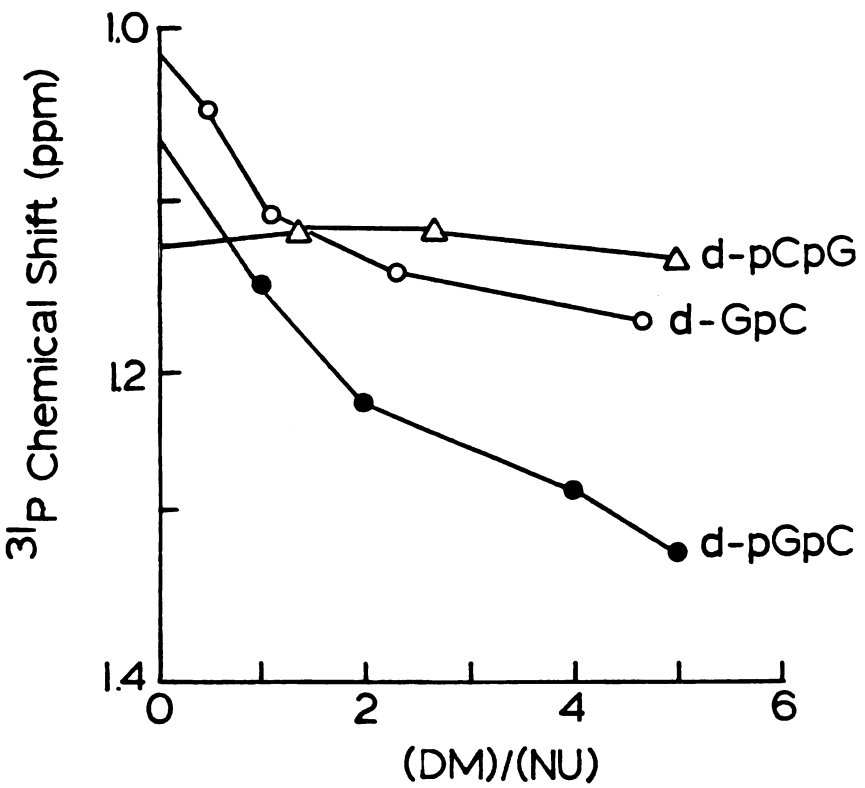

indicating that the magnitude of the binding constant is small. In a separate experiment, the concentration of d-GpC was lowered to 0.3 mM so that very high ratios of daunomycin:nucleotide could be observed. At the ratio of 14.6:1, the chemical shift of the internucleotide phosphate was shifted 0.25 ppm upfield.

A similar experiment was carried out with the sequence isomer d-pCpG. As shown in Figure 3-4, daunomycin had no effect on the internucleotide ^{31}P chemical shift. The internucleotide phosphates of the dinucleotides d-pApT and d-pTpA and the dinucleoside monophosphate d-TpA also showed no change in the presence of daunomycin. Likewise, the non-complimentary dinucleotide d-pGpT showed no effect upon daunomycin titration.

The effect of temperature on the 1:1 mixture of daunomycin:d-GpC was also studied. Lowering the temperature is known to induce the formation of miniature double helicies for dinucleotides (Krugh et al, 1976). Figure 3-5 shows the results of these experiments. Over the temperature range 10-40^{o}, the internucleotide phosphate shifts down field with increasing temperature. However, the chemical shift difference between d-GpC and its daunomycin complex remains at about 0.1 ppm. Increasing the temperature does not dissociate the complex; this implies that the enthalpy accompanying complex formation is small.

Figure 3-5. The effect on temperature on the chemical shift of the internucleotide phosphate of d-GpC (●) and its 1:1 daunomycin complex (▲). Chemical shifts are referenced to an external reference of 85% phosphoric acid at the same temperature.

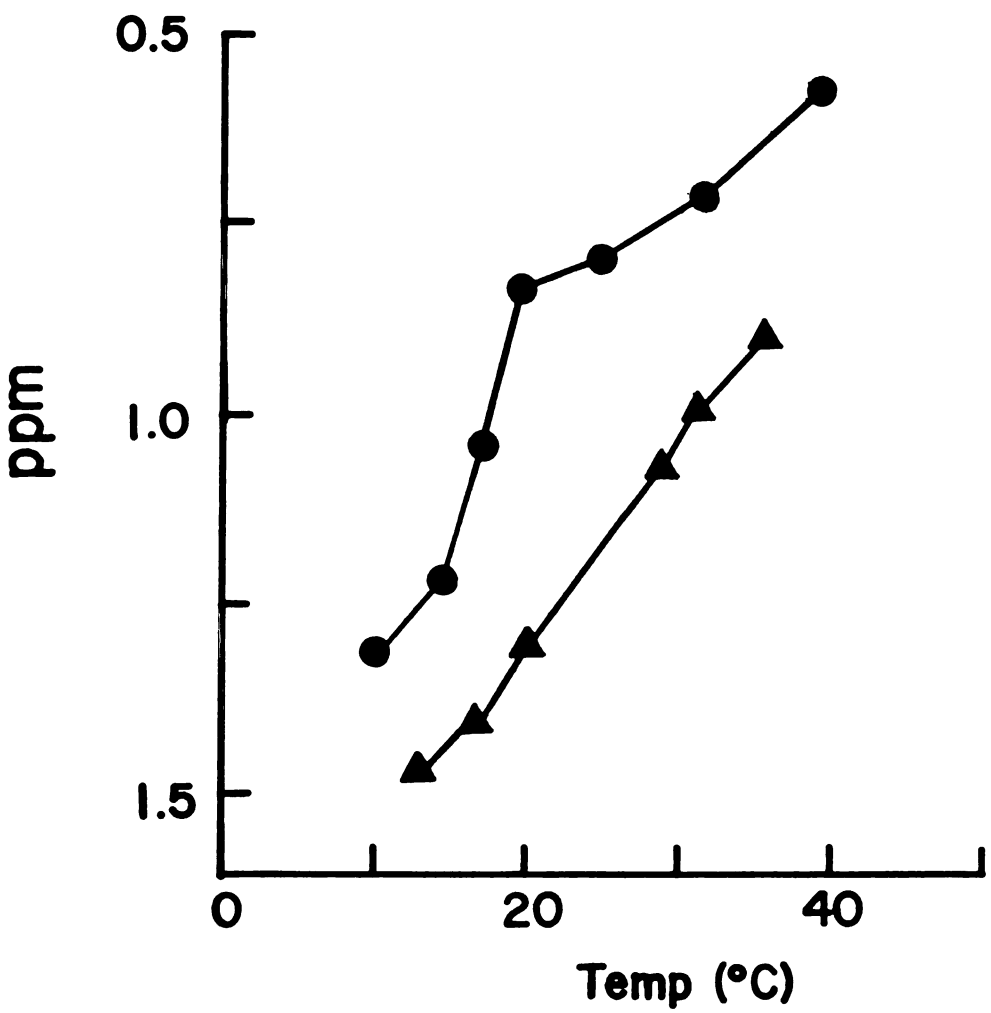

It may be noted in Figure 3-3 that the linewidth of d-pGpC is not altered significantly in the presence of daunomycin at a 1:1 or 2:1 stoichiometry. Linebroadening of the internucleotide phosphate has been observed for dinucleotides in the presence of intercalators ethidium and actinomycin D, which are known to induce the formation of miniature double helicies with the intercalated drug at a 2:1 stoichiometry (Patel, 1974a, Reinhardt and Krugh, 1977). The linebroadening is dependent upon the the drug-to-dinucleotide ratio and presumably arises from the chemical shift inequivalence of the dinucleotide free in solution, in both positions in the 2:1 complex, and possibly the 1:1 complex. Ethidium and actinomycin are known to form 2:1 complexes and at this stoichiometry the internucleotide resonances become considerably sharper. The single sharp line in the daunomycin-dinucleotide complex denotes rapid exchange between the dinucleotide species.

DNA Binding of Daunomycin

Optical absorbance and ^{31}P NMR may also be used to study the binding of daunomycin to higher molecular weight DNA. As mentioned above, daunomycin binds both to native and denatured DNA (Calendi et al, 1965). The absorbance changes which accompany complex formation with denatured DNA are analogous to those observed in the binding to native DNA; the presence of an isosbestic point suggest that the

two species present are the free and the bound drug.

The presence of daunomycin causes alterations in the ^{31}P NMR spectra of DNA. Figure 3-6 shows the 40.5 MHz spectra of calf thymus DNA in the presence and absence of daunomycin. The drug-free sample exhibits a relatively broad resonance (30 Hz) with a chemical shift similar to that of the internucleotide resonance of the dinucleotides. The linewidth is narrower than might be predicted for a polymer of molecular weight about 10^6; it has been proposed that the slow reorientation of the phosphorus-proton vectors is due to a bending of the helix rather than the overall motion of the polymer (Barkley and Zimm, 1979, Bolton and James, 1979, 1980a, 1980b, Early and Kearns, 1979). Thus, the linewidth may reflect the rigidity of the DNA helix. It should also be noted that chemical shift dispersion among the nucleotides also contributes to the DNA linewidth. In the presence of daunomycin at a P/D ratio of 10 the chemical shift is 0.10 ppm downfield from the drug-free sample. This indicates that a change in the average phosphodiester angles and/or torsional angle results from daunomycin binding at 1 of every 5 base pairs. However, binding has no appreciable effect on the linewidth of the sample, suggesting that drug binding does not significantly alter the slower DNA motions (presumably bending) which govern the ^{31}P linewidth at this value of P/D.

Figure 3-6. The ^{31}P NMR spectra of DNA in the presence (top) and absence of daunomycin (bottom). The sample contained 9 mM DNA and 0.9 mM daunomycin.

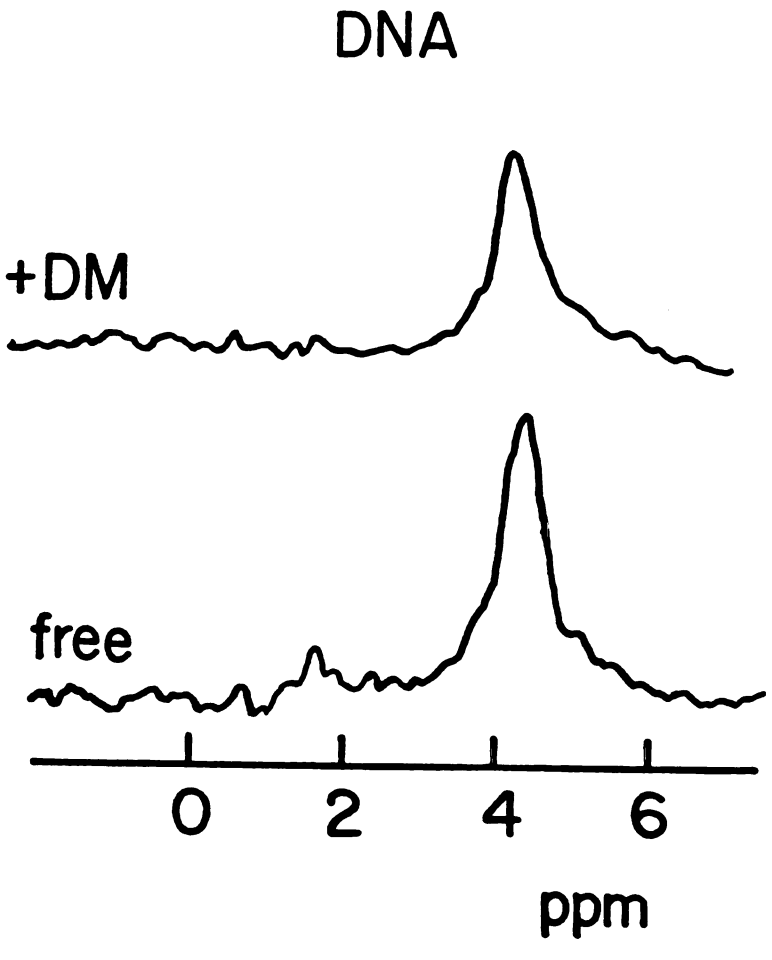

Figure 3-7 shows the effect of daunomycin on the ^{31}P spectrum of d-DNA. Daunomycin has no effect on the chemical shift but the linewidth is increases from 13 Hz to 30 Hz. The increase in linewidth may be accounted for either by a dramatic decrease in conformational flexibility or an increase in chemical shift dispersion which might accompany drug binding.

Helix-to-Coil Transitions of Daunomycin-DNA Complexes

Optical spectroscopy and ^{31}P NMR may both be used to monitor the helix-to-coil transitions of DNA and its daunomycin complexes. The two techniques measure different properties of the transition. When monitored at 260 nm, the UV absorbance of DNA is sensitive to the degree of base stacking and a 37% hyperchromism is observed as the DNA goes from the helix to the coil form. As mentioned above, the ^{31}P chemical shift is sensitive to the conformational features about the phosphodiester linkage and the linewidth is sensitive to the slower conformational fluctuations. The spectra of Figures 3-6 and 3-7 show the difference in linewidth for the native and denatured DNA.

Figure 3-8 shows the effect of temperature on the ^{31}P linewidth of DNA and its daunomycin complex. We noted above that daunomycin binding has no appreciable effect on the DNA linewidth. As the temperature approaches the Tm, a dramatic decrease in linewidth is observed. The ^{31}P linewidth

Figure 3-7. The ^{31}P NMR spectra of denatured DNA in the presence (top) and absence (bottom) of daunomycin. The sample concentration was 3 mM in DNA phosphates and 0.6 mM in daunomycin. Chemical shifts are referenced to an internal reference of 1 mM trimethyl phosphate. See Figure 4-3 for details.

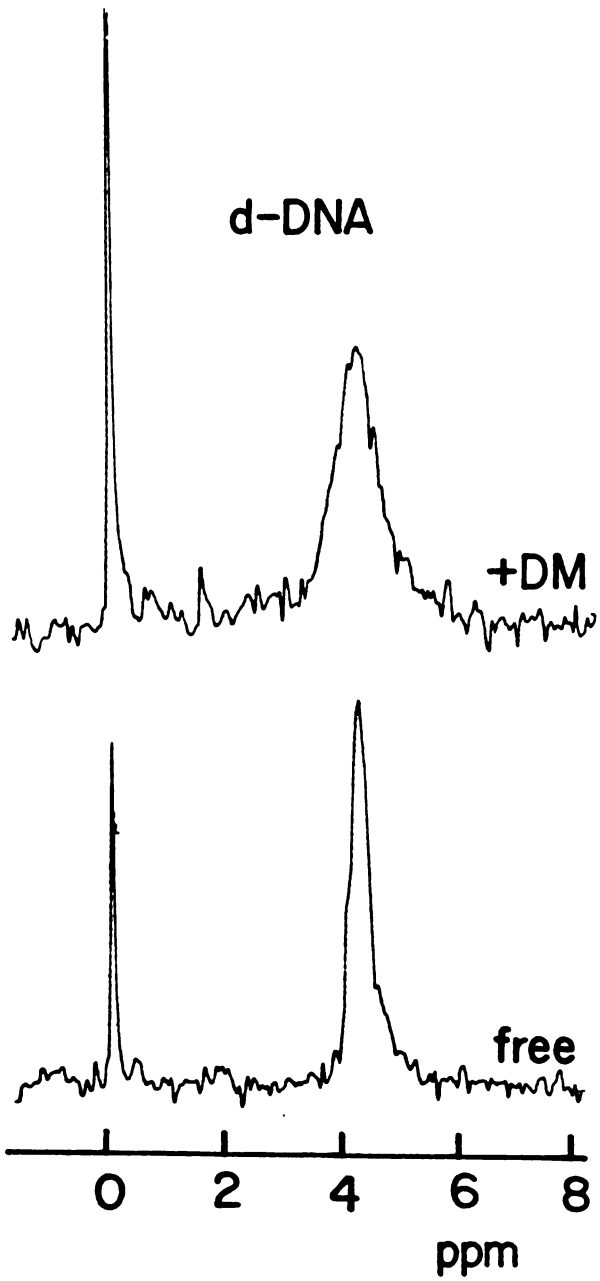

Figure 3-8. The effect of temperature on the linewidth of DNA (●) and its 10:1 daunomycin complex (▲). The concentration of DNA was 17 mM.

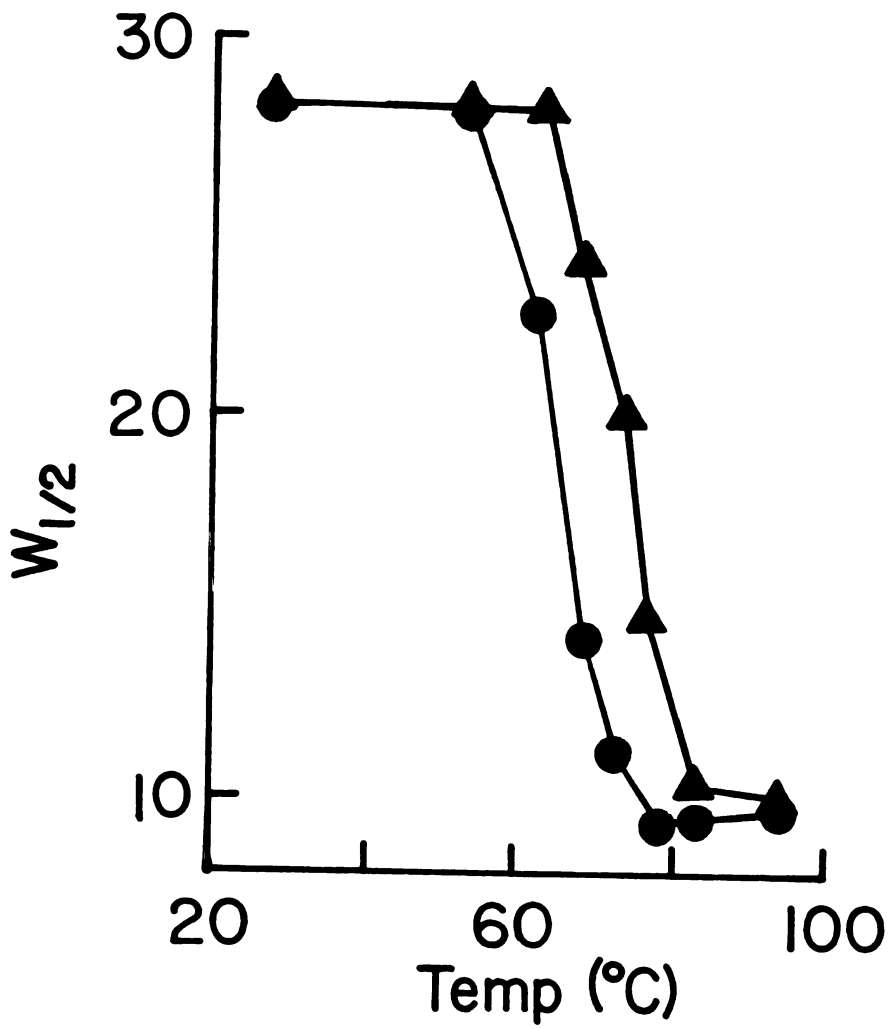

changes in step with the optical absorbance of DNA and its daunomycin complex; thus, the linewidth appears to monitor the rigidity which is supplied by base pairing in the double helix. While daunomycin binding adds no rigidity to the complex, it increases the temperature at which the rigidity is lost. Measurement of the linewidth as a function of temperature gives information analogous to that obtained from monitoring the optical absorbance of the complex.

In contrast, measurement of the ^{31}P chemical shift gives a different picture of the effect of daunomycin on the helix-to-coil transition. Figure 3-9 shows the effect of temperature on the optical absorbance and ^{31}P chemical shift of DNA and its daunomycin complex. For the drug-free sample, the chemical shift varies continuously over the temperature range. This variation, reflecting a conformational change, observed by the ^{31}P chemical shift in the premelting range is not apparent from optical measurements; alteration of the conformation along the sugar-phosphate backbone does not appreciably affect the base stacking or hydrogen bonding of the helix. While the optical absorbance does not change, the circular dichroism spectrum of the helix varies continuously over the temperature range, and it has been proposed on the basis of these data that DNA undergoes a transition from the "B" to "C" form prior to melting (Palecek, 1976). Figure 3-9 shows that daunomycin binding does not alter the ability of the DNA to adopt the premelting conformation (as

Figure 3-9. Helix-to-coil transitions of DNA and its 10:1 daunomycin complex. The left axis is the ^{31}P chemical shift of of DNA (●) and its daunomycin complex (▲); the right axis is the hypochromism of DNA (○) and its daunomycin complex (△) as a function of temperature.

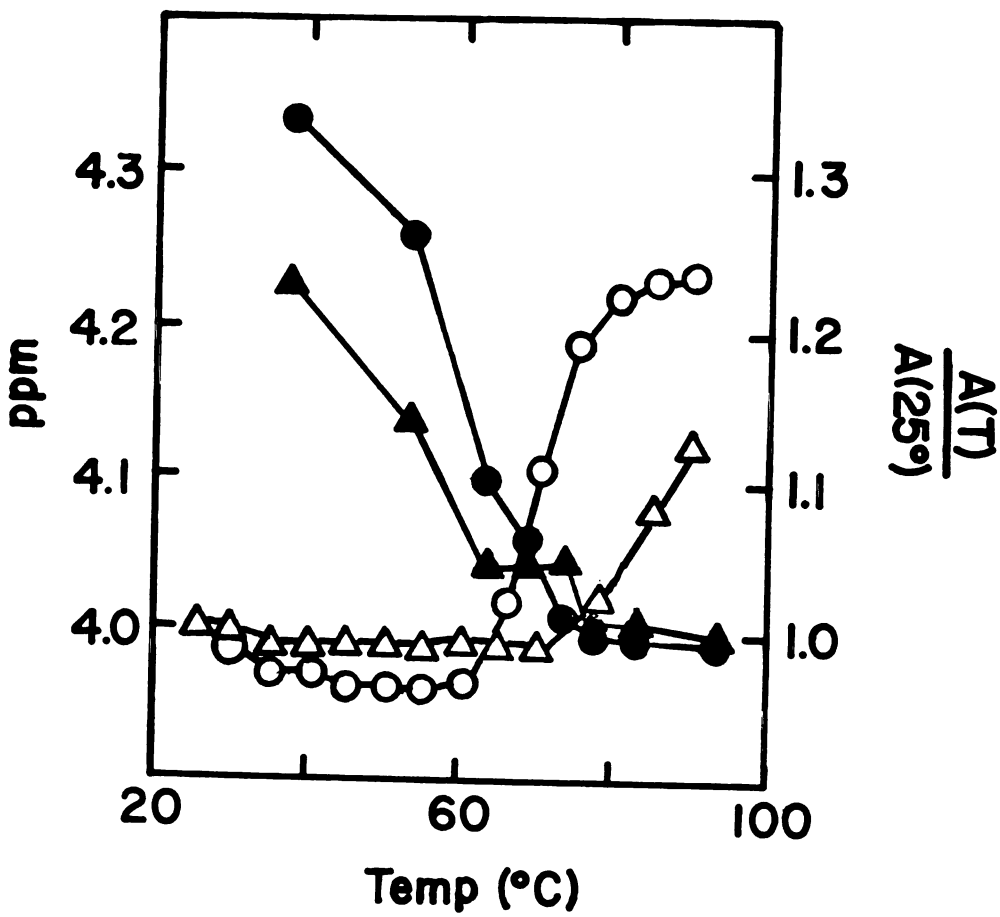

judged by the ^{31}P chemical shift). The chemical shift of the daunomycin-DNA complex approaches that of the drug-free sample far (17^{o}) below the Tm of the complex. Rather, daunomycin exerts its effects most dramatically at the transition temperature.

DISCUSSION

These data demonstrate that ^{31}P NMR may be used to monitor formation of intercalator complexes at both the dinucleotide and polymer level. For the dinucleotides, changes in the internucleotide phosphate are observed only in the case of d-pGpC and d-GpC, suggesting a preference for this 3'-5' purine-pyrimidine sequence. This preference is the same as that observed for actinomycin D and different from that proposed for ethidium binding (Reinhardt and Krugh, 1977). Since only the GC sequence gave rise to changes in the ^{31}P, the interaction appears to be quite specific. While no 3'-5' pyrimidine-purine sequences (d-pCpG, d-TpA) gave rise to changes in the internucleotide phosphate chemical shift, the interaction requires more than any 3'-5' purine-pyrimidine sequence as d-pApT, d-ApT, and d-pGpT also showed no effect. The lack of change in the d-pGpT titration indicates that guanine alone in the 3' position is insufficient to induce complex formation. Figure 3-4 shows that the ^{31}P changes occur at lower ratios of daunomycin:nucleotide for d-pGpC than for d-GpC; this

implies that complex formation is enhanced by the interaction of daunomycin with the phosphate adjacent to the intercalation site. This is most likely attributable to the interaction of the 3' amino on the aminosugar with the negatively charged phosphate.

These data are consistent with the recent x-ray structure of the 2:2 complex of daunomycin with d-CGATCG in which the 2 daunomycins were observed to bind at the CG sequences rather than the AT sequences (Quigley et al, 1981). The important interactions which stabilize this complex are stacking of the "B" and "C" rings of the antibiotic with the bases and a hydrogen bond between the 9 hydroxyl and the guanine exocyclic amino group. It may be the case that this hydrogen bond may play a role in the apparent sequence specificity similar to that proposed for actinomycin (Jain and Sobell, 1972). The amino sugar was observed to lie in the minor groove with no direct interaction with the phosphate backbone. The x-ray data is consistent with the ^{1}H NMR studies on the daunomycin:d-pGpCpGpC complex, which showed only small changes in the in the chemical shift of the "A" ring protons which are not stacked directly under the bases (Patel, 1978). Measurement of the transient electric dichroism has also suggested that daunomycin binding is perpendicular to other intercalators and shows a preference for GC containing DNA (Chairs et al, 1981). This binding geometry may be why the optical changes accompanying dau-

nomycin binding are not as large as those observed for the other intercalators. It should be noted that the daunomycin binding sequence preference does not seem to be as absolute as that observed for actinomycin D binding. Actinomycin does not bind poly(dA-dT)poly(dA-dT) while daunomycin binds this polymer about half as strongly as poly(dG-dC)poly(dG-dC) (Phillips et al, 1978). It has been recently noticed that actinomycin may bind to poly(dA-dT)poly(dA-dT) in the presence of daunomycin but the kinetics of the complex are much faster than for actinomycin binding to DNA (Krugh and Young, 1977, Krugh et al, 1979).

Only small changes in the optical spectra accompany complex formation of daunomycin with the dinucleotides. This makes determination of the stoichiometry of the complex difficult. However, several lines of evidence suggest that the 1:1 complex is formed under our experimental conditions. The precedent for formation of the 1:1 complex is that daunomycin binds strongly to d-DNA. By comparison, actinomycin and ethidium do not appear to bind d-DNA. In contrast to actinomycin and ethidium titrations with dinucleotides, daunomycin complex formation is not accompanied by line broadening of the internucleotide phosphate due to slow exchange among the nucleotide species. Also, from the x-ray and model building studies, it appears that most of the interaction energy in the intercalation complex comes from only one strand of the double helix (Pigram, 1972). Thus,

it might be easily imagined that the interaction energy gained from formation of the 2:1 complex is insufficient to overcome the unfavorable entropy of formation of the 2:1 relative the 1:1 complex at the dinucleotide level.

The DNA binding of daunomycin at one in every five base pairs changes the average environment of the phosphates in the DNA backbone but appears to have a negligible effect on the rate of bending motions in the double helix. At both the dinucleotide and polymer level, changing the temperature leads to changes in the ^{31}P chemical shift. Daunomycin alters the DNA conformation upon binding but does not inhibit the ability of DNA to undergo its premelting transitions. Studies on the NMR relaxation of daunomycin-DNA complexes suggest that drug binding does not interfere with the fast "wobbling" of the phosphates which give rise to ^{31}P NMR relaxation (Jones and Wilson, 1980).

CHAPTER 4

THE NUCLEIC ACID BINDING PROPERTIES OF FLUORINATED INTERCALATORS. ^{19}F NMR, OPTICAL ABSORPTION, AND FLUORESCENCE STUDIES.

INTRODUCTION

Most of the information available on DNA-intercalator interactions has been obtained through the *in vitro* study of the changes in physical properties of the drug or nucleic acid which accompany complex formation. The *in vivo* biochemistry of intercalators is much more difficult to study by the usual techniques. The most common *in vivo* experiments involve measurement of the effect of intercalators on nucleic acid synthesis (Kersten and Kersten, 1974). Fluorescent acridine and anthracycline intercalators have been shown to localize preferentially in the chromosomal material (Johnston et al, 1978). Also, by taking advantage of the energy transfer between fluorescent and non-fluorescent intercalators (such as actinomycin) it is possible to show chromosomal localization of other drugs (Zetalin et al, 1978). Another approach is to monitor the effects of photochemical alkylating (or crosslinking) of intercalators such as the psoralens or ethidium azide (Hyde and Hearst, 1978, Bolton and Kearns, 1978). This provides a probe of the intercalation site through analysis of the photochemical products.

Yet another approach is to label the drug molecule with rare or enriched nuclei which may be observable above the cellular background in NMR experiments. We have chosen to study drug-nucleic acid interaction through the use of fluorine labeled drugs. The choice of the fluorine label

has several advantages over other labels. For example, fluorine is close to protons (94%) in terms of sensitivity and the ^{19}F chemical shift is sensitive to environmental factors so that complex formation is expected to give rise to large changes in the chemical shift (Gerig, 1978). Since cells only rarely contain fluorine, these experiments will not be complicated by large peaks from the solvent or the macromolecule.

The use of fluorine as a probe of biochemical systems is not unprecedented; the fluorine probe has been used both as a ligand and incorporated into the macromolecule of interest. In a series of papers on m-fluorotyrosine labeled alkaline phosphatase, Hull and Sykes (1975a, 1975b, 1975c, 1976) demonstrated the power of ^{19}F NMR in studying the individual environments of the fluorotyrosines and their conformational fluctuations within the enzyme. ^{19}F NMR has been successfully used to study the suicidal inhibition of thymadylate synthetase by 5-fluorodeoxyuridine (Byrd et al, 1977, Lewis et al, 1980, James et al, 1978). Fluorinated substrates have also been used to study enzymatic reactions and the active sites of enzymes (Gerig et al, 1977). It is possible to map out the distance of macromolecular protons to the fluorine probe using the selective $^{19}F^{1}H$ nuclear Overhauser effect (Gerig et al, 1979).

This technique has also been applied to the study of nucleic acids and protein-nucleic acid interactions. While

5-fluorouracil is toxic to many cells, certain strains may be grown on the drug in the presence of thymine (Kaiser, 1980). This results in fluorine labeling of the cellular RNA. The fluorine spectra and some NMR relaxation parameters have been reported for unfractionated tRNA, $tRNA^{val}$, and 5S RNA labeled with fluorouracil (Horowitz et al, 1978, Marshall and Smith, 1980). Also, fluorotyrosine labeled gene 5 protein, a DNA unwinding protein, has been used to study protein- nucleic acid interactions (Coleman and Armitage, 1976, Coleman et al, 1976). We have used 5-fluorotryptamine to monitor the the role of planar aromatic amino acids in protein-nucleic acid interactions (Mirau et al, 1981).

We have studied DNA-intercalator interactions using the fluorinated intercalators fluoroquine and fluoroquinacrine shown in Figure 4-1. These are analogs of the well-characterized intercalators chloroquine and quinacrine in which the chlorine of chloroquine or the methoxy of quinacrine has been replaced with the fluorine nucleus. These studies have characterized the interaction of the drug with poly(A), tRNA, and DNA <u>in vitro</u> as a prelude to the study of the fate of intercalators in <u>in vivo</u> systems. Before these results may be extrapolated to intercalators in general, it first must be demonstrated that introduction of the fluorine atom does not perturb the drug-nucleic acid complex. Besides the environmental information obtained from the

Figure 4-1. The structure of fluoroquine (top) and fluoroquinacrine. Relaxation parameters were calculated assuming rotation about the C-N bond ($\alpha = 109^{o}$) as indicated. Also depicted is the axes system for the chemical shift tensor with δ_z normal to the plane of the acridine ring.

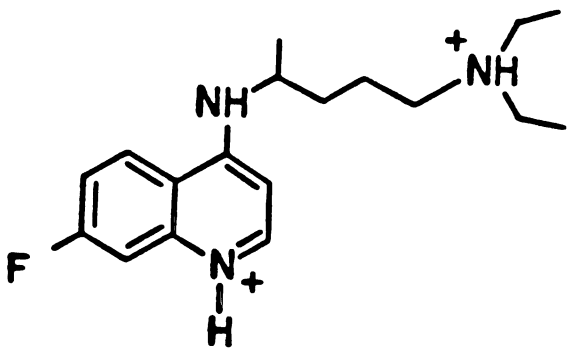

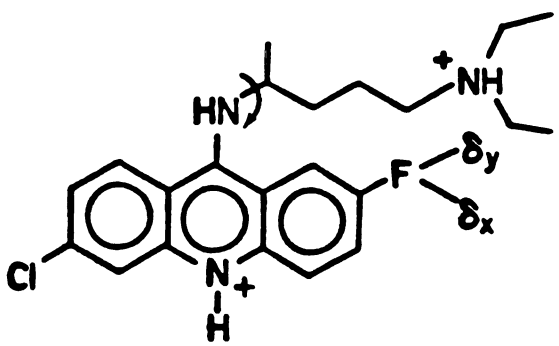

induced chemical shifts which accompany complex formation, we may also probe the dynamics of the drug-receptor complex through measurement of the ^{19}F NMR relaxation parameters. This approach offers information on the internal motion (here modeled as the sliding of the intercalator between the base pairs) and the slower reorientation of the nucleic acid (bending of the helix). With this information gathered, it should be possible to interpret the ^{19}F NMR spectra of cells which have been incubated with the fluorinated intercalator.

MATERIALS AND METHODS

Synthesis of Fluorinated Intercalators

Fluoroquine, 7-fluoro-4-(diethylamino-1-butylamino) quinoline was synthesised in a manner similar to chloroquine (Price and Roberts, 1948) except that 3-fluoroanaline was used in place of 3-chloroanaline (Bolton et al, 1981). The 4-chloro-7-fluoroquinoline was converted to the phenoxy-derivative by the method of Surry and Cutler (1951), which gave good crystals. The phenoxy derivative was condensed with 2-amino-5-diethylaminopentane (nonol diamine) to give fluoroquine. The product identity was confirmed by ^{1}H and ^{19}F NMR, fluorescence and UV/visible spectroscopy.

Fluoroquinacrine, 3-fluoro-7-chloro-9-(diethylamino-1-methylbutylamine)acridine, was prepared using the standard synthesis of quinacrine (Addock, 1973), except that 4-fluoroanaline was used in place of 4-methoxyanaline (Bolton et al, 1981). The product was confirmed by ^{1}H and ^{19}F NMR,

UV/visible, and mass spectroscopy.

Sample Preparation

Poly(A) (PL Biochemicals) and unfractionated tRNA (Boeheringer Mannheim) were prepared by dialysis against 0.01 M NaCl, 0.01 M sodium cacodylate at pH 7.0. Calf thymus DNA (Sigma) was briefly sonicated in BPES buffer and dialysised against the buffer described above. This sonication procedure generally yields polydisperse DNA fragments with molecular weight between 10^5 and 10^6, as measured by its intrinsic viscosity. Concentrations were determined spectrophometrically using the extinction coefficients 9400 per nucleotide of poly(A), 13,600 per base pair of DNA, and $6x10^5$ per mole of tRNA at 260 mn at pH 7.0. The extinction coefficients for fluoroquine and fluoroquinacrine were assumed the same as chloroquine and quinacrine; 18,000 at 340 nm and 8,000 at 416 nm, respectively. The NMR samples typically contained 20 mM poly(A), 1 to 2 mM tRNA, and 10 to 20 mM DNA base pairs. Binding experiments were performed at high ratios of phosphate-to-drug to insure that all of the drug was bound in the strongest mode and that the NMR parameters contained no contribution from the free drug. The complexes contain 1 drug per 10 nucleotides of poly(A), 2 drugs per molecule of tRNA, and 1 drug per 10 DNA base pairs.

Fluorescence and Optical Absorption

Steady state fluorescence measurements were performed on a Perkin-Elmer MPF2 fluorimeter. Fluorescent lifetimes were determined by Dr. P. Bolton in the laboratory of Dr. J. Yguerabide at the University of California at San Diego. Fluorescent experiments were performed at low concentrations ($<10^{-5}$M) to insure that the results were not complicated by inner filter effects. Absorption and thermal denaturation experiments were performed on a Beckman Acta CIII equipped with a circulating water bath. The temperature was measured by insertion of a temperature probe into the reference chamber.

NMR Methods

^{19}F NMR experiments were performed on a Varian XL-100 spectrometer equipped with a Fourier transform accessory at 94.1 MHz. The NMR relaxation parameters were measured as describe elsewhere (James, 1975, James et al, 1978). Briefly, the spin-lattice relaxation time (T_1) was measured using the inversion recovery sequence. Linewidths were measured using the line-fitting routine on the Nicolet 10-80 computer. Nuclear Overhauser enhancements were measured by comparing the intensity of the fluorine resonance obtained with broad band ^{1}H decoupling with that obtained by decoupling only during acquisition, using sufficient delay times to insure that the maximum NOE was observed. The off-resonance intensity ratio (R) and the rotating frame spin-

lattice relaxation time ($T_{1\rho}^{off}$) were obtained by comparing the intensity of the fluorine resonance in the presence of a 0.23 gauss field 5.6 KHz off-resonance with that obtained with the radiofrequency field 100 KHz off-resonance.

The solvent induced shifts (SIS) were measured by comparing the chemical shift of fluoroquine samples in 10% ^2H_2O/90% H_2O with that obtained in 90% ^2H_2O/10% H_2O. Chemical shifts to higher field are reported as positive with the chemical shift of the free drug taken as the origin.

Analysis of NMR Relaxation

Values for the overall and sliding motion correlation time were obtained from analysis of the data plotted in Figure 4-2. The reported values are the pair which gave the lowest value for the residual sum of squares R^2

$$R^2=\sum\left\{\frac{\text{observed}-\text{predicted}}{\text{observed}}\right\}^2 \qquad (4\text{-}1)$$

when summed over the five measured relaxation parameters. Typically, changing the overall motion correlation time by a factor of two increased R^2 by an order of magnitude while a similar change in the sliding motion correlation time doubled R^2. Uncertainty in the measured relaxation parameters is expected to be about 15%. Since $T_{1\rho}^{off}$ requires measurement of both T_1 and R, the errors in this parameter are expected to be somewhat larger. Figure 4-2 shows that while $T_{1\rho}^{off}$ and T_1 are sensitive to errors of this magnitude, the linewidth, NOE, and R value are relatively unaffected.

THEORY

The molecular motions of drug bound to nucleic acids may be investigated via ^{19}F NMR. This section describes the calculation of ^{19}F NMR relaxation parameters due to dipolar interactions and chemical shift anisotropy, and the relationship of drug motion to the spectral density functions.

Dipolar Interactions

The spin-lattice relaxation time, T_1, linewidth, $W_{1/2}$, nuclear Overhauser effect, NOE, and the rotating frame spin-lattice relaxation time in the presence of an off-resonance field, $T_{1\rho}^{off}$ are given in terms of the spectral density $J_n(\omega)$ for dipolar coupling to N protons by (Abragam, 1961, James et al, 1977):

$$\frac{1}{T_1}=NK\left\{J_0(\omega_H-\omega_F)+3J_1(\omega_F)+6J_2(\omega_H+\omega_F)\right\} \tag{4-2}$$

$$W_{\frac{1}{2}}=\frac{1}{\pi}\left\{\frac{1}{2T_1}+NK\left[2J_0(0)+3J_1(\omega_H)\right]\right\} \tag{4-3}$$

$$NOE=1+\frac{\gamma_H}{\gamma_F}\frac{\left[6J_2(\omega_H+\omega_F)-J_0(\omega_H-\omega_F)\right]}{\left[J_0(\omega_H-\omega_F)+3J_1(\omega_F)+6J_2(\omega_H+\omega_F)\right]} \tag{4-4}$$

$$\frac{1}{T_1^{off}}=NK\left\{\sin^2\theta\left[2J_0(\omega_e)+\frac{3}{2}J_1(\omega_H+\omega_e)+\frac{3}{2}J_1(\omega_H-\omega_e)\right]+\frac{1}{T_1}\right\} \tag{4-5}$$

$$K=\frac{\hbar^2\gamma_F^2\gamma_H^2}{20r^6} \tag{4-6}$$

The symbols γ_F and γ_H are the respective gyromagnetic ratios of the ^{19}F and ^{1}H, ω_F and ω_H are the respective angular Larmor frequencies of the ^{19}F and ^{1}H, and r is the

proton-fluorine internuclear distance. The other terms are

$$\theta=\tan^{-1}\left[\frac{\gamma_F H_1}{\cos\delta}\right] \qquad (4\text{-}7)$$

and

$$\omega_e=\frac{2\pi\nu_{off}}{\cos\theta} \qquad (4\text{-}8)$$

where ω_e is the angular frequency about the effective field H_e created by the application of the rf field H_1 at a frequency ν_{off} off-resonance. The expression for $1/T_{1\rho}^{off}$, equation 4-5, is valid only if H_1 is applied sufficiently off-resonance:

$$\nu_{off}\geq\frac{5\gamma_F H_1}{2\pi} \qquad (4\text{-}9)$$

A steady state magnitization along the effective field H_e is due to competition between $T_{1\rho}^{off}$ and T_1 relaxation (James et al, 1978)

$$M_{eff}=M_o\frac{T_{1\rho}^{eff}}{T_1} \qquad (4\text{-}10)$$

where M_{eff} is the steady-state magnitization in the presence of the off-resonance rf field and M_o is the magnitization in the absence of the rf field, i.e., thermal equilibrium.

A convenient experimental parameter is the ratio of the intensity of an ^{19}F resonance in the presence of an off-resonance field to the intensity in the absence of the off resonance field, which can be identified as the ratio

$$R=\frac{M_{off}}{M_0}=\frac{J_0(\omega_H-\omega_F)+3J_1(\omega_F)+6J_2(\omega_H+\omega_F)}{2\sin^2\theta J_0(\omega_0)+J_0(\omega_H-\omega_F)+3J_1(\omega_F)+6J_2(\omega_H+\omega_F)} \qquad (4\text{-}11)$$

It may be noted that, analogous to the NOE, the value of R is independent of the internuclear FH distance but does depend on the motional properties of the fluorine nucleus as manifest in the spectral density functions.

The spectral densities for the case of random reorientation about an axis of internal rotation (with correlation time τ_i) which itself is reorienting isotropically (with correlation time τ_o) have been described by Woessner (1962) and have been subsequently applied to motion in macromolecules (Doddrell et al, 1972, Hull and Sykes, 1975a, 1975b):

$$J_0(\omega)=A\frac{2\tau_0}{1+\omega^2\tau_0^2}+B\frac{2\tau_B}{1+\omega^2\tau_B^2}+C\frac{2\tau_c}{1+\omega^2\tau_c^2} \qquad (4\text{-}12)$$

$$A=\frac{1}{4}(3\cos 2\alpha-1)^2 \qquad \tau_B=\left[\frac{1}{\tau_0}+\frac{1}{6\tau_i}\right]^{-1}$$

$$B=\frac{3}{4}(\sin^2 2\alpha) \qquad \tau_C=\left[\frac{1}{\tau_0}+\frac{2}{3\tau_i}\right]^{-1}$$

$$C=\frac{3}{4}(\sin^4\alpha)$$

where α is the angle between the F-H internuclear vector and is the axis of internal rotations, τ_i is the correlation time for random reorientation of the F-H vector about the axis of internal rotation, and τ_o is the correlation time for the isotropic tumbling of the drug-nucleic acid complex.

Chemical Shift Anisotropy Relaxation

Hull and Sykes (1975a) have described the the contribution of the chemical shift anisotropy of the ^{19}F to its T_1 and linewidth in macromolecules for internal motions superimposed on isotropic tumbling. Their expressions for T_1 and linewidth, as well as the chemical shift anisotropy contributions to the $T_{1\rho}^{off}$ and R are (Bolton et al, 1981)

$$\frac{1}{T_1} = \frac{3}{20}\gamma_F^2 H_o^2 \delta_z^2 \left[c_o J_o(\omega_F) + c_1 J_1(\omega_F) + c_2 J_2(\omega_F)\right] \tag{4-13}$$

$$W_2 = \frac{1}{2\pi T_1} + \frac{1}{10}\pi\gamma_F^2 H_o^2 \delta_z^2 \left[c_o J_o(0) + c_1 J_1(0) + c_2 J_2(0)\right] \tag{4-14}$$

$$\frac{1}{T_{1\rho}^{off}} = \frac{1}{T_1} + \frac{1}{10}\gamma_F^2 H_o^2 \delta_z^2 \left[c_o J_o(\omega_e) + c_1 J_1(\omega_e) + c_2 J_2(\omega_e)\right] \tag{4-15}$$

$$R = \frac{6\left[c_o J_o(\omega_F) + c_1 J_1(\omega_F) c_2 J_2(\omega_F)\right]}{6\left[c_o J_o(\omega_F) + c_1 J_1(\omega_F) + c_2 J_2(\omega_F)\right] + 4\sin^2\theta\left[c_o J_o(\omega_e) + c_1 J_1(\omega_e) + c_2 J_1(\omega_e)\right]} \tag{4-16}$$

$$c_o = \frac{1}{4}\left[(3\cos^2\beta - 1) + \eta\sin^2\beta 2\gamma\right]^2 \tag{4-17}$$

$$c_1 = \frac{1}{3}\sin^2\beta\left[\cos^2\beta(3 - \eta\cos 2\gamma)^2 + \eta^2\sin^2 2\gamma\right] \tag{4-18}$$

$$c_2 = \left[\sqrt{\frac{3}{4}}\sin^2\beta + \frac{\eta}{2\sqrt{3}}(1 + \cos^2\beta)\cos 2\gamma\right] + \left(\frac{\eta^2}{3}\right)\sin^2 2\gamma\cos^2 2\beta \tag{4-19}$$

Rotation of the principal axes for the internal rotational diffusion into the chemical shift principal axes yields the Euler angles β and γ. The anisotropy of the chemical shift is represented by δ_z, and the asymmetry is represented by η, which reflect the deviations from axial symmetry of the ^{19}F nucleus.

The spectral densities appropriate for equations 4-13 through 4-16 are given by

$$J_i(\omega)=\frac{2\tau_i}{1+\omega^2\tau_i^2} \qquad (4\text{-}20)$$

$$j=0,1,2 \quad \tau_0=\tau_c \quad \tau_1=\left[\frac{1}{\tau_c}+\frac{1}{6\tau_i}\right]^{-1} \quad \tau_2=\left[\frac{1}{\tau_c}+\frac{2}{3\tau_i}\right]^{-1}$$

^{19}F Relaxation in Fluorinated intercalators

The relaxation parameters for the fluorinated drugs may have contributions from both dipolar interactions and chemical shift anisotropy. Since fluoroquine and fluoroquinacrine both contain aromatic fluorines which are adjacent to two aromatic protons and have similar amino side chains, the drugs are expected to bind in a similar fashion to nucleic acids. Thus, identical calculations may be made for the two drugs. The model for the internal motion which gives rise to NMR relaxation was chosen from model building studies on the binding of the drugs to dinucleotides. One possible orientation of the drug bound to polynucleotides is with the chromophore of the drug intercalated between the bases and the amino side chain aligned along the phosphate backbone.

With the drug bound in this orientation, rotation about the bond shown in Figure 4-1 (α=109.5^{o}) would allow the chromophore of the drug to slide between the bases.

The principal axis of the chemical shift (δ_x, δ_y, δ_z) are also depicted in Figure 4-1. In order to calculate the chemical shift anisotropy contribution to relaxation, the values for the chemical shift anisotropy and the asymmetry need to be known. Unfortunately the chemical shift tensors for the fluorinated drugs have not yet been determined. As a reasonable approximation, however, we may use the values which have been determined for fluorobenzene: δ_z=51.2 ppm and η= -1.27 ppm (Mehring et al, 1974, Hull and Sykes, 1975a). The appropriate Euler angles for the motion depicted in Figure 4-1 are β= 19^{o} and γ=30^{o}.

Theoretical curves depicting the dependence of the relaxation rates, NOE, R, and linewidth on τ_i for ^{19}F in the fluorinated drugs relaxed by two protons 0.26 nm distant from the fluorine are given in Figures 4-2A through 4-2E for a series of overall motion correlation times. The curves were calculated assuming a magnetic field of 2.35T, an H_1 field of 0.23 gauss, and an off-resonance frequency of 5.6 KHz. The theoretical curves, with the exception of those for the NOE, contain contributions from both the dipolar and chemical shift anisotropy mechanisms. To the extent that chemical shift anisotropy is important, the actual NOE value will be somewhat diminished.

Figure 4-2A,B,C,D,E. Theoretical dependence of the spin-lattice relaxation time, nuclear Overhauser effect, rotating frame spin-lattice relaxation time in the presence of an off-resonance field, off-resonance peak intensity ratio, and linewidth on the internal motion correlation time for a series of overall motion correlation times. The values for the overall motion correlation time are (a) $3x10^{-8}$ s, (b) 10^{-7} s, (c) $3x10^{-7}$ s, (d) 10^{-6} s, (e) $3x10^{-6}$ s, and (f) 10^{-5} s.

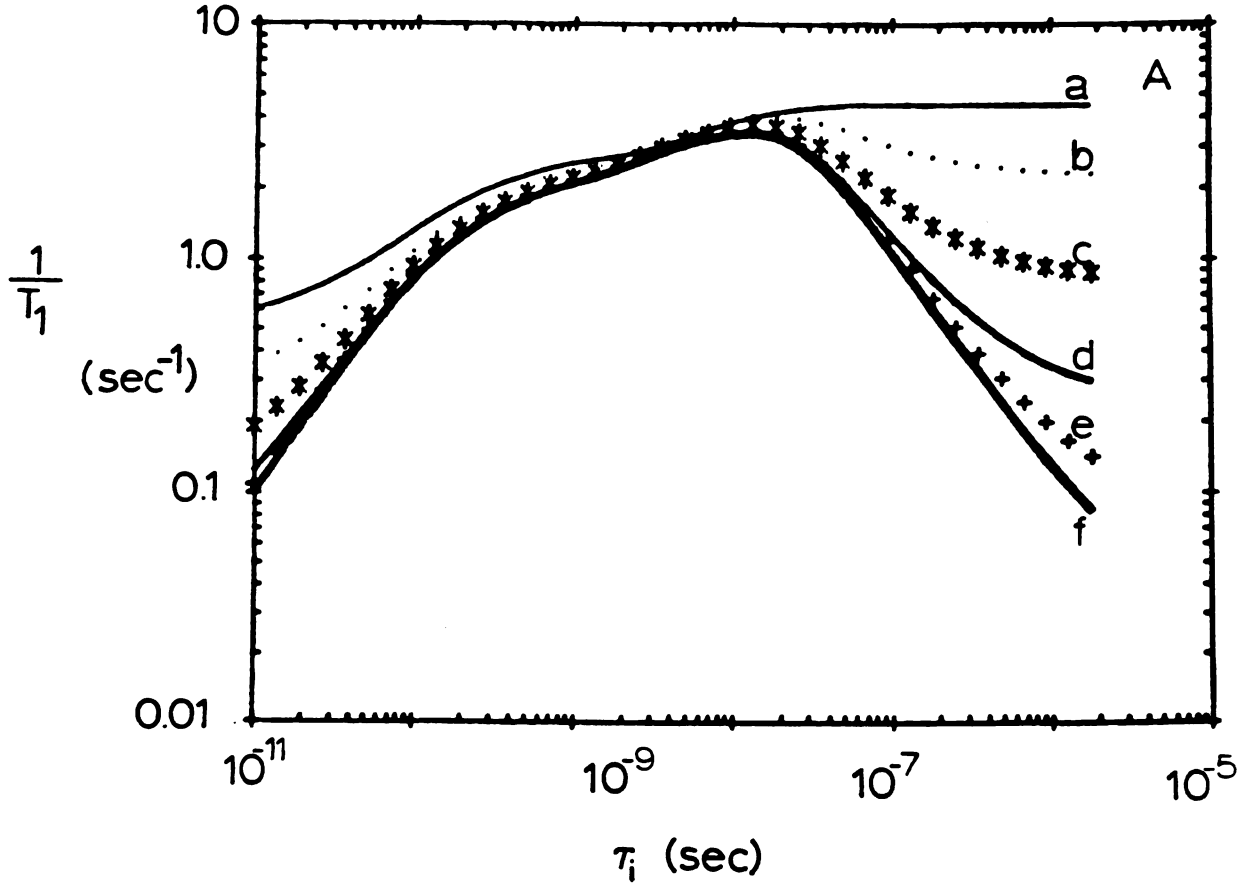

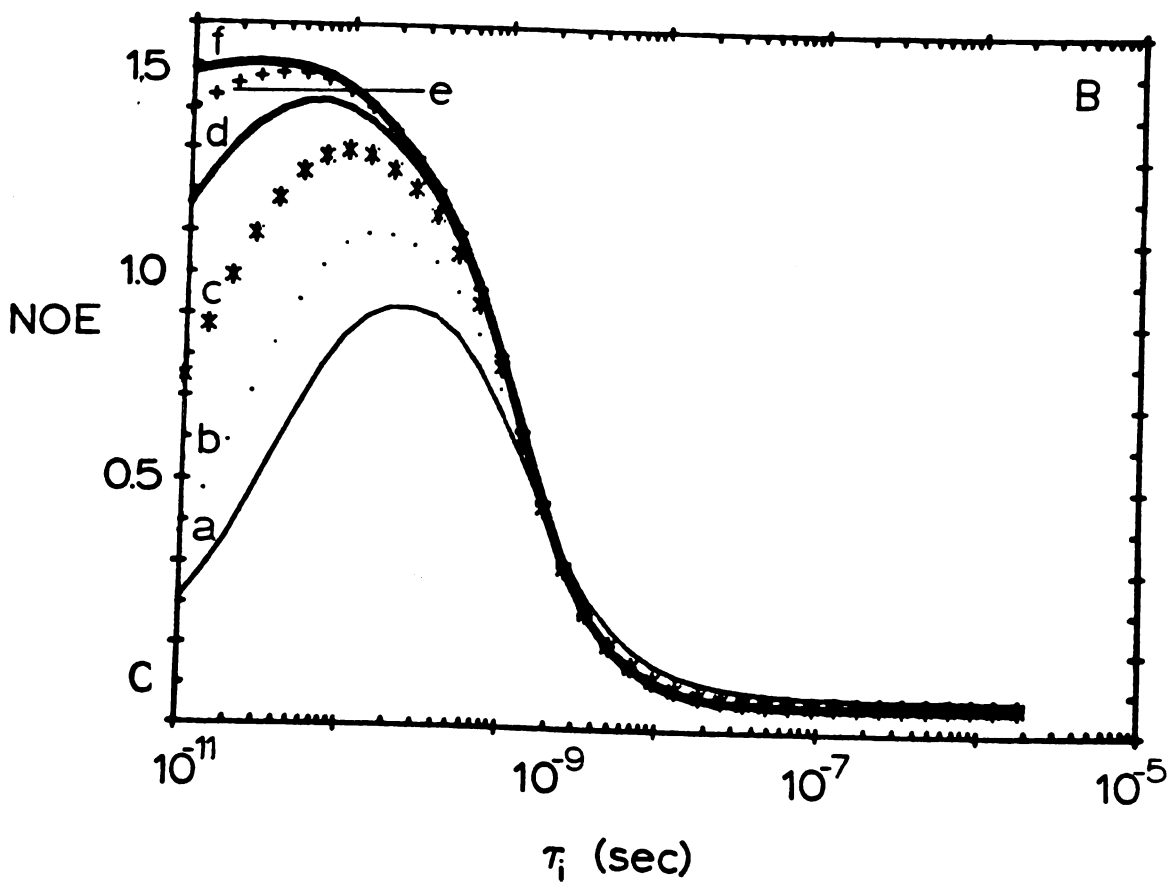
f
e
d
c
b
a
B
1.5
1.0
0.5
0
NOE
10^{-11}
10^{-9}
10^{-7}
10^{-5}
τ_i (sec)

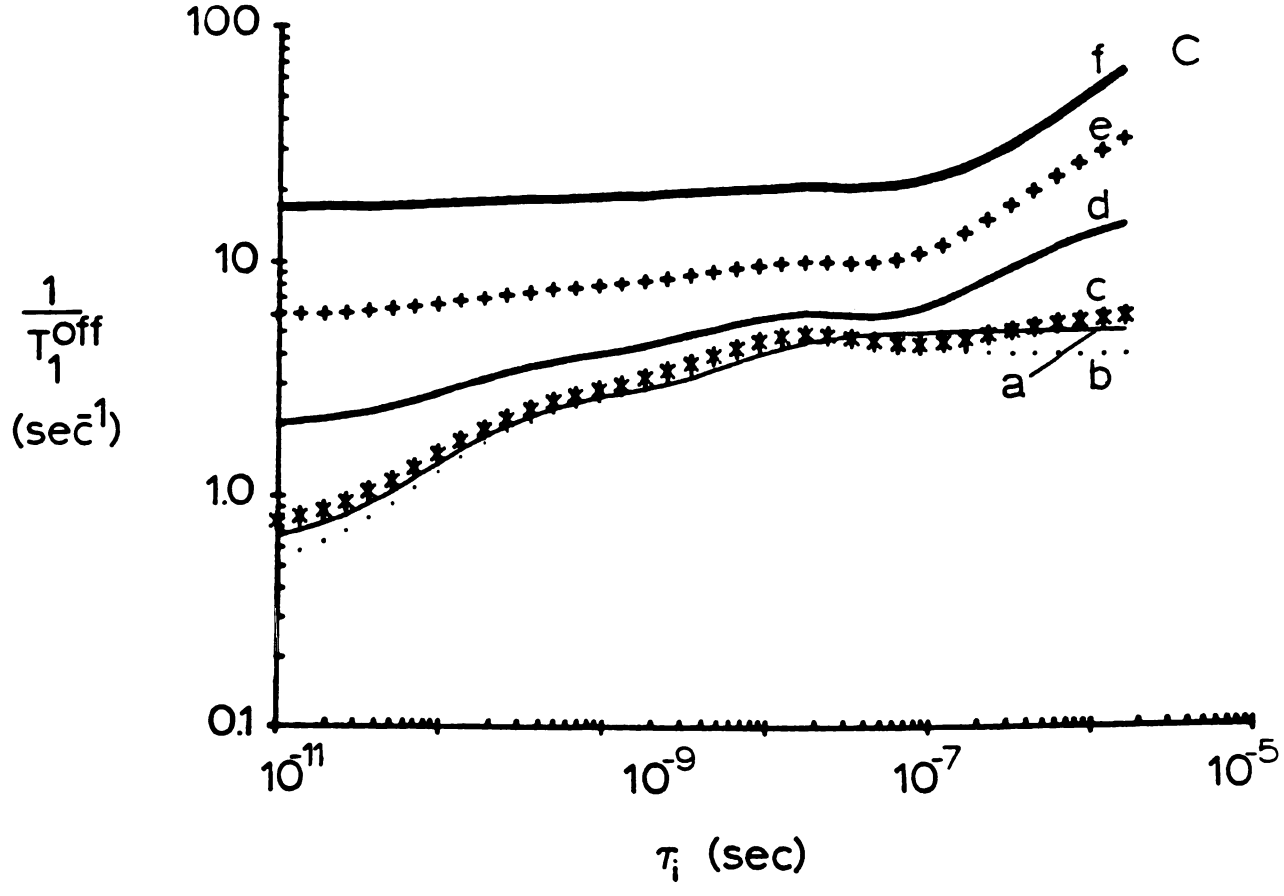
100
10
1.0
0.1
$\frac{1}{T_1^{off}}$
(sec^{-1})
10^{-11}
10^{-9}
10^{-7}
10^{-5}
τ_i (sec)
a
b
c
d
e
f
C

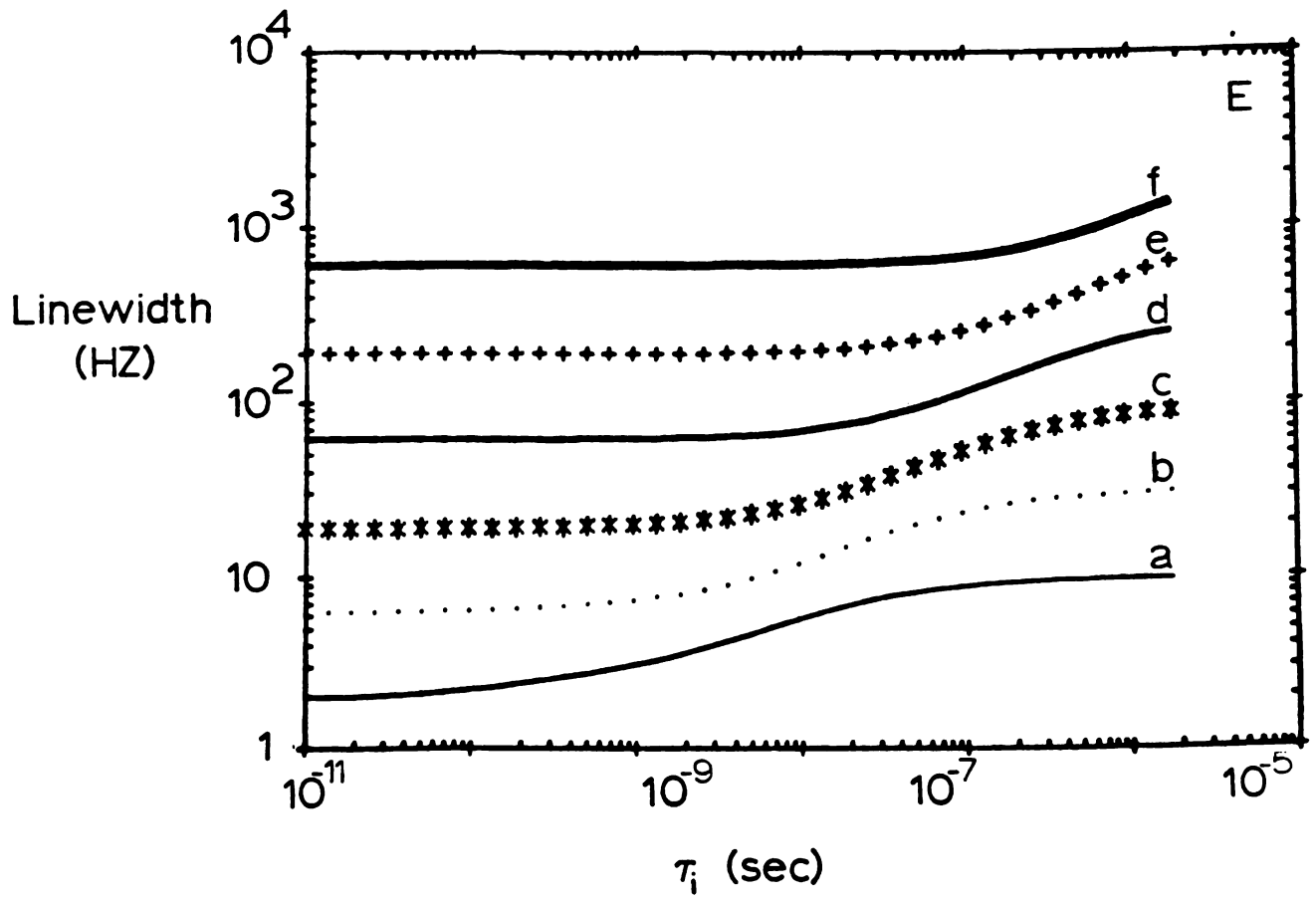
Linewidth
(HZ)
10^4
10^3
10^2
10
1
E
f
e
d
c
b
a
10^{-11}
10^{-9}
10^{-7}
10^{-5}
τ_i (sec)

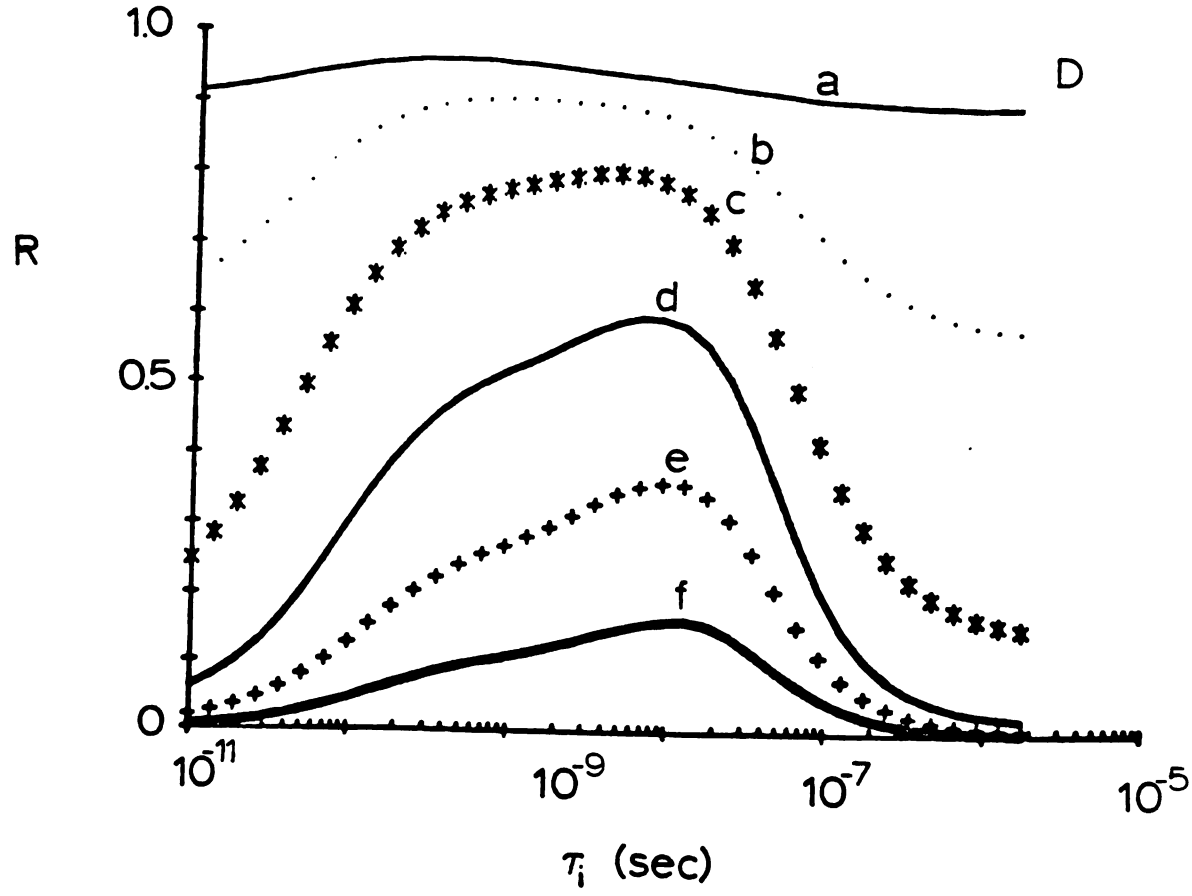
1.0
0.5
0
R
a
D
b
c
d
e
f
10^{-11}
10^{-9}
10^{-7}
10^{-5}
τ_i (sec)

RESULTS

Nucleic Acid Binding

To extrapolate the results of these studies on fluorinated intercalators to intercalators in general, it is necessary to demonstrate that the fluorinated intercalators bind in a manner similar to the more extensively studied intercalators. Binding by intercalation is usually characterized by a shift of the absorbance maximum to longer wavelength, a change in the fluorescent intensity of the bound drug, and an increase in the thermal denaturation temperature of double-stranded polynucleotides (Peacock, 1973). Itercalative binding is also characterized by a strong binding constant ($K > 10^5$) and at least two base pairs are excluded by the bound drug. While any of the above criteria is insufficient proof for intercalation, the total of the criteria is very strong circumstantial evidence for this mode of binding.

The interaction of fluoroquine with nucleic acids leads to changes in the above properties. The extinction coefficient at 340 nm decreases by 35% in the presence of DNA and 20% in the presence of tRNA. The changes observed upon complex formation are entirely analogous to those observed for chloroquine in the presence of nucleic acids (Hann et al, 1966, Cohen and Yielding, 1965). The presence of chloroquine at a phosphate-to-drug ration of 10 increased the thermal denaturation temperature by 10^{o} while similar

conditions led to a 12^{o} increase in Tm for fluoroquine. The Scatchard plots constructed from fluorescence quenching of chloroquine and fluoroquine in the presence of DNA were almost superimposable. As mentioned above, intercalative binding leads to an increase in the fluorescent lifetime of the drug, presumably because of the hydrophobic environment of the drug. We note this behavior for fluoroquine binding, where the fluorescent lifetime increases from 10 to 15 nsec in the presence of DNA (Bolton et al, 1981).

A similar situation is observed for fluoroquinacrine. Figure 4-3 shows the effect of DNA on the absorbance spectra of quinacrine and fluoroquinacrine. The isosbestic point observed in Figure 4-3 is usually taken as evidence of two absorbing species in solution; in this case, the free drug and the intercalated drug. Figure 4-4 shows the effect of various polynucleotides on the intensity of fluoroquinacrine fluorescence and Figure 4-5 shows a Scatchard plot for the binding of fluoroquinacrine to DNA constructed from the fluorescence quenching data. The DNA binding constant of fluoroquinacrine was found to be 1.6×10^{6} with 2.4 sites excluded per bound drug when analyzed by the method of McGhee and von Hippel (1974). These numbers are close to the literature value for the DNA binding quinacrine binding under our experimental conditions (Wilson and Lopp, 1980). For the acridine dyes there is often a weaker mode of interaction at lower ratios of P/D, a stacking of the drugs

Figure 4-3. Effect of DNA on the absorbance spectra of quinacrine (A) and fluoroquinacrine (B). The values represent the ratios of phosphate-to-drug.

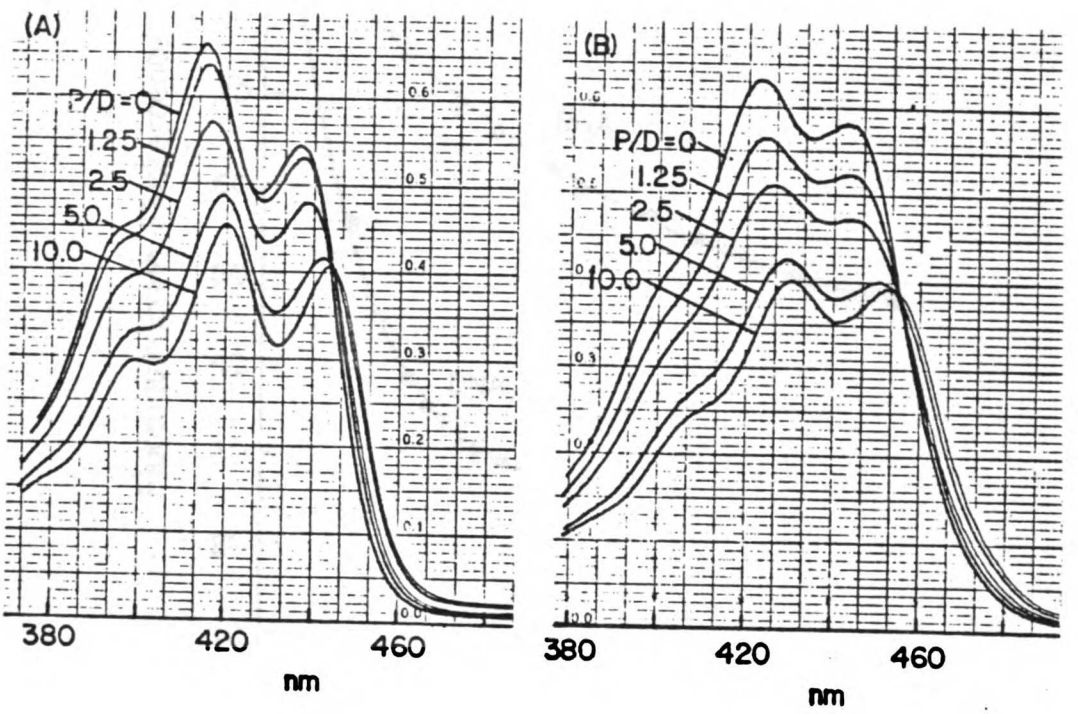

Figure 4-4. Effect of polynucleotides on the fluorescent quenching of fluoroquinacrine at ambient temperature for poly(A), tRNA, and DNA. The concentration of fluoroquinacrine was about 10^{-6} M.

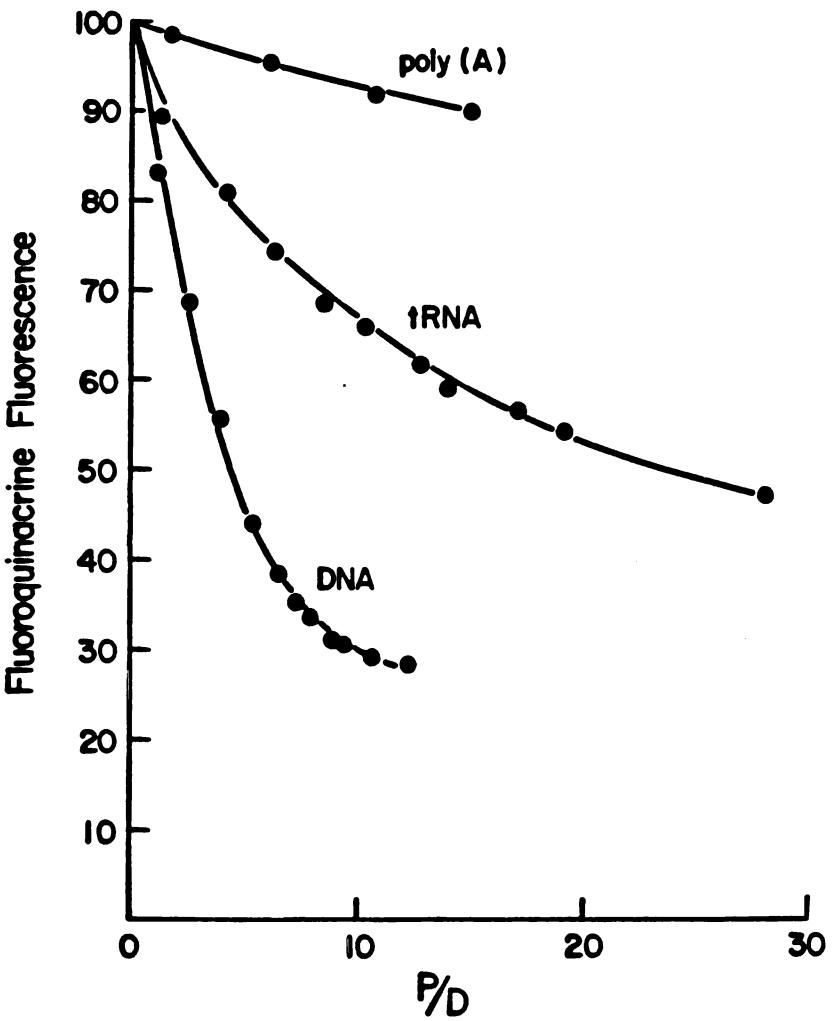

Figure 4-5. Scatchard plot constructed from the fluorescence quenching of fluoroquinacrine in the presence of DNA at ambient temperature. The binding constant (1.6×10^6 M) and number of binding sites (2.3) were obtained using the proceedure of McGhee and von Hippel (1974). The concentration of drug was 1×10^{-6} M.

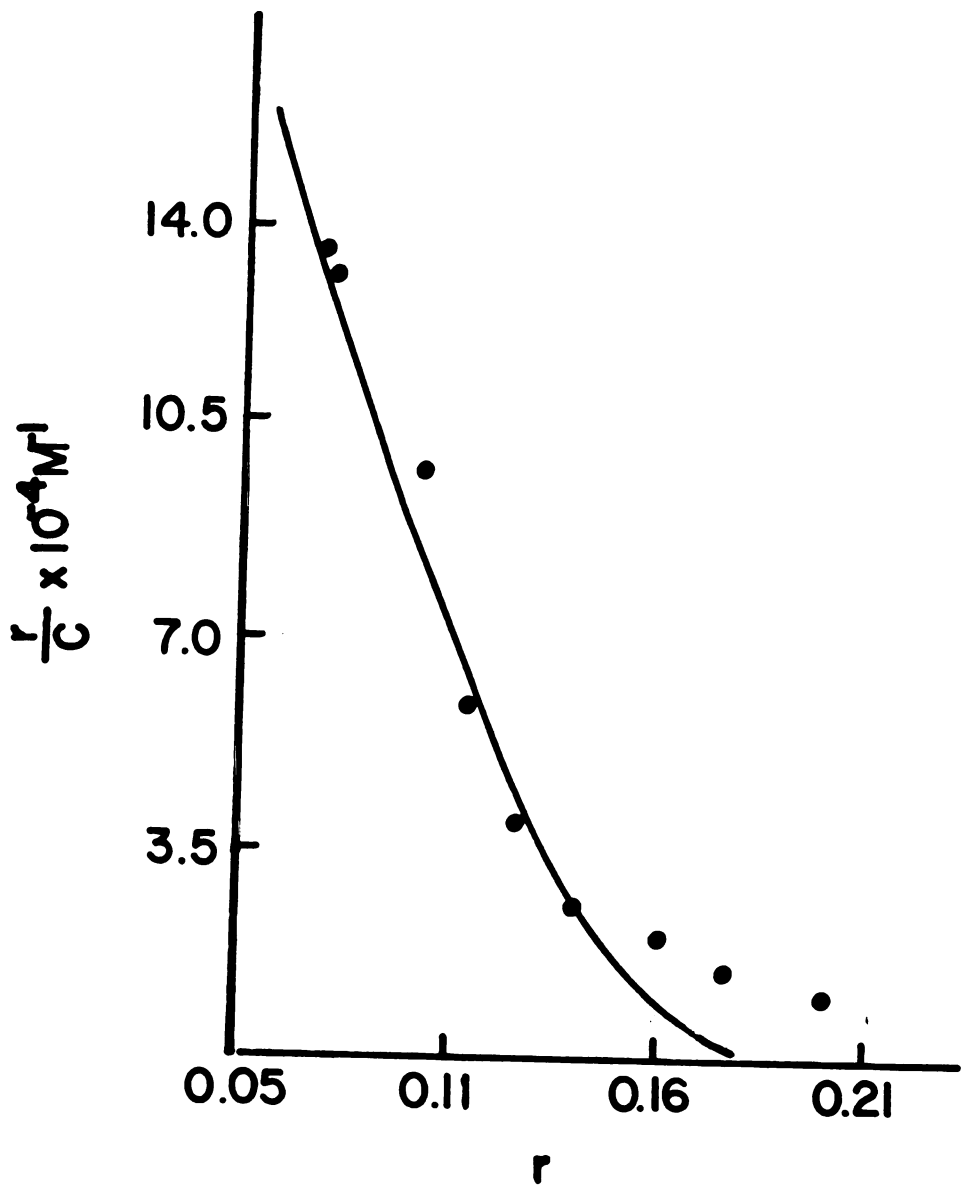

on the exterior of the helix (Peacock, 1973, Bontemps and Fredricq, 1974). Care was taken such that in all NMR experiments greater than 95% of the drug was bound by the strongest binding mode. At a P/D ratio of 20, fluoroquinacrine increased the Tm of DNA 12^{o} while quinacrine led to a 10^{o} increase.

Taken together these data are strong indicators that the fluorinated intercalators bind nucleic acids in a fashion similar to the parent compounds. Thus, the substitution of the fluorine for the chlorine of fluoroquine or the substitution of fluorine for the methoxy group of fluoroquinacrine may regarded as a non-perturbing probe of the intercalation complex.

Induced Chemical Shifts

The interaction of the fluorinated drugs with polynucleotides changes the ^{19}F properties of the drugs. Figures 4-6 and 4-7 show the effect of DNA, tRNA, and poly(A) on the chemical shift and linewidth of fluoroquine and fluoroquinacrine. The induced chemical shifts compiled in Table 4-1 are reported with respect to the free drug. As illustrated in Figure 4-2E, the linewidths are especially sensitive to the slower overall motions of the complexes; thus the linewidths indicate that the drugs are intimately associated with the polynucleotides. For fluoroquine the induced chemical shifts are relatively insensitive to the nature of the

Figure 4-6. 94.1 MHz ^{19}F spectra of fluoroquine free in solution and in the presence of poly(A), tRNA and DNA at 37°. The spectra were gathered in 2 K data points with a sweep width of 2 KHz using a 60 ° nonselective rf pulse, and broad band proton decoupling. Five minutes of signal averaging were required for the spectrum of the free drug, 15 minutes for the poly(A) sample, 30 minutes for the tRNA sample, and 4 hours for the DNA sample. The concentration of fluoroquinacrine was 2 mM in the free, poly(A), and tRNA samples and 1 mM in the DNA sample.

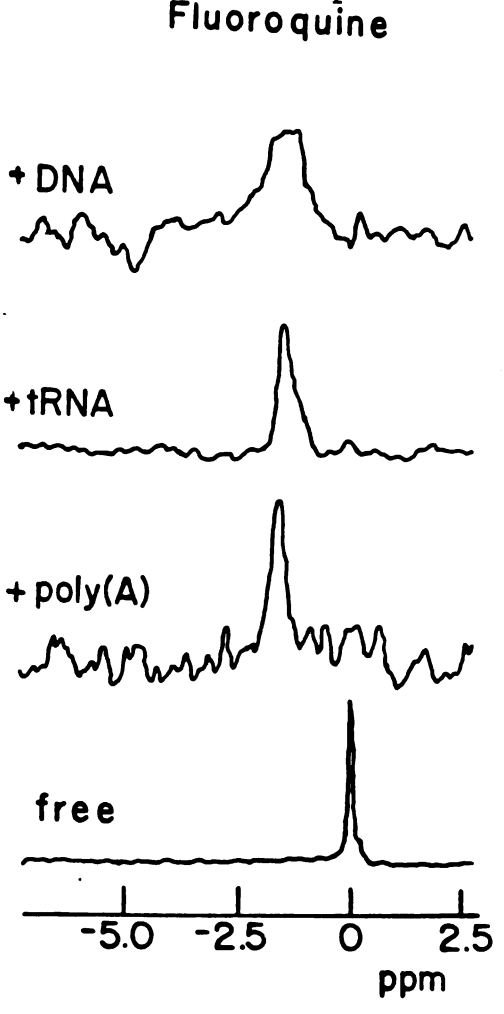

Figure 4-7. ^{19}F NMR spectra of fluoroquinacrine free and in its complexes with poly(A), tRNA, and DNA at 37°. See Figure 4-6 for details.

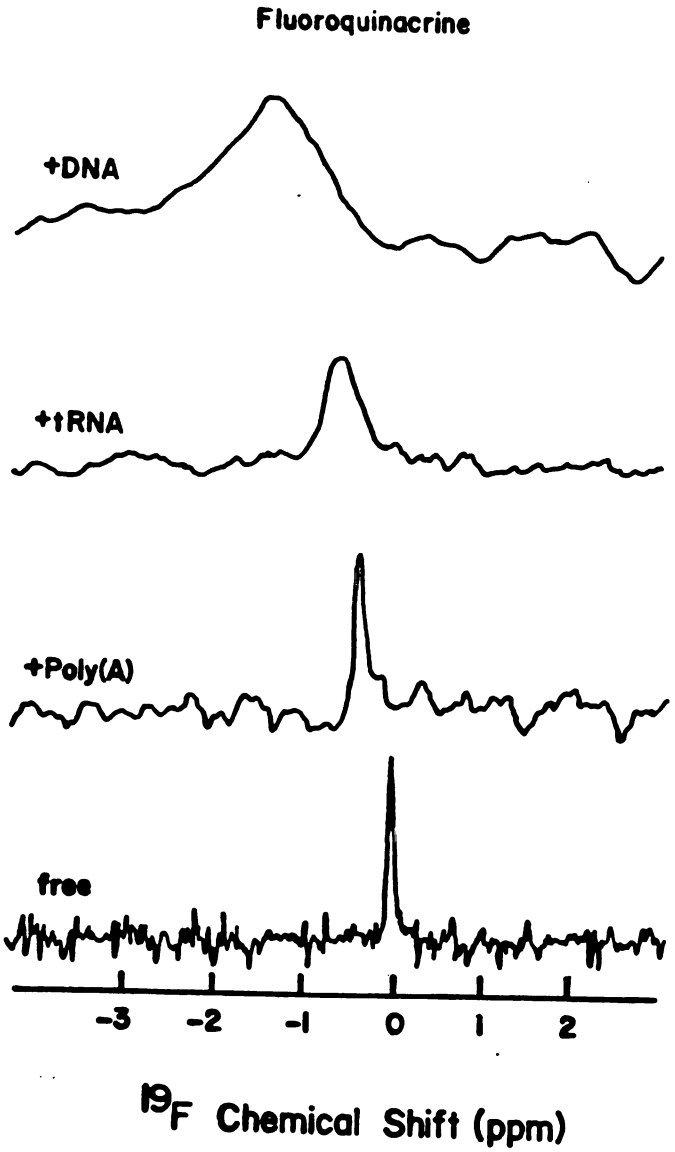

Table 4-1. ^{19}F chemical shifts and solvent induced shifts for fluoroquine, fluoroquinacrine, and their nucleic acid complexes.

Sample	T (°C)	Δδ (ppm)	SIS (ppm)
fluoroquine	25	0	-1.7
fluoroquine + poly(A)	25	-1.6	-0.6
fluoroquine + tRNA	25	-1.5	-0.1
fluoroquine + DNA	25	-1.7	-0.1
fluoroquine + E. Coli	37	-1.5	-
fluoroquine + Yeast	37	-1.7	-
fluoroquinacrine	25	0	0.3
fluoroquinacrine + poly(A)	25	-0.4	-
fluoroquinacrine + tRNA	25	-0.9	-
fluoroquinacrine + DNA	37	-1.6	0.3

a. See Materials and Methods.

b. Chemical shifts referenced to the free drug.

c. Solvent induced shifts.

polynucleotide; the fluorine nucleus must experience a similar environment in all complexes. In the fluoroquinacrine complexes, the induced chemical shifts roughly parallel the induced fluorescent quenching shown in Figure 4-5 and thus probably reflects the different environment of the acridine ring in the various complexes.

The chemical shifts of fluoroquinacrine-tRNA complexes have also been investigated under conditions under which tRNA is in its "native" conformation (Bolton and Kearns, 1977). Under such conditions, tRNA has one strong ethidium binding site (Wells and Cantor et al, 1970). Chemical shift titrations of fluoroquinacrine in the presence and absence of the native buffer are shown in Figure 4-8. It is clear from this data that the presence of high salt and magnesium has an effect on binding. It is not possible, however, to separate the two factors which may be responsible for the effect; a change in the structure of tRNA or a decreased binding affinity of the drug in the presence of high salt and magnesium.

The induced chemical shifts are opposite in sign and larger in magnitude than is expected if the shifts were due to ring current shifts from stacking between the bases (Krugh and Nuss, 1980). ^{19}F chemical shifts are known to be sensitive to environmental effects and the environment of the drug is expected to change significantly upon binding (Gerig, 1978). The observed chemical shifts are most likely

Figure 4-8. ^{19}F chemical shift of fluoroquinacrine in the presence of varying amounts of tRNA. Experiments were performed in a buffer which contained 0.01 M NaCl and 0.01 M cacodylate (△) or 0.1 M NaCl, 0.01 M cacodylate, and 0.01 M Mg^{+2} (▲) at pH 7 at 25°.

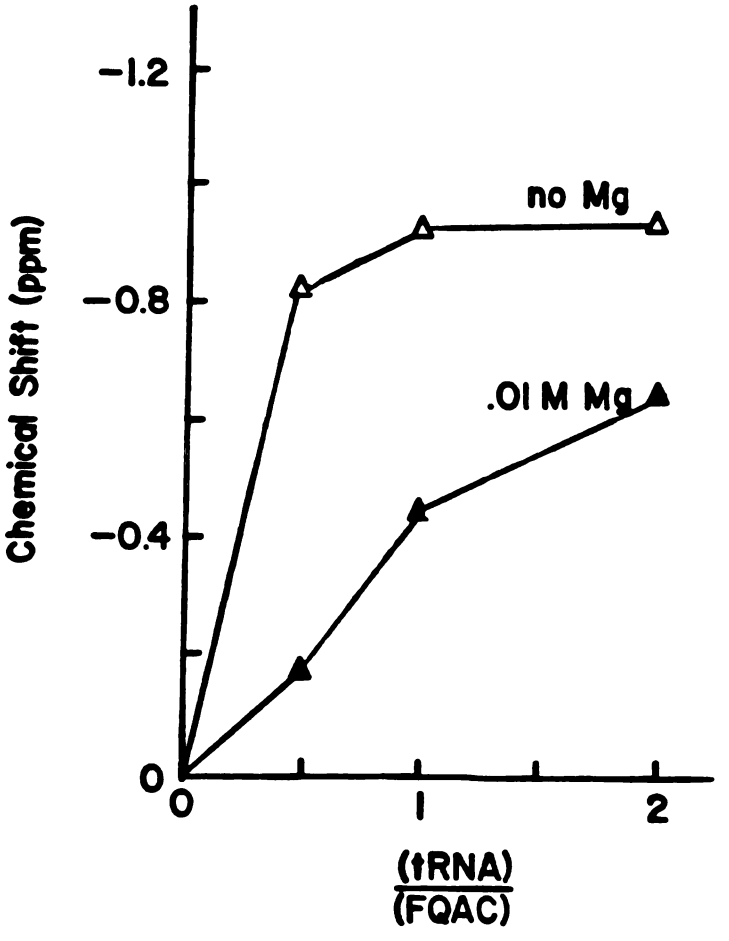

attributable to a sum of contributions from ring current shifts (upfield) and the change from an aqueous to a hydrophobic environment (downfield).

Solvent Induced Shifts

As mentioned above, the ^{19}F chemical shifts are sensitive to environmental factors. It has been noted that the chemical shift is sensitive to the isotopic composition of the solvent (Hull and Sykes, 1976, Hagen et al, 1980). For free fluoroquine, the ^{19}F resonance is shifted 1.7 ppm downfield as the solvent is changed from 90% H_2O/10% ^2H_2O to 10% H_2O/ 90% ^2H_2O. This shift is opposite in sign and larger in magnitude that the previously reported solvent induced shifts (SIS) for fluorine nuclei, which are usually between 0.1 to 0.4 ppm. In the reported studies it was speculated that the chemical shift difference is related to the hydrogen bonding ability of the fluorine; apparently the difference in the ^1H hydrogen bonding ability in comparison to the ^2H ability is significant enough to alter the electronic distribution about the fluorine nucleus and the difference in chemical shift is observed. It should be noted that changing from H_2O to ^2H_2O also has the effect of changing the apparent pH from 7.0 to 7.4. Increasing the pH of fluoroquine solutions to pH 7.4 shifts the fluorine to only slightly higher field. Increasing the pH to the pK_a (8.2) shifts the resonance several ppm upfield. Since the SIS is

opposite of the pH effect, the SIS cannot be due to a change in protonation (deuteration) of the acridine ring. Whatever the physical basis for this effect, however, the SIS may be used to examine the accessibility of the drug to solvent in the nucleic acid complexes.

Figure 4-9 demonstrates the SIS for fluoroquine free and in its nucleic acid complexes. The value for these and all of the SIS of the fluoroquine complexes are compiled in Table 4-1. The binding of fluoroquine to DNA and tRNA effectively shields the drug from solvent. The SIS is reduced by a factor of 17; the drug must spend greater than 90% of its time effectively isolated from the solvent pool. Single-stranded poly(A) offers less solvent protection for the bound drug. A study of the temperature dependence of the SIS for the poly(A) complexes showed that the increase in solvent accessibility correlates with the non-cooperative melting of poly(A) (Stanard and Felsenfeld, 1975).

The SIS for fluoroquinacrine (0.34 ppm) was similar to that reported for other fluorinated molecules. Approximately half of this shift may be accounted for by the pH change which accompanies the solvent substitution. The broad lines observed for the fluoroquinacrine complexes make quantitation of this effect difficult for such small values of the SIS.

Helix-to-Coil Transitions

Figure 4-9. Solvent induced shifts (SIS) for fluoroquine free and in its tRNA complex, The spectra were gathered at 25° in a buffer which contained either 10% H_2O/90% ^2H_2O or 90% H_2O/10% ^2H_2O.

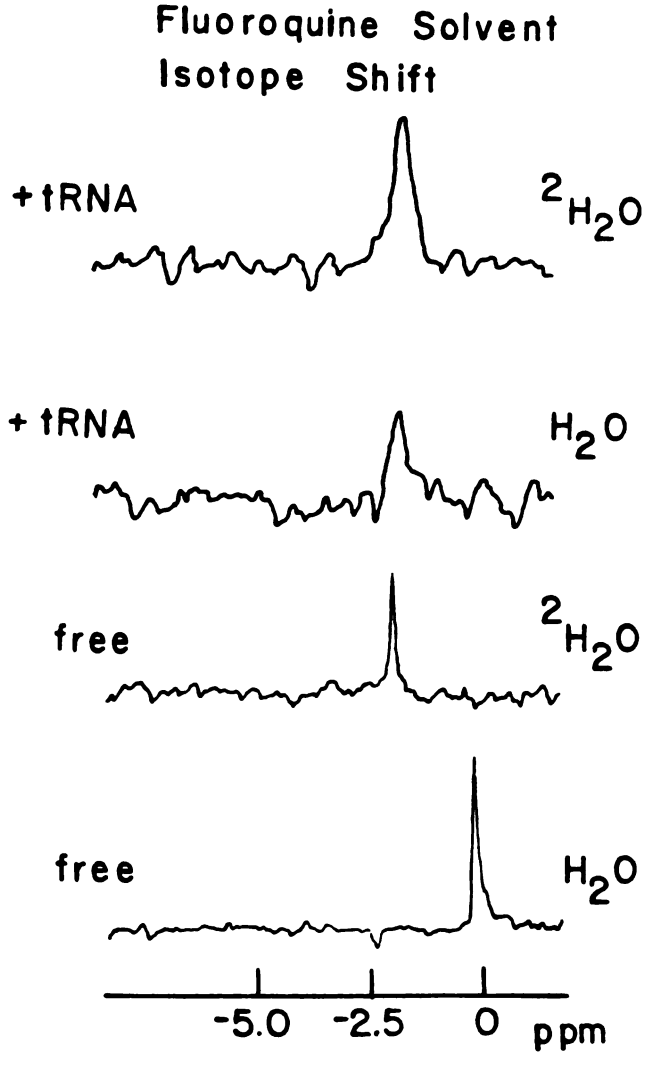

The ^{19} NMR parameters may also be used to monitor the helix-to-coil transitions of the polynucleotide complexes. Optical spectroscopy may be used in some cases to monitor the transitions in the drug free and the drug binding sites, however, ^{19}F NMR may offer dynamic and geometric information about the complex not obtainable by other methods.

The chemical shift of the ^{19}F of fluoroquinacrine bound to poly(A) does not change appreciably over the range of 25 to 85°. The data plotted in Figure 4-10 are in contrast to the optical melting of poly(A) which is non-cooperative and has a Tm of about 50° (Stanard and Felsenfeld, 1975, Bloomfield et al, 1974). The data suggest that the binding to poly(A) is not changed appreciably by the loss in poly(A) secondary structure. It should be noted that the poly(A) is still about 20% stacked at 80°.

The DNA binding of fluoroquinacrine has also been monitored at several temperatures by ^{19}F NMR and optical spectroscopy. The data plotted in Figure 4-11 show that the chemical shift of fluoroquinacrine changes in step with the optical absorbance of the complex when monitored at 260 nm. Both methods indicate a cooperative transition at 78°. The data also show that at high temperature the chemical shift approaches that of the free drug, indicating that the drug has a much higher affinity for the double-stranded DNA.

The optical absorbance of the tRNA complex indicates a cooperative transition at about 50° as shown in Figure 4-10.

Figure 4-10. Effect of temperature on the ^{19}F chemical shift of fluoroquinacrine in its poly(A) (△) and tRNA complexes (▲) and the absorbance at 260 nm of the tRNA complex (●). The concentrations were 20 mM for poly(A), 1 mM for tRNA, and 2 mM for fluoroquinacrine in the NMR experiments and the concnetration of tRNA in the optical experiments was $1x10^{-6}$ M.

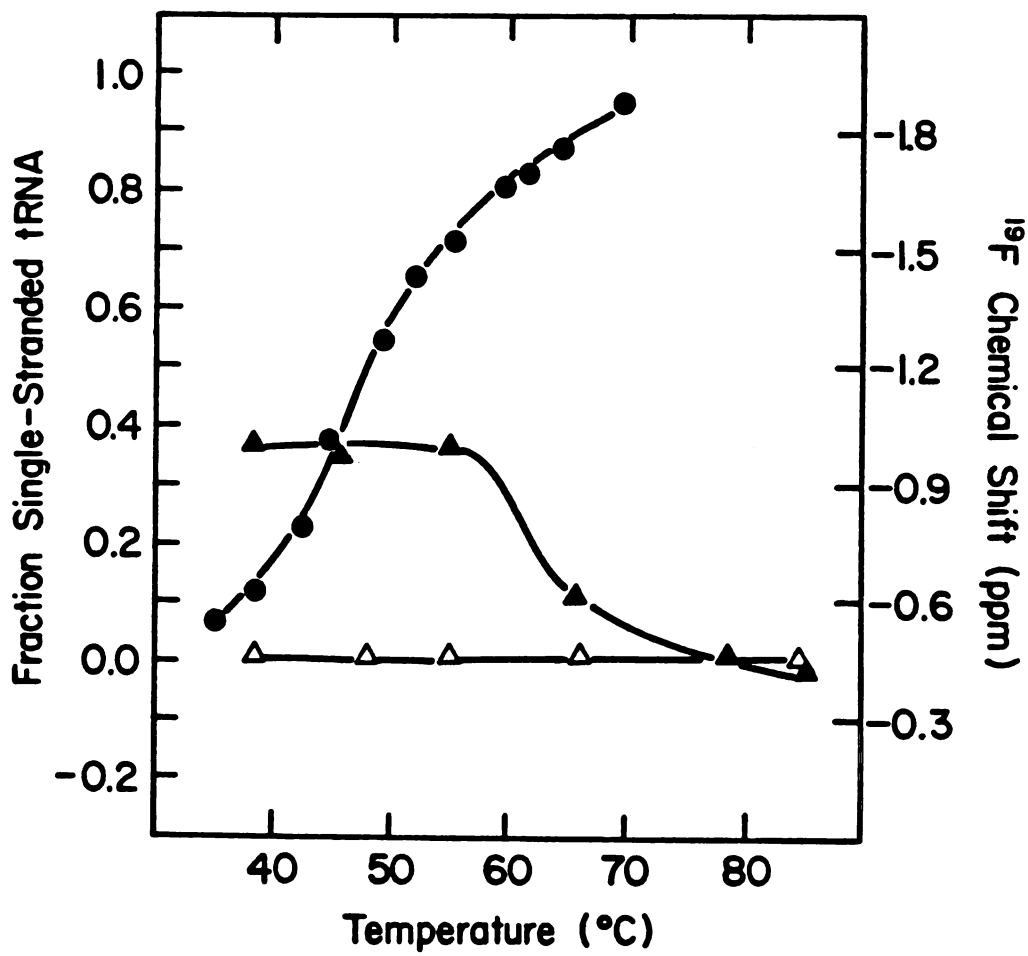

Figure 4-11. Helix-to-coil transitions of fluoroquinacrine in its DNA complex as monitored by its ^{19}F chemical shift (▲) and absorbance at 260 nm (●). See Figure 5-7 for NMR details. The concentration of DNA was $7x10^{-5}M$ for the optical experiments.

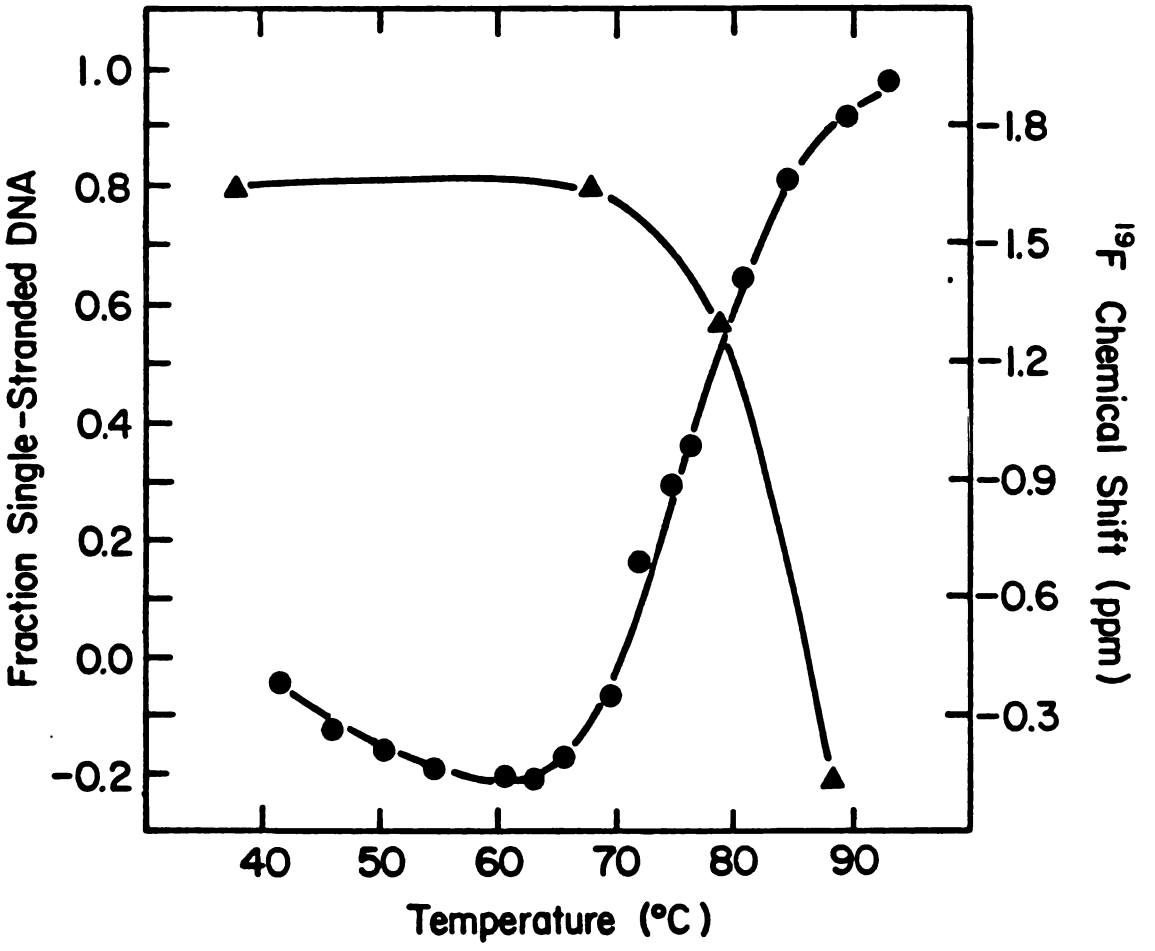

Figure 4-12. Effect of temperature on the ^{19}F NMR spectra of fluoroquinacrine in its tRNA complex. The sample contained 1 mM tRNA and 2 mM fluoroquinacrine.

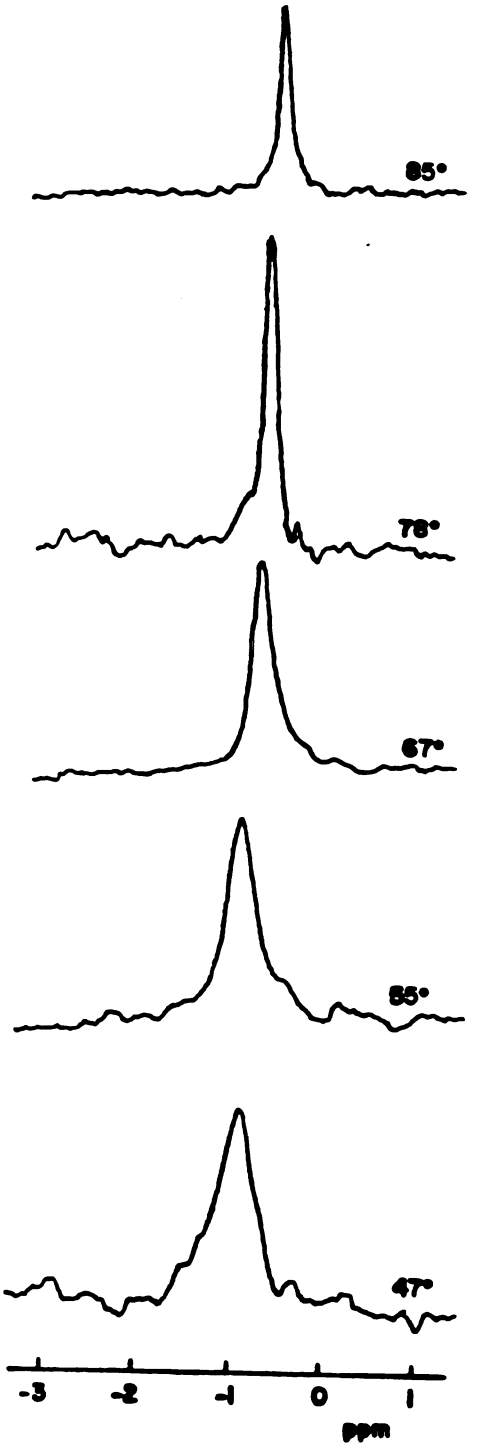

However, at this temperature there is no indication that the environment of the drug has changed appreciably. When the tRNA is 70% melted, as judged by the optical absorbance, a cooperative transition is noted in the ^{19}F NMR. This result indicates that fluoroquinacrine binds to the most stable region of the tRNA which are, of course, the double-helical stems.

Another interesting aspect of the helix-to-coil transition of the fluoroquinacrine-tRNA complex is shown in Figure 4-12, which shows the effect of temperature on the ^{19}F spectra of the complex. As discussed in the next section, the linewidth for the tRNA complex is broader than expected from the drug binding to a molecule with an overall tumbling time of 30 nsec. This broadening is most likely due to the proximity of the fluorine nucleus to the tRNA ribose protons. The change in chemical shift at the transition temperature is accompanied by a drastic decrease in linewidth. Evidently in the melted structure the ^{19}F is no longer close (and dipolar coupled to) the tRNA ribose protons.

These data illustrate a difference in the interaction of fluoroquinacrine with DNA vs RNA. In the DNA sample at high temperature the chemical shift approached that of the free drug, indicating little binding to the single-stranded form. In contrast, the RNA samples showed a residual -0.4 ppm chemical shift which is not dependent upon secondary structure. This is the only type of interaction observed

Figure 4-11. Helix-to-coil transitions of fluoroquinacrine in its DNA complex as monitored by its ^{19}F chemical shift (▲) and absorbance at 260 nm (●). See Figure 5-7 for NMR details. The concentration of DNA was 7×10^{-5}M for the optical experiments.

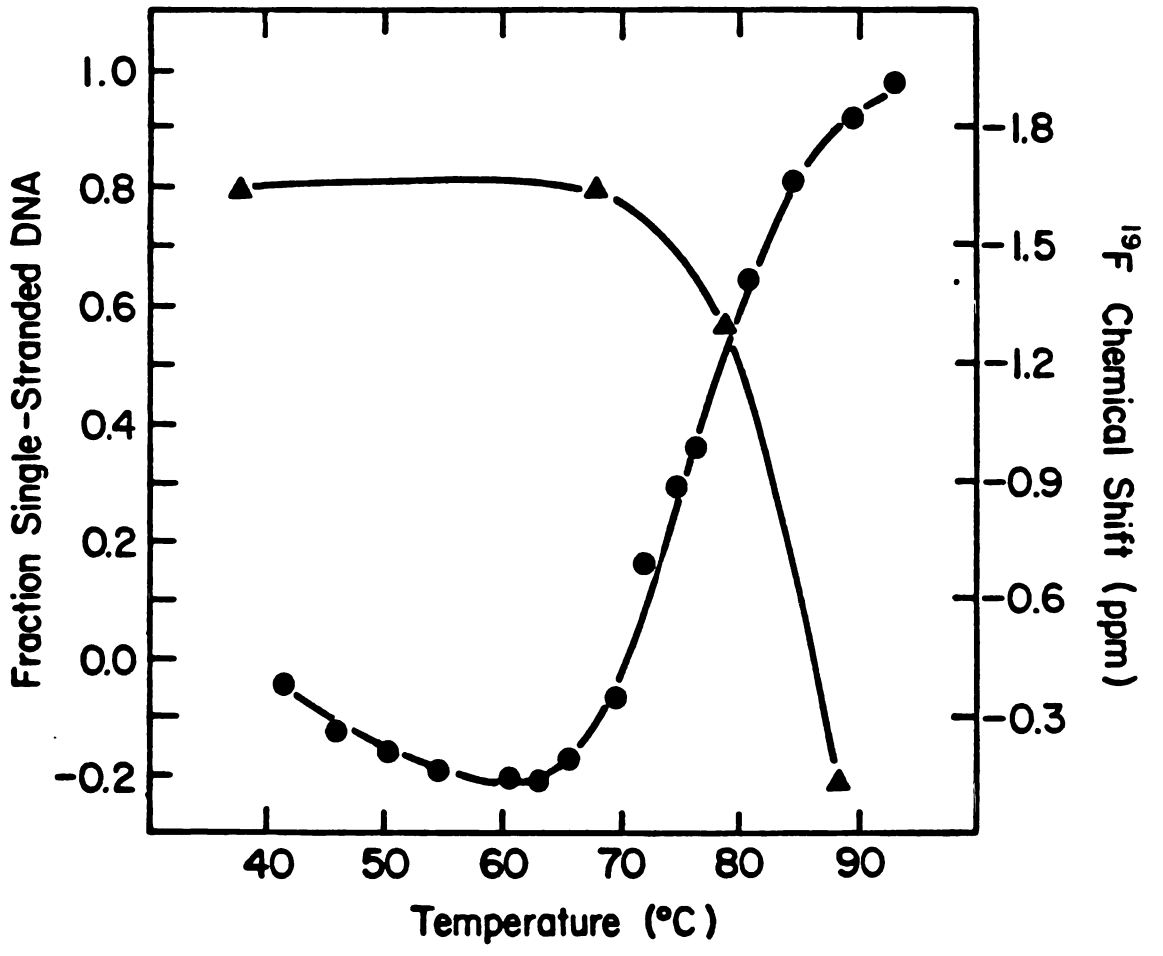

for poly(A).

^{19}F NMR Relaxation

The NMR relaxation parameters linewidth, $W_{1/2}$, spin-lattice relaxation time, T_1, rotating frame spin-lattice relaxation time in the presence of an off-resonance field, $T_{1\rho}^{off}$, and the off-resonance peak intensity ratio, R, may provide an insight into the dynamic nature of the drug-nucleic acid complex. The molecular motions of the drug are related to the relaxation parameters through the spectral densities as discussed in the Theory section. In addition, selective $^{19}F^{1}H$ NOE experiments may provide geometric information on the complex.

The NMR relaxation parameter values for fluoroquine and fluoroquinacrine in their nucleic acid complexes are presented in Tables 4-2 and 4-3. Like the chemical shift measurements, the relaxation experiments were performed at high ratios of P/D such that changes in the ^{19}F NMR reflects the strongest mode of interaction (intercalation). All of the relaxation parameter values change in the presence of nucleic acids. The effect of polynucleotides on the linewidth is dramatically illustrated in the ^{19}F NMR spectra of Figures 4-5 and 4-6, which show the nucleic acid complexes of fluoroquine and fluoroquinacrine. The Theory section shows that the linewidth and the off-resonance peak intensity ratio are sensitive to the slower overall motions

Table 4-2. ^{19}F NMR relaxation parameter values for fluoroquine free and in its nucleic acid complexes.

Sample	T_1 (sec)	NOE	R	$T_{1\pi}^{off}$ (sec)	$W_{1/2}$ (Hz)
fluoroquine, 25°	2.7	1.5	-	-	~1
fluoroquine, 10° + poly(A)	0.2	1.0	0.65	0.13	~15
fluoroquine, 25° + poly(A)	0.3	1.5	0.73	0.22	~10
fluoroquine, 25° + tRNA	0.2	0.8	0.56	0.11	~30
fluoroquine, 37° + tRNA	0.2	0.8	0.75	0.15	~30
fluoroquine, 37°	0.4	0.8	0.29	0.12	~100

Table 4-3. ^{19}F NMR relaxation parameter values for fluoroquinacrine free and in its nucleic acid complexes.

Sample	T_1 (sec)	NOE	R	$T_{1\pi}^{off}$ (sec)	$W_{1/2}$ (Hz)
fluoroquinacrine, 25°	2.0	1.5	-	-	~1
fluoroquinacrine, 25° + poly(A)	0.2	0.9	0.60	0.13	~50
fluoroquinacrine, 37° + poly(A)	0.3	0.7	0.66	0.15	~35
fluoroquinacrine, 25° + tRNA	0.15	0.52	0.56	0.08	~75
fluoroquinacrine, 37° + tRNA	0.14	0.51	0.60	0.08	~80
fluoroquinacrine, 37°	0.30	0.47	0.22	0.06	~180

and are clear indicators that complexes are being formed under the experimental conditions. The relaxation parameters for the DNA complexes are well-described by the model proposed in the Theory section. The values of the internal motion correlation times inferred from Figures 4-2A through 4-2E are 1 and 2 nsec for the sliding motion of fluoroquine and fluoroquinacrine respectively. Both complexes are well-described by an overall bending motion correlation time of 3000 nsec. The internal motion correlation time is shorter than predicted if the motion of the drug was rigidly coupled to the motion of the bases. Studies on the decay of fluorescence anisotropy of ethidium bound to DNA and spin labeled ethidium EPR studies suggest the time scale of this motion to be about 30 nsec (Genest and Wahl, 1978, Barkley and Zimm, 1979, Robinson et al, 1980). The 1 to 2 nsec correlation time is indicative of a sliding of the drug relative to the bases in the intercalation cavity. The overall motion correlation time is longer than that measured for drug-free samples of DNA by ^{31}P and ^{13}C NMR. This difference presumably reflects a local stiffening of the helix about the intercalation site and, hence, a slowing of the bending motion.

In a similar manner, the NMR parameters of fluoroquinacrine bound to poly(A) may be well described by a 1 nsec sliding motion and a 500 nsec overall correlation time. This indicates that the bases restrict the internal motion

of the drug. The faster overall motion is expected for the more flexible single-stranded polynucleotide. Tables 4-2 and 4-3 show that temperature variation does not appreciably alter the nature of the complex. In all samples the overall correlation time shows a slight temperature dependence; it has been estimated that the activation energy for this motion is about 4 kcal/mole (Barkley and Zimm, 1979, Hogan and Jardetski, 1980b, Bolton and James,1979).

The relaxation parameters for the fluoroquine-poly(A) complex, the fluoroquine tRNA, and the fluoroquinacrine-tRNA complexes are not well described by the model presented in the Theory section. The linewidths are greater than expected and Tables 4-2 and 4-3 show that the T_1 for these complexes are less than the T_1 minimum (0.3 sec) predicted by our model. The most obvious reason for this discrepancy is that the fluorine nucleus is being relaxed by some channel not accounted for; i.e. by dipolar interactions with protons on the polynucleotide.

To determine which protons are dipolar coupled to the fluorine nucleus we have performed a series of selective $^{19}F^{1}H$ NOE experiments on fluoroquine and its nucleic acid complexes. In these experiments a region of about 50 Hz of the proton spectra was irradiated and the effect on the fluorine intensity was monitored. For fluoroquine free in solution it was found that the $^{19}F^{1}H$ NOE originated from protons with chemical shifts between 7 and 8 ppm. These are

the aromatic ring protons adjacent to the fluorine on the quinoline ring. Figure 4-13 shows the effect of irradiation frequency on the intensity of the fluoroquine-tRNA and DNA complexes. In the DNA complex, the NOE originated from protons with chemical shifts between 7 and 8, ppm as was observed for fluoroquine free in solution. The fluorine in the poly(A) and tRNA complexes also showed an effect when these protons were irradiated. In addition, there was a selective $^{19}F^{1}H$ effect when the protons between 3 and 5 ppm were irradiated; this is the region in which the tRNA ribose protons appear. The experiments were performed in $^{2}H_2O$ to eliminate any contribution from the solvent.

The dipolar coupling to the macromolecule protons invalidates the approach of the Theory which assumes a set of proton-fluorine relaxation vectors. However, the NOE is not directly dependent on the number of dipolar coupled protons and thus may be used to estimate the sliding motion correlation time. Using Figure 4-2 with the estimated rotational tumbling time of 30 nsec for tRNA and 100 nsec for poly(A) (Tao et al, 1975, Bolton and James, 1979) we estimate the internal motion correlation time to be 1 nsec for the fluoroquine-the fluoroquine-tRNA and fluoroquinacrine-poly(A) complexes, and 2 nsec for the fluoroquinacrine-tRNA complex.

Cellular Binding Studies

Figure 4-13. Selective $^{19}F^{1}H$ nuclear Overhauser enhancement for fluoroquine in its DNA and tRNA complex. The spectra compare the intensity of the fluorine resonance in the presence of a 50 Hz ^{1}H irradiation field centered at 0 ppm and 4 ppm (the tRNA ribose protons).

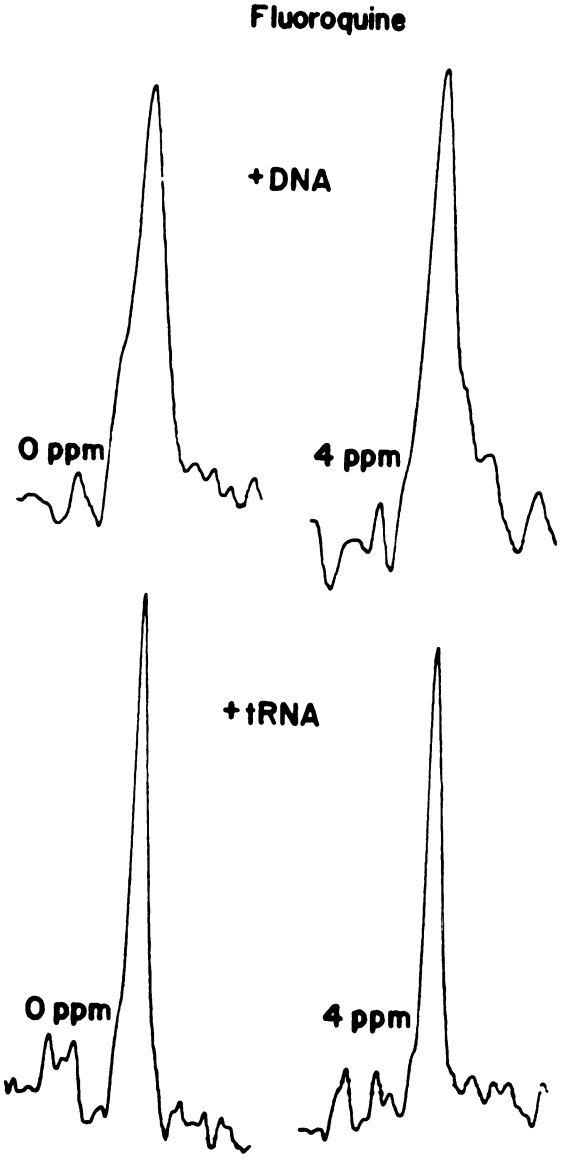

Initial studies on the fate of fluoroquine in whole cells has been investigated by ^{19}F NMR to demonstrate the power of ^{19}F NMR as a cellular probe. Figure 4-14 shows the ^{19}F spectra of fluoroquine (1 mM) which has been incubated for 2 hr. with a thick cellular suspension of E. coli and Yeast cells. The induced chemical shifts (Table 4-1) are indistinguishable from those obtained in the presence of nucleic acids. In addition, the linewidth, spin-lattice relaxation time, and the nuclear Overhauser enhancement (Table 4-2) are similar to those observed for fluoroquine in its poly(A) and tRNA complexes. While the control experiments were not performed to insure that lipid, protein, or carbohydrate binding did not contribute to the NMR properties, these data show how NMR may probe the fate of drugs.

DISCUSSION

This chapter illustrates how a variety of physical techniques may be used in conjunction to obtain a more detailed picture of DNA-ligand interactions. The first experiments were designed to demonstrate that fluorine substitution into the drug did not perturb the nature of the drug-nucleic acid complex. While minor differences in the Tm are noted for the analogs, the data very strongly indicate that the drugs bind like the parent compounds. On the basis of the optical measurements and the Scatchard analysis

Figure 4-14. ^{19}F NMR spectra of fluoroquine incubated with E. coli and Yeast cells at 37^{o}. The cells were incubated with fluoroquine (1 mM) for 2 hours prior to NMR experiments.

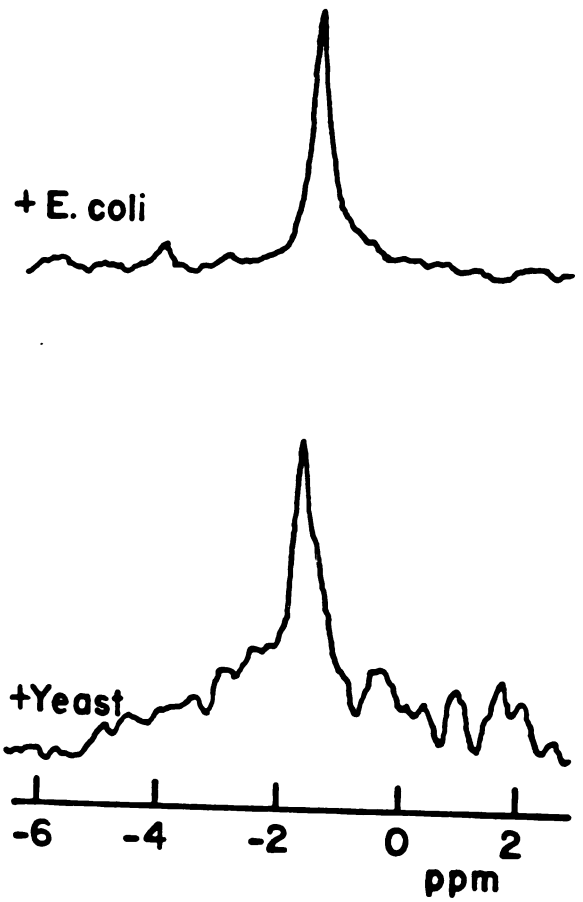

we conclude that fluorine substitution may be regarded as a non-perturbing probe of the intercalation complex.

Fluorine NMR provides a convenient method for monitoring intercalator complex formation. The linewidths of fluoroquine and fluoroquinacrine in the presence of nucleic acids (Figures 4-6 and 4-7) are clear indicators that a complex is formed under our experimental conditions. The induced chemical shifts and solvent induced shifts (Table 4-1) are indicators that the drug environment changes significantly upon binding. Unfortunately, an analysis of the geometry of the complex is not obtainable through analysis of the induced chemical shifts. Solvation plays an important role in ^{19}F chemical shifts, presumably because of the ability of the fluorine atom to hydrogen bond to the solvent. However, several conclusions may be drawn from the induced chemical shifts. It has been pointed out that there is a correlation between the chemical shift of the fluorine nucleus incorporated into fluorotyrosines of alkaline phosphatase and their "buriedness" within the protein (Hull and Sykes, 1976). In general, it is thought that the change to a hydrophobic environment decreases the shielding about the fluorine nucleus so downfield shifts are observed. The environment of the intercalator is expected to be essentially hydrophobic when intercalated. The chemical shifts observed in the presence of nucleic acid are most likely due to both ring current shifts which result from stacking of

the drug with the bases of the polynucleotide (upfield) and the change in environment from an aqueous to a hydrophobic one (downfield). The selective nuclear Overhauser effect indicates that in the fluoroquine-tRNA and fluoroquine-poly(A) complexes that the fluorine nucleus is within a few angstroms of the ribose protons of the polyribonucleotide.

The induced chemical shifts for fluoroquine and fluoroquinacrine binding to DNA (-1.5 and -1.6 ppm) suggest that the two intercalators experience a similar environment when bound to DNA. The induced chemical shifts of the fluoroquine complexes are not very sensitive to the nature of the polynucleotide (Figure 4-6 and Table 4-1). One explanation for this insensitivity is that the interaction energy for complex formation comes predominately from one chain of the polynucleotide. Thus, similar complexes may be formed with the single and double-stranded polynucleotides because the quinoline ring system is not large enough to fill the intercalation site. This is not true for fluoroquinacrine, in which the acridine ring may occupy a larger volume of the intercalation "cavity" and a sensitivity to polynucleotide structure and conformation is observed.

Since similar chemical shifts are observed for fluoroquine binding to all polynucleotides, this analog will provide only a limited amount of information on the cellular fate of intercalators. The cellular system contains a mixture of nucleic acids to which the drug may bind. The

sharper lines which result from formation of the tRNA or poly(A) type complexes would make difficult observation of the broader resonance from the DNA complex at the same chemical shift. The sensitivity of fluoroquinacrine to polynucleotide structure may be a much more useful probe of the cellular fate of intercalators.

The solvent induced shifts of fluoroquine allow us to evaluate the interaction of the bound drug with the solvent pool. When bound to DNA and tRNA (Table 4-1) fluoroquine showed little interaction with the solvent. These data provide both kinetic and geometric information about the complex. A quenching of the SIS could only be observed if the drug were in slow exchange with the solvent pool. These data also indicate that fluoroquine binds in such a way as isolate the drug from the solvent pool. While this may be expected for acridines, it would not be true for all drugs. For example, if daunomycin (chapter 3) were fluorinated in either the "A" or "D" ring, binding would have only a minor effect on the SIS, as these portions of the drug are open to the solvent in the DNA complex.

^{19}F NMR also provides an interesting insight into the fate of drugs in the helix-to-coil transitions of polynucleotides. While thermal denaturation may not be important in cells, some denaturation process is required for transcription of of genetic information; thermal denaturation is used to model this process. The binding of fluoroquinacrine

to poly(A) is not dependent upon secondary structure. Similarly, at high temperature the tRNA binding of fluoroquinacrine exhibits the same residual chemical shift of -0.4 ppm. However, in the presence of DNA the drug chemical shift approaches that of free fluoroquinacrine above the Tm, suggesting that dissociation of the complex accompanies the helix-to-coil transition. These data demonstrate a difference in the drug binding of RNA and DNA. Since, at high temperature, the macromolecules are in an unfolded state, these data suggest that the recognition is most likely related to a structural feature (i.e. the 2' hydroxyl) rather than a conformational one.

It is possible to monitor the conformational fluctuations of the drug-receptor with ^{19}F NMR. DNA is a hydrodynamically complex molecule and several motional models have been proposed to account for the observed ^{1}H, ^{13}C , and ^{31}P NMR relaxation behavior (Bolton and James, 1979, 1980a, Hogan and Jardetski, 1979, 1980b, Shindo and Cohen, 1978). The models generally consider two types of motion, a slow overall isotropic motion and a fast anisotropic internal motion. For chunks of DNA of molecular weight less than 250,000, the hydrodynamics of DNA are best approximated by a rigid rod and the overall motion may be explicitly described (Bloomfield et al, 1974). For larger segments of DNA there appears to be another motion (on a microsecond time scale) which dominates the slower reorientation of the relaxation

vectors. This was dramatically illustrated in a study which monitored the linewidth of the exchangeable proton resonances of discretely sized DNA fragments from 10 to 2000 base pairs long (Early and Kearns, 1979). The linewidths were less than predicted for the larger fragments, indicating that some process other than rotational reorientation was dominating NMR relaxation. It has been proposed that this motion is a bending of the helix (Barkley and Zimm, 1979). In addition, a "wobbling" of the phosphate backbone (1 nsec) and psuedorotation (puckering) of the sugar (1-6 nsec) must be invoked to explain the relaxation data (Bolton and James, 1979, 1980a, Hogan and Jardetski, 1979, 1980b). Although it has not been measured by ^{13}C NMR (^{1}H NMR studies are complicated by spin diffusion) the motion of the bases is expected to occur on a time scale of about 30 nsec (Barkley and Zimm, 1980). This is predicted from studies on the decay of fluorescence anisotropy of ethidium bound to DNA and electron paramagnetic resonance (EPR) studies on spin labeled ethidium analogs (Genest and Wahl, 1978, Robinson et al, 1980).

The ^{19}F NMR data on the two drugs studies so far indicate that the intercalators show considerable motion when intercalated. The 1 and 2 nsec internal motion correlation times indicate that the motions of the drugs are not rigidly coupled to those of the bases. This motion is on the time scale of the fastest motion which gives rise to the decay of

fluorescence anisotropy of ethidium bound to DNA (Genest and Wahl, 1978). A 1 nsec motion has been proposed to account for the the EPR linewidths of spin labeled acridine bound to DNA (Robinson et al, 1980). The presence of the rapid sliding motion observed in these ^{19}F NMR experiments implies that the intercalation "cavity" is quite large and offers sufficient room for intercalators to slide about. It may be the case that examination of larger intercalators (actinomycin) may have significantly reduced internal motion.

It is interesting to note that the bending motion correlation time measured for the fluorinated intercalators is longer than that measured for the drug free samples by ^{13}C and ^{31}P NMR (Bolton and James, 1979, 1980). At high ratios of phosphate-to-drug, P/D=20, the increase in contour length is expected to be about 10%. Therefore, the increase in overall motion correlation time is most likely attributable to the stiffening of the DNA helix when the drug binds. Such long range effects of intercalator binding may be related to the <u>in vivo</u> effects, such as the inhibition of RNA polymerase, which occur at low levels of drug binding.

Finally, these experiments demonstrate the potential power of ^{19}F NMR to study the fate of drugs in cellular systems. With no interference from cellular NMR resonances, this technique allows us to monitor complex formation in a mixture of nucleic acids.

REFERENCES

Abner, W. (1974) Prog. Mol. Biol. Nucl. Acids Res. 14, 1.

Abragam, A. (1961) "The Principles of Nuclear Magnetism, " Clarendon Press, Oxford.

Addock, B. (1973) in "Acridines" (Acheson, R. Ed.) John Wiley and Sons, New York, 109.

Arison, B. and Hoogsteen, K. (1970) Biochemistry 9, 3978.

Ascoli, F., De Santis, P., Lener, M., and Savino, M. (1972) Biopolymers 11, 1173.

Barkley, M. and Zimm, B. (1979) J. Chem. Phys. 70, 2991.

Bittman, R. and Blau, L. (1976) Biochemistry 14, 2138.

Bloomfield, V., Crothers, D., and Tinocco, I. (1974) "The Physical Chemistry of Nucleic Acids," Harper and Row, New York.

Bolton, P. and James, T. (1979) J. Chem. Phys. 83, 3359.

Bolton, P. and James, T. (1980a) Biochemistry 19, 1388.

Bolton, P. and James, T. (1980b) J. Amer. Chem. Soc. 102, 25.

Bolton, P. and Kearns, D. (1977) Biochemistry 16, 5729.

Bolton, P. and Kearns, D. (1978) Nucleic Acids Res. 5, 4891.

Bolton, P., Mirau, P., Shafer, R., and James, T. (1981) Biopolymers 20, 435.

Bontemps, J. and Fredricq, E. (1974) Biophysical Chemistry 2, 1.

Bovey, F., Brewster, A., Patel, D., Tonelli, A., and Torchia, D. (1972) Acct. Chem. Res. 6, 193.

Brandts, J., Halvorson, H., and Brennon, M. (1975) Biochemistry 14, 4953.

Bresloff, J. and Crothers, D. (1975) J. Mol. Biol. 95, 103.

Brockmann, H. and Manegold, J. (1958) Naturwissenschaften 45, 310.

Brockmann, H. and Manegold, J. (1960) Chem. Ber. 93, 2971.

Byrd, R., Dawson, W., Ellis, P. and Dunlap, R. (1978) J. Amer. Chem. Soc. 100, 7748.

Bystrov, V., Ivanov, V., Portnova, S., Balashara, T., and Ovshinnikova, V. (1973) Tetrahedron. 29, 873.

Calendi, E., Di Marco, A., Reggioni, M., Scarpinato, B., and Valentini, L. (1965) Biochim. Biophys. Acta 103, 25.

Cantor, C. and Schimmel P. (1980) "Biophysical Chemistry," Part III, W.H. Freeman and Co., San Francisco.

Caruthers, M.(1980) Acct. Chem. Res. 13, 155.

Cerami, A., Reich, E., Ward, D., and Goldberg, I. (1967) Proc. Nat. Acad. Sci. 57, 1036.

Chaio, C. and Krugh, T. (1977) Biochemistry 16, 747.

Chairs, J., Dattagupta, N., and Crothers, D. (1981) Biophysical J. 33, 314a.

Cohen, S. and Yielding, K, (1965) J. Biol. Chem. 240, 3123.

Coleman, J., Anderson, R., Ratcliffe, R., and Armitage, I. (1976) Biochemistry 15, 5410.

Coleman, J. and Armitage, I. (1976) in "NMR in Biology" (Dwek, R., Campbell, I., Richards, R., and Williams, R., Eds) Academic Press, San Francisco, 171.

Conti, F. and De Santis, P. (1970) Nature 227, 1239.

Davanloo, P. and Crothers, D. (1976) Biochemistry 15, 5299.

Deslauriers, R, and Smith, I. (1977) Biopolymers 16, 1245.

Deslauriers, R. and Smith, I. (1980) in "Biological Magnetic Resonance" (Berliner, L. and Reubens, J. Eds.) vol. 2, Pleunum Press, New York, 243.

Deslauriers, R., Walters, R., and Smith, I. (1974) J. Biol. Chem. 249, 7006.

De Tar, D. and Luthra, N. (1977a) J. Amer. Chem. Soc. 99,

1232.

De Tar, D. and Luthra, N. (1977b) J. Org. Chem. 44, 3299.

Doddrell, D., Glushko, V., and Allerhand, A. (1972) J. Chem. Phys. 56, 3683.

Du Vernay, V., Mong, S., and Crooke, S. (1980) in "Anthracyclines" (Crooke, S. and Reich, S., Eds.) Academic Press, San Francisco, 61.

Early, T. and Kearns, D. (1979) Proc. Nat. Acad. Sci. 76, 4165.

Fico, R., Chen, T., and Canellakis, E. (1977) Science 198, 53.

Formica, J. Shatkin, A., and Katz, E. (1968) J. Bacteriol. 95, 2139.

Formica, J. and Apple, M. (1976) Antimicrob. Agents Chemother. 9, 214.

Gabbey, E., Greier, D., Fingerle, R., Reiner, R., Levy, R., Pearce, W., and Wilson, W. (1976) Biochemistry 15, 2062.

Gellert, N., Smith, C., Neville, D., and Felsenfeld, G. (1965) J. Mol. Biol. 11, 445.

Genest, D. and Wahl, P. (1975) Biochem. Biophys. Acta 521, 502.

Gerig, J. (1975) in "Biological Magnetic Resonance" (Berliner, L. and Reubens, Eds.) vol. 1, Plenum Press, chapter 4.

Gerig, J., Halley, B., and Ortiz, C. (1977) J. Amer. Chem. Soc. 100, 6217.

Gerig, J., Luk, K., and Roc, D. (1979) J. Amer. Chem. Soc. 101, 7698.

Goldberg, I., Rabinowitz, M., and Reich, E. (1962) Proc. Nat. Acad. Sci. 48, 2094.

Gorrenstein, D., Findlay, J., Momii, R., Luxon, B., and Kar, D. (1976) Biochemistry 15, 3796.

Gorrenstein, D. and Kar, D. (1975) Biochem. Biophys. Res. Commun. 65, 1073.

Hagen, D., Weiner, J., and Sykes, B. (1979) Biochemistry 18, 3590.

Hamilton, L., Fuller, W., and Reich, E. (1963) Nature 198, 538.

Hann, F., O'Brien, R., Ciak, J., Allison, J., and Olenick, J. (1966) Military Medicine 1071.

Hogan, M., Dattagupta, N., and Crothers, D. (1980) Biochemistry 18, 280.

Hogan, M. and Jardetski, O. (1979) Proc. Nat. Acad. Sci. 76,

6341.

Hogan, M. and Jardetski, O. (1980a) Biochemistry 19, 2079.

Hogan, M. and Jardetski, O. (1980b) Biochemistry 19, 3460.

Hopfinger, A. (1977) "Intermolecular Interactions and Biomolecular Organization" John Wiley and Sons, New York.

Huang, C., Mong, S., and Crooke, S. (1980) Biochemistry 19, 5537.

Hull, W. and Kricheldorf, H. (1980) Biopolymers, 19, 1103.

Hull, W. and Sykes, B. (1975a) J. Mol. Biol. 98, 121.

Hull, W. and Sykes, B. (1975b) Biochemistry 17, 3431.

Hull, W. and Sykes, B. (1975c) J. Chem. Phys. 63, 867.

Hull, W. and Sykes, B. (1976) Biochemistry 17, 1535.

Hyman, R. and Davidson, N. (1970) J. Mol. Biol. 50, 421.

Israel, M., Wilkinson, P., and Osteen, R. (1980) in "Anthracyclines" (Crooke, S. and Reich, S., Eds.) Academic Press, San Francisco, 61.

Jain, S. and Sobell, H. (1972) J. Mol. Biol. 68, 1.

James, T. (1975) "Nuclear Magnetic Resonance in Biochemistry" Academic Press, New York.

James, T., Matson, G., Kuntz, I., Fisher, R., and Buttlaire,

D. (1977) J. Mag. Res. 28, 417.

James, T., Pogolotti, A., Ivanetich, K., Wataya, Y., Loni, S., and Santi, D. (1977) Biochem. Biophys. Res. Commun. 72, 404.

Johnston, F., Jorgenson, K., Lin, C., and van de Sand, J., (1978) Chromosoma 68, 115.

Jones, R., Lanier, A., Keel, R., and Wilson, W. (1980) Nucl. Acids Res. 8, 1613.

Jones, R. and Wilson, W. (1980) J. Amer. Chem. Soc. 102, 7776.

Kaiser, I. (1980) Biochemistry 8, 231.

Karplus, M. (1959) J. Chem. Phys. 30, 11.

Kastorp, R., Young, M., and Krugh, T. (1978) Biochemistry 17, 4855.

Kersten, H. and Kersten, W. (1974) "Inhibitors of Nucleic Acid Synthesis" Springer-Verlag, New York.

Kollman, P. and Weiner, P. (1981) J. Comp. Chem. Submitted.

Krugh, T. (1972) Proc. Nat. Acad. Sci. 69, 1911.

Krugh, T., Hook, J., Lin, S., and Chen, F. (1979) in "Steriodynamics of Molecular Systems" (Sarma, R., Ed.) Pergamon Press, New York, 423.

Krugh, T., Laing, J., and Young, M. (1976) Biochemistry 15, 1224.

Krugh, T. and Mooberry, E. (1973a) Biochemistry 12, 1775.

Krugh, R. and Mooberry, E. (1973b) Biochemistry 12, 4418.

Krugh, T., Mooberry, E., and Chaio, C. (1977) Biochemistry 16, 740.

Krugh, T. and Neely, J. (1973a) Biochemistry 12, 1775.

Krugh, T. and Neely, J. (1973b) Biochemistry 12, 4418.

Krugh, T. and Nuss, M. (1980) in "Biological Applications of Magnetic Resonance" (Schulmann, R. Ed.) Academic Press, San Francisco.

Krugh, T. and Young, M. (1977) Nature 269, 627.

Lackner, H. (1977) Angew. Chem. Internat. Edit. 74, 375.

Le Pecq, J. and Paoletti, C. (1967) J. Mol. Biol. 27, 87.

Lerner, D. and Kearns, D. (1980) J. Amer. Chem. Soc. 102, 7776.

Lewis, C., Ellis, P., and Dunlap, D. (1980) Biochemistry 19, 116.

Li., H. and Crothers, D. (1975) J. Mol. Biol. 39, 461.

London, R. (1978) J. Amer. Chem. Soc. 100, 2678.

Madison, V. (1977) Biopolymers 16, 2671.

Marshall, A. and Smith, J. (1977) J. Amer. Chem. Soc. 99, 635.

Mauger, A. (1975) in "Peptides: Chemistry, Structure, and Biology" (Walters, R. and Meinhoffer, J. Eds.) Ann Arbor Sci. Publishing Co., New York, 181.

Mauger, A. (1980) in "Topics in Antibiotic Chemistry," vol. 5. (Sammes, P., Ed.) John Wiley and Sons, New York, 223.

McGhee, J. (1976) Biopolymers 15, 1345.

McGhee, J. and von Hippel, P. (1974) J. Mol. Biol. 86, 469.

Mehring, M., Raber, H., and Sinning, G. (1974) 18th Ampere Congress, Nottingham (Allen, P., Andrews, E., and Bates, C., Eds.) University of Nottingham.

Meienhoffer, J. and Atherton, E. (1977) in "Structure Activity Relationships Among Semisynthetic Antibiotics" (Pearlman, D., Ed.) Academic Press, New York, 427.

Meraldi, J., Blout, E., Boni, R., and Verdini, A. (1978) Biopolymers 17, 2401.

Mirau, P., Shafer, R., and James, T. (1981) Biochemistry submitted.

Mosher, C., Kuhlmann, K., Kleid, D., and Henry, D. (1977) J. Med. Chem. 20, 1055.

Muller, W. and Crothers, D. (1968) J. Mol. Biol. 35, 251.

Olmsted, J., and Kearns, D. (1977) Biochemistry 16, 3647.

Patel, D. (1974a) Biochemistry 13, 2388.

Patel, D. (1974b) Biochemistry 13, 2396.

Patel, D. (1976) Biopolymers 15, 533.

Patel, D. (1978) Biopolymers 18, 533.

Peacock, (1973) in "Acridines" (Acheson, R., Ed.) John Wiley and Sons, New York, 723.

Phillips, D., Di Marco, A., and Zunino, F. (1977) Eur. J. Biochem. 85, 481.

Pigram, W., Fuller, W., and Hamilton, L. (1972) Nature New Biology 235, 17.

Plumbridge, T. and Brown, J. (1977) Biochem. Biophys. Acta 479, 441.

Pogliani, L., Ellenberger, M., and Volat, J. (1975) J. Mag. Res. 7, 61.

Prado, F., Giessner-Prettre, C., Pullman, B., and Daudey, J. (1979) J. Amer. Chem. Soc. 101, 1751.

Pratt, W. and Ruddon, R. (1979) "The Anticancer Drugs" Oxford Press, New York.

Price, C. and Roberts, R. (1948) Org. Synth. 28, 38.

Quigley, G., Wang, A., Ughetto, G., van der Marel, G., van Boom, J., and Rich, A. (1981) Proc. Nat. Acad. Sci. 77, 7204.

Ramachandran, G., Lakshiminaryanan, A., Balasubramanian, R., and Tegoni, G. (1970) Biochem. Biophys. Acta 221, 165.

Reich, E., Goldberg,I., and Rabinowitz, M. (1962) Nature 196, 743.

Reinhardt, C. and Krugh, T. (1977) Biochemistry 16, 2890.

Remers, W. (1978) "The Chemistry of Antitumor Antibiotics," vol. 1, Wiley Interscience, New York.

Robinson, B., Lerman, L., Beth, A., Frisch, H., Dalton, L., and Auer, C. (1980) J. Mol. Biol. 139, 19.

Shafer, R. (1978) Biochem. Pharmacol. 26, 1729.

Shafer, R., Burnette, R., and Mirau, P. (1980) Nucl. Acids Res. 6, 1121.

Shindo, H., McGhee, J., and Cohen, J. (1979) Biopolymers 19, 523.

Sobell, H. (1974) Cancer Chemother. Rep. 58, 101.

Sobell, H. and Jain, S. (1972) J. Mol. Biol. 68, 21.

Stanard, B. and Felsenfeld. G. (1975) Biopolymers 14, 299.

Surry, A. and Cutler, R. (1951) J. Amer. Chem. Soc. 73, 2623.

Tao, T., Nelson, J., and Cantor, C. (1970) Biochemistry 9, 3514.

Tsang, T., and Baldwin, R. (1972) J. Mol. Biol. 69, 145.

Tsang, T., Baldwin, R., and Elson, E. (1972) Proc. Nat. Acad. Sci. 69, 1809.

Tubbs, R., Ditmars, W., and van Winkle, Q. (1964) J. Mol. Biol. 9, 545.

Venkatachalaphti, V. and Balaram, P. (1981) Biopolymers 20, 65.

Wang, J. (1974) J. Mol. Biol. 89, 783.

Waring, M. (1965) Mol. Pharmacol. 1, 1.

Waring, M. (1974) J. Mol. Biol. 54, 247.

Wells, B. and Cantor, C. (1970) Nucl. Acids Res. 4, 1667.

Wells, R. and Larson, J. (1970) J. Mol. Biol. 49, 319.

Wilson, W. and Lopp, I. (1980) Biopolymers 19, 1257.

Winkle, S. and Krugh, T. (1981) Nucl. Acids Res. submitted.

Wossner, W. (1962) J. Chem. Phys. 36, 1.

Young, M. and Krugh, T. (1977) Biochemistry 14, 4841.

Zelenin, A., Kitianova, E., Kolesnikov, V., and Stepanova, N. (1976) J. Histochem. Cytochem. 24, 1169.

Zunino, F., Gambetta, R., Di Marco, A., Velich, A., Zaccara, A., Quadrifoglio, F., and Crescenzi, V. (1977) Biochim. Biophys. Acta 476, 38.